MEGATHRUST SPLAY FAULT GEOMETRY IN PRINCE WILLIAM SOUND, ALASKA

by

Shaun Patrick Finn

A thesis

submitted in partial fulfillment

of the requirements for the degree of

Master of Science in Geophysics

Boise State University

December 2012

BOISE STATE UNIVERSITY GRADUATE COLLEGE

DEFENSE COMMITTEE AND FINAL READING APPROVALS

of the thesis submitted by

Shaun Patrick Finn

Thesis Title: Megathrust Splay Fault Geometry in Prince William Sound, Alaska

Date of Final Oral Examination: 20 August 2012

The following individuals read and discussed the thesis submitted by student Shaun Patrick Finn, and they evaluated his presentation and response to questions during the final oral examination. They found that the student passed the final oral examination.

Lee M. Liberty, M.S.	Chair, Supervisory Committee
Clyde J. Northrup, Ph.D.	Member, Supervisory Committee
John R. Pelton, Ph.D.	Member, Supervisory Committee

The final reading approval of the thesis was granted by Lee M. Liberty M.S., Chair of the Supervisory Committee. The thesis was approved for the Graduate College by John R. Pelton, Ph.D., Dean of the Graduate College.

ACKNOWLEDGEMENTS

First I want to thank my loving and supportive grandparents: Barbara and Jack Ohl; and Margaret and Dennis M. Finn. Next, I want to thank my parents, Lori and Dennis P. Finn, whose love and support have made my education a reality, and allowed me to pursue my childhood dreams. I gratefully acknowledge the friendship and support extended to me by the faculty, staff, and students of the Geoscience department at BSU during these three years. I am extremely grateful to Dr. Peter J. Haeussler and Dr. Thomas L. Pratt who shared their knowledge of structural and stratigraphic geology. Lastly, I must acknowledge the special role Lee M. Liberty played in maintaining my enthusiasm for near-surface geophysical research. Without his insight, advice and endless patience, this thesis would not have been possible.

ABSTRACT

I present marine seismic reflection results from Prince William Sound, Alaska that document the location of active faults related to the subduction zone processes.

Subduction zones along convergent margins experience large earthquakes, magnitude >8, with recurrence intervals on the order of centuries. Smaller magnitude earthquakes with shorter recurrence intervals are probable along the same subduction zone fault zones. Convergent margin earthquakes also are associated with high uplift rates and tsunami generation, yet the location and uplift history of most tsunamigenic faults are unknown. In this thesis, I present the processed results of high resolution marine seismic reflection data of Prince William Sound (PWS), Alaska. I then use these results to create a new tectonic model for the region that constrains fault histories, earthquake hazards, and distribution of active faults within a megathrust subduction zone system.

The epicenter of the M9.2 Great Alaska Earthquake of 1964 was in northern PWS. This earthquake caused tsunamis that impacted shoreline communities as far as California. Earthquake damage and local tsunamis affected towns and infrastructure throughout the PWS region. Future earthquakes may occur independently on these faults or they may rupture only during a large earthquake.

Data were collected in four locations within PWS: Gravina Bay, Orca Bay, Hinchinbrook Entrance, and Montague Strait. Seismic results show high angle faults that

offset three primary stratigraphic layers (Holocene, older Quaternary, and Tertiary). Regionally extensive bathymetric lineations connect mapped faults on seismic reflection profiles to define fault lengths that are a proxy for maximum earthquake magnitude. Bathymetric lineations where bedrock surfaces on the sea floor help identify additional active or relic faults. Megathrust splay faults that control motion along the subduction plate boundary surface on Montague Island and recorded the greatest offset during the M9.2 Great Alaska Earthquake of 1964. I interpret Montague Island as the outerarc high of the subduction zone system and suggest splay faults may extend across PWS. Lineations in Hinchinbrook Entrance represent the surface expression of splay faults identified in unpublished crustal seismic data. I interpret normal faults in Orca Bay and Montague Strait, within the forearc of the subduction zone, to form in the hanging wall of the main PWS splay fault that defines the outer arc high. I calculate slip rates along hanging wall normal faults of 1.8 m/kyr in Orca Bay and 6.25 m/kyr in Montague Strait. These faults may extend 40 km, potentially causing an independent M7 earthquake that could damage local infrastructure. Furthermore, landslides identified in Orca Bay and Montague Strait demonstrated a potential hazard from local tsunamis within these locations.

TABLE OF CONTENTS

LIST OF FIGURES

LIST OF ABBREVIATIONS

3-D	Three dimensional
BP	Before present (years before present)
CMP	Common Midpoint
BSU	Boise State University
GPS	Global Positioning System
Hz	Hertz
J	Joules (unit of energy)
ka	“kiloannum” (thousand years ago)
km	Kilometers
m	Meters
M9.2	magnitude 9.2
m/ky	meters per kiloyear (meters per 1000 years)
m/s	meters per second (velocity measurement)
Ma	“megaannum” (million years ago)
mGal	milligal (1 Gal= 1 cm per second squared) Unit of Gravity
min	minutes

mm	millimeters
mm/yr	millimeters per year
N32˚W	North 32 degrees west (example)
NMO	Normal Moveout
NOAA	National Oceanic and Atmospheric Administration
PWS	Prince William Sound
RPM	Revolutions per minute
s	seconds
sec	seconds
TACT	Trans-Alaska Crustal Transect
US	United States
USGS	United States Geological Survey
UTM	Universal Transverse Mercator (meters)
UW	University of Washington

CHAPTER ONE

Introduction

Subduction zones at oceanic/continental plate boundaries are responsible for a significant percentage of the worldwide seismic energy release (Kanamori, 1977). In recent years, the 2004 Sumatra and 2011 Japan subduction zone earthquakes incurred more than 286,000 and 20,000 casualties respectively with damage estimates in the billions of US dollars (USGS, 2012). Alaska experienced the second largest historic earthquake, M9.2, in 1964 that devastated local communities. The earthquake and related tsunamis caused 115 fatalities and more than $300 million in damages to local infrastructure (Haas, 1973). After a local tsunami and regional subsidence, residents of Valdez rebuilt the town 10 km to the northwest; an area more protected from future earthquakes and tsunamis. Tsunamis from the earthquake damaged coastline infrastructure of the U.S as far south as northern California. The causes of these tsunamis were landslides and offset of megathrust splay faults both offshore and near Montague Island (Plafker, 1969). My objective is to identify active faults and characterize Holocene deformation in Prince William Sound (PWS), Alaska. Furthermore, I discuss the seismic hazards of PWS based on my observations.

I collected approximately 300 km of high-resolution marine seismic reflection data to identify and characterize active faults in PWS. I process and interpret the seismic profiles to map the geologic stratigraphy and identify stratigraphic offsets that define

either active or inactive faults. I combine these interpretations with surface geologic information and new bathymetric surveys to interpret active fault geometries and lengths used to build probabilistic hazard maps. I integrate my fault interpretations with legacy crustal reflection seismic data and relocated earthquake location maps to create transects of active fault geometries to mid-crustal depths. For an expanded description of the Holocene deformation history of PWS, I combine these interpretations with other geophysical datasets, including aeromagnetic surveys, regional Global Positioning System (GPS) surveys, water bottom sediment cores, and thermochronology.

Geologic Framework

Tectonic Setting-Southern Alaska

Interaction between North American plate, Pacific plate, and Yakutat terrane result in tectonic deformation of southern Alaska and a unique surface geomorphic expression. Southern Alaska is a subset of the Northern Cordillera of the North American plate (Figure 1; Figure 2). Geomorphic features include mountain ranges and islands along the southern Alaska margin, including a 3,000 km coastline with nearly 2,000 km of plate convergence. Since Jurassic age, southern Alaska has been an active margin, with the modern trench approximately 150 km south of the Alaskan coastline (Plafker and Berg, 1994). Inland from the trench, the subduction related volcanic arc extends from the Wrangell Mountains to the Aleutian Islands (Plafker et al., 1994). Slip along active faults produce large earthquakes (greater than M8) along the Alaskan subduction zone, including three of the fifteen largest worldwide historic earthquakes recorded (USGS, 2012).

Southern Alaska is an amalgamation of accreted blocks including the Prince William terrane. Accretion of the Yakutat terrane to the North American plate is presently south of the Saint Elias Mountains (Figure 1). The Pacific plate subducts beneath the North America plate and portions of the Yakutat terrane along the southern margin of Alaska (Figure 1) (Fuis et al., 2008; Plafker et al., 1994).

Since Cretaceous time, convergence and accretion of terranes uplifted the Chugach and St. Elias Mountain ranges (Nokleberg et al., 1994; Plafker et al. 1994). Southern Alaska averages an elevation of 2 km for high relief coastal mountains (Figure 3) (Plafker et al., 1994). Regional faults and lineations are common along the mountainous coastal islands south of the Chugach mountain ranges (Nokleberg et al., 1994; Condon and Cass, 1958). Glacial processes along the coastal mountains also contribute to the high relief terrain.

Alpine glaciers partially cover mountains and migrate towards sheltered inlets and bays along the Alaska coast line. The numerous glaciations of southern Alaska are associated with proximity to moisture sources within the northern Pacific Ocean coupled with mountainous relief along the Alaska Range (Hamilton, 1994; Clark et al., 2006; Plafker and Berg, 1994). Glaciers initiated in southern Alaska in the Miocene (Berger et al., 2008). During the Pleistocene age, the Cordilleran ice sheet formed as a union of numerous glaciers and extended to the continental shelf. The latest glacial retreat began 12-15 kya before present and the majority of inlets and fjords were ice-free by 10 kya (Hamilton, 1994). Glacial retreat and related erosion in mountain ranges continues to provide a significant sediment source in areas such as the Copper River delta and locally within PWS (Klein, 1983; Jaeger et al., 1998).

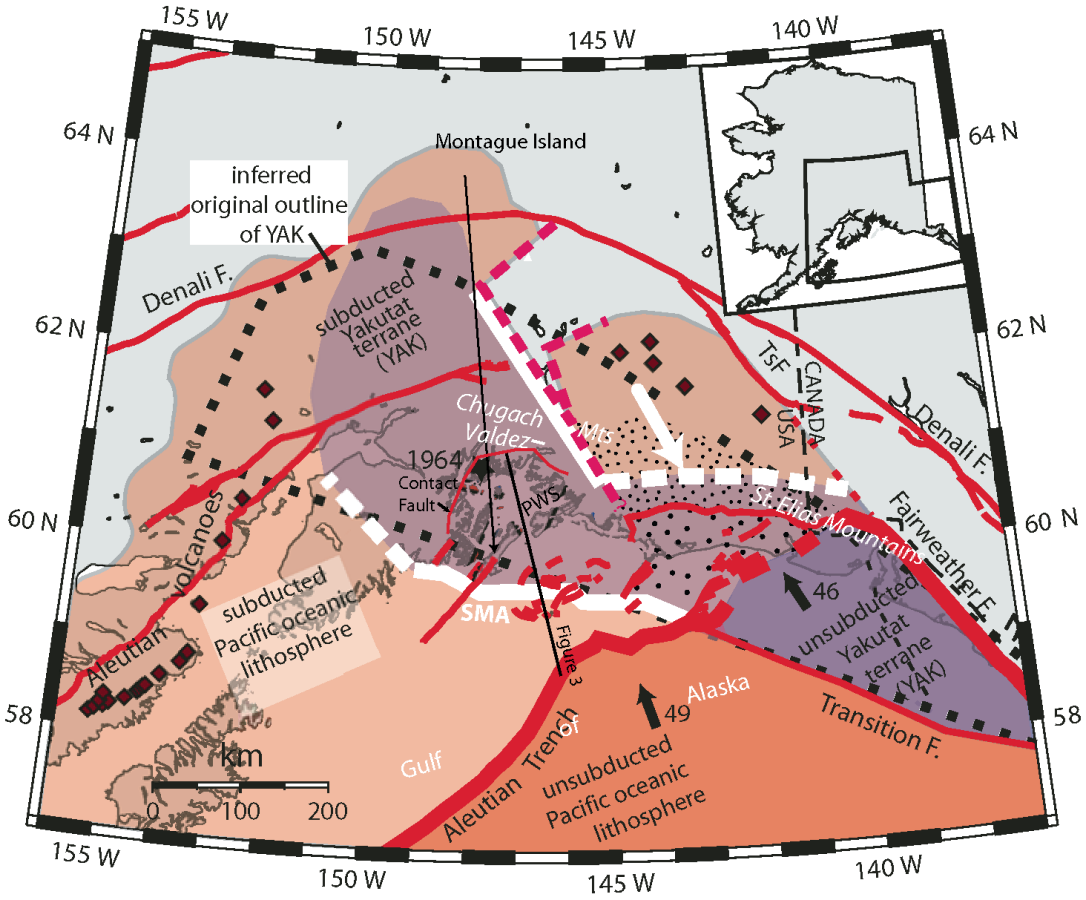

Figure 1: Southern Alaska tectonic map (modified from Fuis et al., 2008) illustrating structural interaction of northward subducting plates (Yakutat terrane and Pacific plates) and North American plate. Interpreted fault locations are shown in bold red lines. Pacific plate subduction direction and rate is different from Yakutat terrane by approximately 5 degrees and 4 mm/yr respectively. SMA=slope magnetic anomaly that defines the western margin of the subducted Yakutat terrane.

North American Plate

The southern Alaska block, subset of North America plate, internally deforms and rotates counter-clockwise relative to North American plate with a pole of rotation south of Montague Island (Figure 2) (Freymueller et al., 2008). GPS data throughout southern

Alaska document block rotation and internal deformation (Lahr and Plafker, 1980; Freymueller et al., 2008; Elliott et al., 2010).

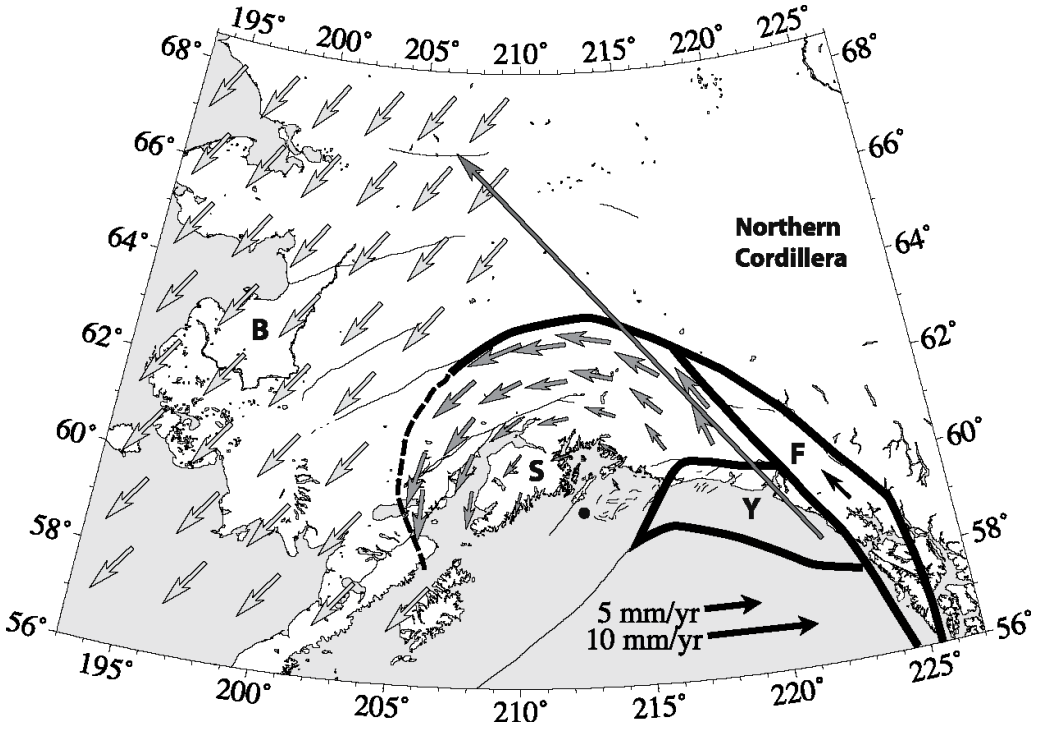

Figure 2: Map of southern Alaska showing southern Alaska block (S), Yakutat block (Y), Fairweather block (F), Bering block (B), and Pacific plate (P). The Transition fault separates (F) and (Y). Southern Alaska block rotates counter-clockwise around a pole located south of PWS (figure modified from Freymueller et al. 2008).

The 1,350 km long Trans-Alaska Crustal Transect (TACT) reflection and refraction profiles collected between 1983 and 1990 record the crustal structure of southern Alaska (Figure 3) (e.g., Fisher et al., 1989; Brocher et al., 1994; Fuis et al., 2008). Along the continental margin, Fuis et al. [2008] interpret significant crustal deformation including underplating of primitive oceanic-arc basalts, continental suturing and plutonism. Underplating in southern Alaska generates regional deformation as far as

northern Alaska. Furthermore, within southern Alaska, unusually thick island arc terranes are present (Gulick et al., 2007).

Yakutat Terrane

The Yakutat terrane is accreting to the North American plate south of the intersection between the St. Elias Range and Chugach Range (Figure 1). The Yakutat terrane motion is N32°W at nearly 40 mm/yr (Figure 2) (Freymueller et al., 2008). The western extent of the subducted Yakutat terrane lies beneath western PWS (Griscom and Sauer, 1990; Brocher et al., 1994). Total field anomalies from aeromagnetic data show a linear feature along the proposed edge of the Yakatut terrane, a feature termed the slope magnetic anomaly (Figure 1) (Griscom and Sauer, 1990; Brocher et al., 1994; Fuis et al., 2008). Freymueller et al. [2008] suggested locked subduction and accretion between the Yakutat terrane and North American plate deforms the Yakutat terrane.

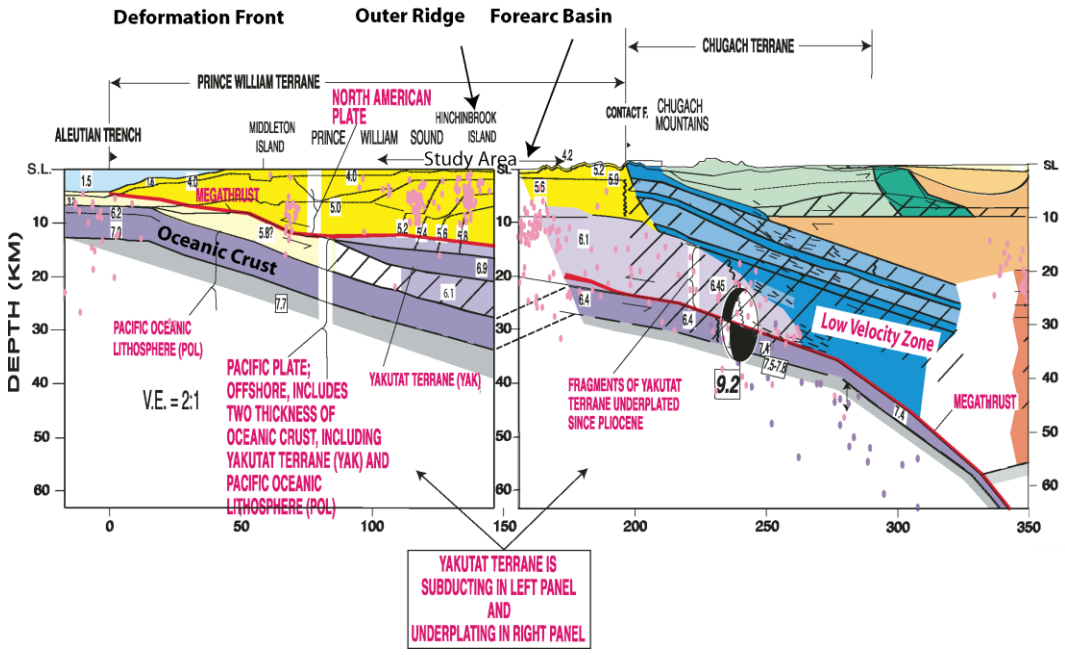

Figure 3: Anatomy of the PWS subduction zone in profile from TACT dataset (revised from Fuis et al., 2008). Yellow color represents the Prince William terrane, purple represents oceanic crust.

TACT data and geologic mapping provide interpretations of the Yakutat terrane accretion (Brocher et al., 1994; Fuis et al., 2008; Wilson and Hults, 2008). The Yakutat terrane is predominantly composed of a thick, oceanic plateau with flysch and mélange sequences (Bruns, 1983; Plafker et al., 1994; Gulick et al. 2007). The Yakutat terrane subducts beneath the North American plate at less than 10˚ (Brocher et al., 1994; Eberhart and Phillip, 2006). Fuis et al. [2008] suggested crustal thickening and plate tearing changed the subduction magnitude and direction of the Yakutat terrane around 35 Ma. The Transition fault, a strike slip fault between the southern Yakutat terrane and the Pacific plate is a non-subduction contact between the Yakutat terrane and Pacific plate (Figure 1). The strike-slip boundary explains the lack of subduction of the Yakutat terrane beneath North America except within PWS (Bruns, 1983).

The Yakutat terrane is locked to the overriding North American plate near the Copper River region east of PWS (e.g., Freymueller et al., 2008); the arc is spatially near the trench in this region. Moving westward, the already subducted and locked Yakutat terrane underthrusts the North American plate in the PWS region. The lack of volcanic arc materials and a more exposed outer arc high may result from buoyant Yakutat terrane rocks.

Pacific Plate

Freymueller et al. [2008] suggested the Pacific plate subducts beneath the North American plate at a rate between 44 and 70 mm/yr along the Alaskan subduction zone with a motion of N12°W relative to the North American plate (Figure 2). Fuis et al. [2008] interpreted the Pacific plate as subducting beneath the accreting Yakutat terrane in the region of PWS (Figure 2). Freymueller et al. [2008] interpreted the Pacific plate as actively deforming the North American margin west of PWS and west of the Yakutat terrane margin (Figure 2). Furthermore, subduction angle determined by passive and active seismic data is known to be shallower in PWS than to the west of PWS near Kodiak Island (e.g., Brocher et al., 1994; Eberhart-Phillips et al., 2006; Doser et al., 2008).

Prince William Terrane

Subduction Zone Geology/Anatomy

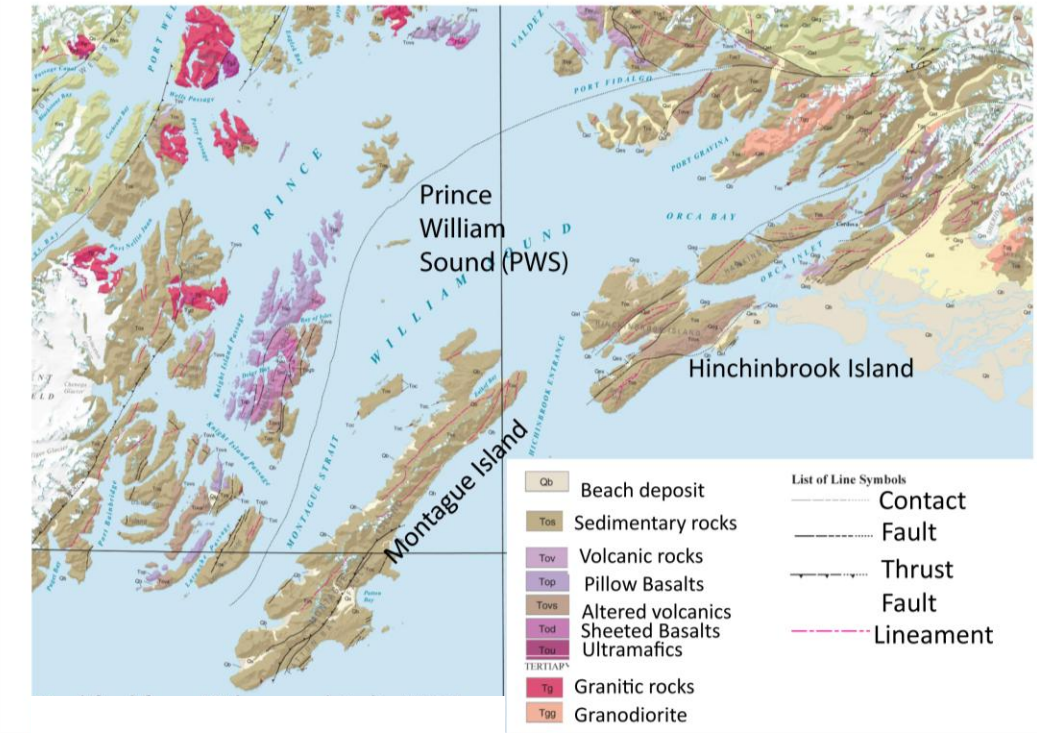

Figure 4: Geologic and structure map of Prince William Sound, Alaska (modified from Wilson and Hults, 2008).

The Prince William terrane is located in the PWS region of Alaska north of the boundary of the subducting Pacific plate (Figure 3). The Prince William terrane accreted to the North American plate during the Cretaceous (Plafker et al., 1994).

The dominant stratigraphic units within PWS include Holocene marine and glacial deposits; Quaternary Yakataga formation, Tertiary Orca group rocks, and Valdez group rocks (Figure 4). The Holocene stratigraphy can be subdivided into end moraine

deposits, marine sediments, glacial wash deposits, and beach deposits (Molnia, 1977). An erosional unconformity exists at the boundary of the Holocene and Orca group sedimentary and reflects a time hiatus between Yakataga deposition and onset of the latest glacial retreat (Carlson and Molnia, 1978). The Yakataga formation is exposed predominantly offshore and composed of Quaternary glacial marine sediments (Molnia, 1977). Orca group rocks are characterized by Middle Eocene to upper Paleocene flysch (composed of greywacke and argillite) or other Tertiary continental clastics (conglomerates) and/or basalts (pillow basalts, tuffs, and dikes) (Silberling et al., 1994). A Cretaceous-Tertiary flysch Valdez group rock underlies the Orca Group strata. Knight Island and portions of Hinchinbrook Island are composed of lower Tertiary mafic volcanic (Figure 4). Other localized land units include Oligocene to Eocene granitic plutonic rocks (Plafker et al., 1994). Orca group rocks exposed on land are highly deformed due to millions of years of accretion and exhumation (Winkler and Plafker, 1981).

Barnes and Morin [1990] interpreted gravity data throughout PWS with a multilayered subduction zone model with decreasing Bouguer gravity values to the north and west. Gravity highs, greater than 10 mGal, result from dense igneous intrusions. A modeled 2 km thick igneous intrusion correlates with 55 mGal gravity high on Knight Island (Figure 4) (Barnes and Morin, 1990). Low gravity values in central PWS suggest loosely consolidated, low-density marine sediments dominate the upper crust. The central gravity low continues eastward towards Cordova and results from increasing thicknesses of granitic plutons or flysch deposits (Barnes and Morin, 1990).

Based on seismic results, Fuis et al. [2008] summarized the structural geometry of the Prince William terrane (Figure 3). A changing refractor velocity on TACT seismic profiles suggest subducted Yakutat terrane may result in crustal doubling in the offshore region and underplating in the onshore region. Brocher et al. [1994] forward modeled the 1,100 km of TACT offshore wide-angle seismic reflection/refraction data to develop a seismic velocity and tectonic model. Brocher et al. [1994] interpreted a multilayered subduction system with the subducted Yakutat terrane underthrusting the North American plate. In addition, they modeled a high velocity refractor associated with the megathrust decollement that activated during the 1964 Great Alaska Earthquake.

PWS Active Faults

During the 1964 earthquake, the Hanning Bay and Patton Bay faults on Montague Island accommodated south directed coseismic slip from the seismic release (Plafker, 1969) (Figure 4). Terraces in Hanning Bay and Patton Bay show uplifted coastlines and offsets of Orca group rocks (Figure 4). The Rude River and Etches faults offset Tertiary rocks on Hinchinbrook Island are two along strike lineations to the northeast of Montague Island with questionable offset from the 1964 earthquake. Although Hanning Bay and Patton Bay faults on Montague Island cannot be traced beyond central Montague Island, Patton Bay fault may continue offshore toward Hinchinbrook Island (Plafker, 1969). The Rude River fault, Etches fault, and Patton Bay fault all strike between N20˚E and N50˚E (Winkler and Plafker, 1981; Plafker et al., 1993; Condon and Cass, 1958; Condon, 1966). Hanning Bay and Patton Bay experienced regional uplift by as much as

twelve meters whereas regional uplift near the Rude River and Etches faults was approximately two meters (Plafker et al., 1993).

The seismic hazard in PWS is high even after the stress drop from the 1964 earthquake. Bufe [2004] hypothesized that stress transfers among faults after large earthquakes based on stress transfer during the Alaskan earthquake swarm between 1938 and 1964. Lahr and Plafker [1980] suggested the possibility of reactivation of the eastern portion of 1964 rupture zone that could uplift Middleton Island as much as 4 m. Estimated stress states from mapped seismicity, less than M7.5, show a risk along the Denali fault and the 1964 thrust zone (Bufe, 2004; Doser and Brown, 2001; Freymueller et al., 2008; Ruppert et al. 2008).

Using the vertical component of GPS data, Freymueller et al. [2008] suggested central PWS is currently subsiding while inland regions are uplifting from post-seismic reloading of a locked subduction zone after the 1964 Great Alaska Earthquake (Figure 5). The current Prince William terrane horizontal motion is N30°W at 5 mm/yr relative to the North American plate (Plafker and Berg, 1994).

Geomorphic Expression/Setting

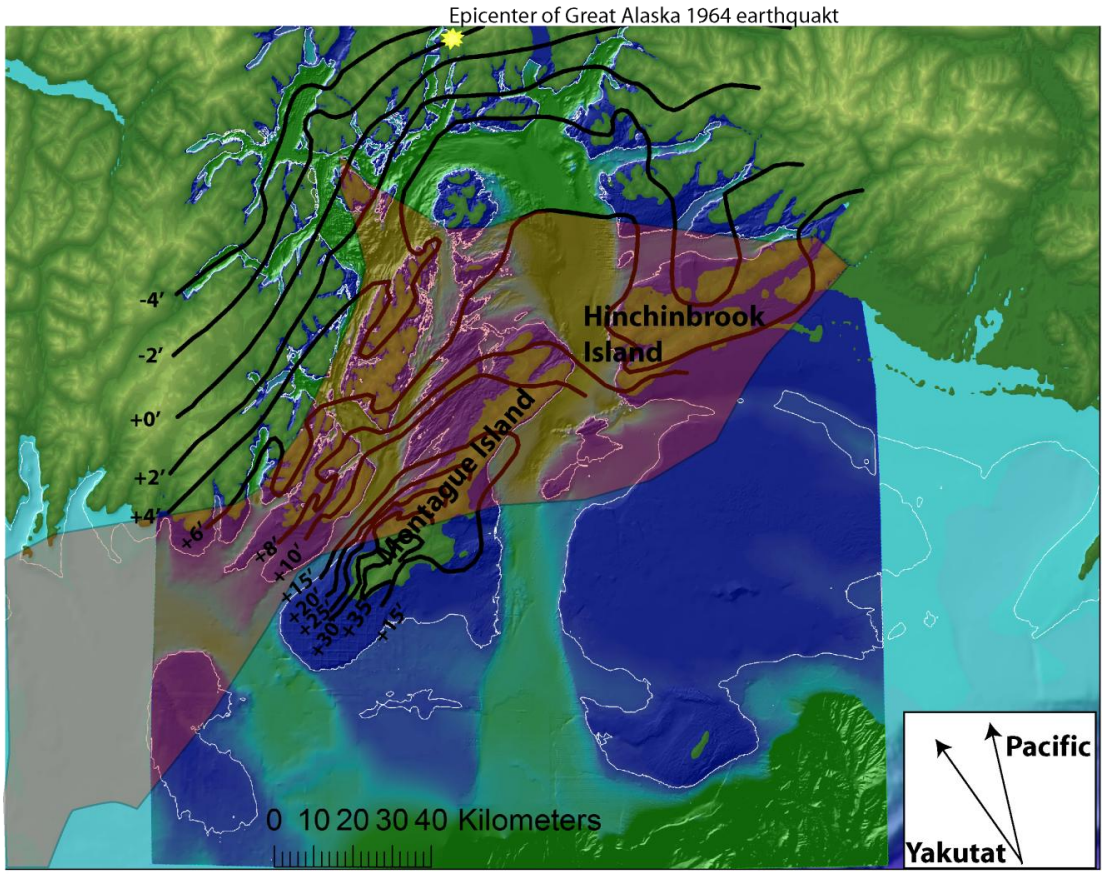

Figure 5: PWS study area with contours that show regional vertical uplift (in feet) related to the 1964 earthquake . The figure also shows motion of Pacific and Yakutat terranes relative to North American plate and epicenter of the 1964 earthquake. Montague Island had the greatest uplift from the 1964 earthquake (Plafker, 1969). The Contact fault is closely approximated by the zero uplift contour. Zone of red shows area of maximum subsidence from 1964-2008 (Freymueller et al., 2008)

An archipelago of mountainous barrier islands (Montague and Hinchinbrook Islands) is located along the south and southwest boundary of PWS, nearly 100 km north of the subduction trench (Figure 1; Figure 4). Carver and Plafker [2008] theorized that interseismic periods of subsidence are followed by greater amounts of uplift during megathrust earthquakes that created the barrier islands. While alternating exhumation and subsidence is possible, the lack of sedimentation throughout PWS suggests that this

pattern is not likely (Klein, 1983; Carver and Plafker 2008; Freymueller et al., 2008). Uplift of the barrier islands during the seismic events outpaces the inter-seismic period subsidence. Exhumation of the region both onshore and offshore occurs along these barrier islands. (Figure 5) (Plafker, 1969; Carver and Plafker, 2008)

Modern Sedimentation

During the Holocene, the maximum sedimentation rates have occurred within the central area of PWS (Figure 6) (Klein, 1983; Jaegar et al., 1998). Presently, a portion of the Gulf of Alaska current enters PWS at Hinchinbrook Entrance and exits at the southern outlet of Montague Strait (e.g., Jaegar et al., 1998), depositing predominantly distal sediments from the Copper River. Additional sediment sources derived from local rivers, drainages, and glacial headwalls appear throughout PWS. These sources mostly deposit meters of sediments in the deep glacially scoured channels.

Glacial History - Holocene Strata

From sparker and airgun surveys in the Gulf of Alaska and PWS, von Huene et al. [1967] characterized seismic facies. The shallowest unit is identified as Holocene age sediments that is composed dominantly of glacial and fluvial sands carried by the Gulf of Alaska Current entering PWS through Hinchinbrook Entrance (Molnia, 1977; Hamilton, 1994; Jaegar et al., 1998). An unconformity between Holocene and older Quaternary or Tertiary strata resulted from the low stand of sea level and subareal exposure to 110 m depth during the last ice age (Hamilton, 1994). Glacial retreat initiated about 15-13 kya and was complete for the majority of PWS around 10 kya (Hamilton, 1994).

Von Huene et al. [1967] described the Holocene seismic unit as only slightly faulted and folded with little evidence of Holocene age deformation. Von Huene et al. [1967] also suggested deformation in PWS during the last 10,000 years is predominantly tilting or arching.

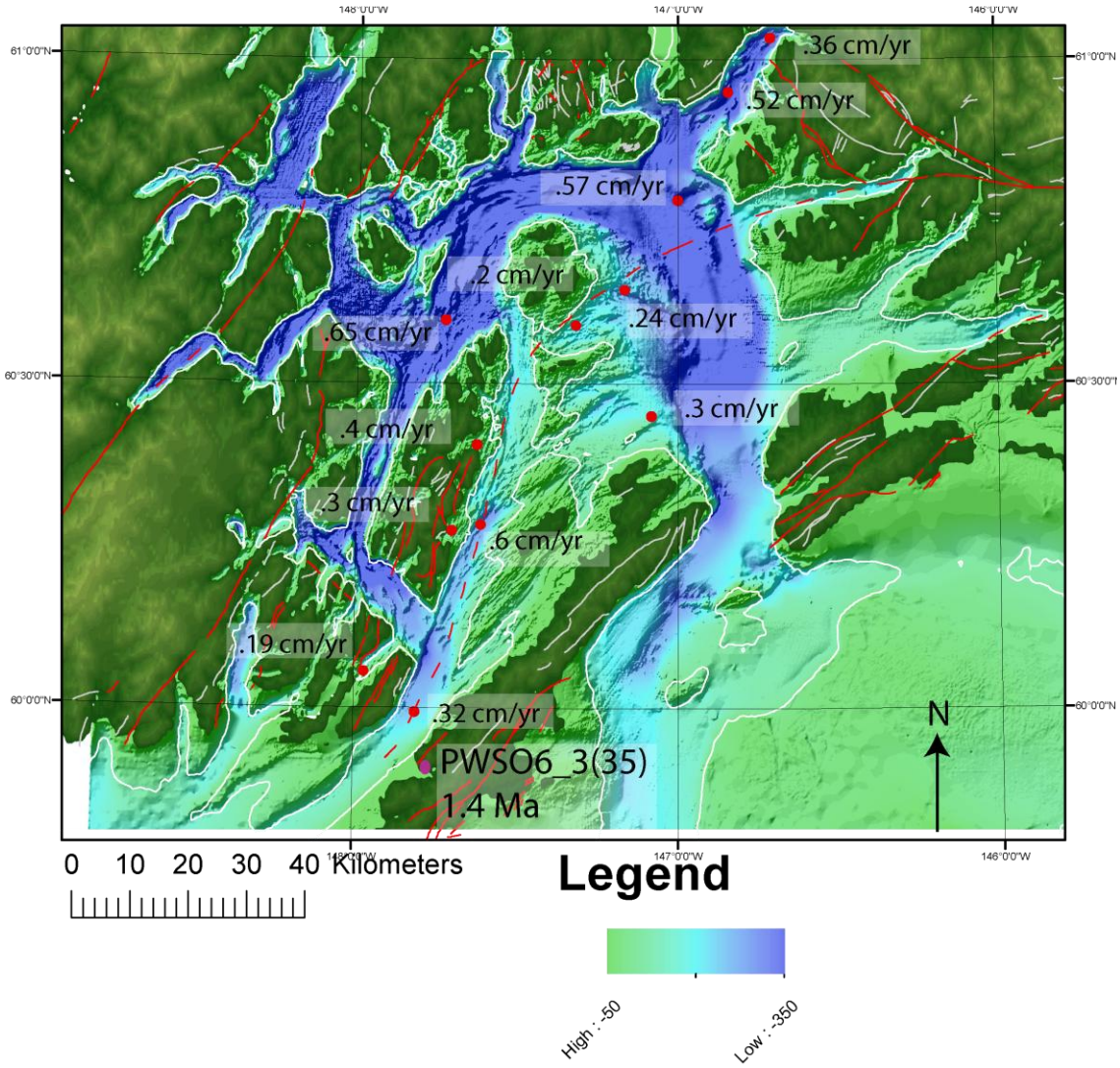

Figure 6: Bathymetric map of central PWS with sedimentation rates added from USGS measurements (Page et al., 1995) and Klein [1983] (red dots). High deposition rates are located near Valdez and along western PWS toward Montague Strait.

Historic Seismicity

1964 Great Alaska Earthquake

The Mw 9.2 Great Alaska Earthquake occurred on March 27, 1964. The earthquake occurred at a depth of 25 km at the boundary between the North American plate and the Pacific plate (Stauder and Bollinger, 1966). The epicenter of the earthquake was located about 50 km west of Valdez, Alaska (Figure 2; Figure 3). Coseismic uplift occurred over an area nearly 2,600 km long and as much as 1,000 km wide, with maximum uplift of nearly 12 m (Figure 5) (Plafker, 1969). Aftershock events occurred over an area of 250,000 km^2. The duration of surface waves was from 1.5 to 7 min, with a mode of 3.5 min. The event was felt throughout most of Alaska (Cloud and Scott, 1972). Tsunamis generated by the earthquake affected regions as far as northern California. Ports in PWS were greatly impacted when local tsunamis as large as 50 m displaced ships and destroyed buildings (Plafker, 1969; Haas, 1973).

Relocated pre-1964 historic earthquakes are concentrated near mapped splay faults associated with the 1964 earthquake (Figure 4; Figure 7) (Doser and Brown, 2001; Fuis et al., 2008). Within PWS, there are records of at least three historic earthquakes within the vicinity of the 1964 rupture zone. Earthquakes M_w>4.5 have been far less common since 1964 within the region. Ratchkovski and Hansen [2002] provided evidence of the segmented subduction on the Alaskan-Aleutian trench using 14,099 relocated earthquakes. Their results suggested a seismic break along western PWS related to the edge of the subducted Yakutat terrane.

Doser et al. [2008] characterized upper and lower plate seismicity as related to the structure of the subduction zone. They determined that earthquakes in the upper 14 km

are predominantly related to thrust faulting while earthquakes grouped at a depth of 15-25 km are related to the interface between the Yakutat block and North American plate. Earthquakes clusters appear near an interpreted stress build up near Valdez and Columbia Bay while earthquakes grouped between 25 and 35 km depth beneath Valdez and Columbia Bay are likely related to faulting within the Pacific plate. Due to accretion of the Yakutat terrane and continued subduction of the Pacific plate earthquakes tend to be concentrated in the upper (0-14 km) or lower (25-35 km) depths. Doser et al. [2004] suggested deformation and seismic moment release were lower following the 1964 Great Alaska earthquake. Furthermore, a M7 earthquake is probable in the region every 40 to 50 years (Doser et al., 2004), but no large earthquake has been experienced since 1964.

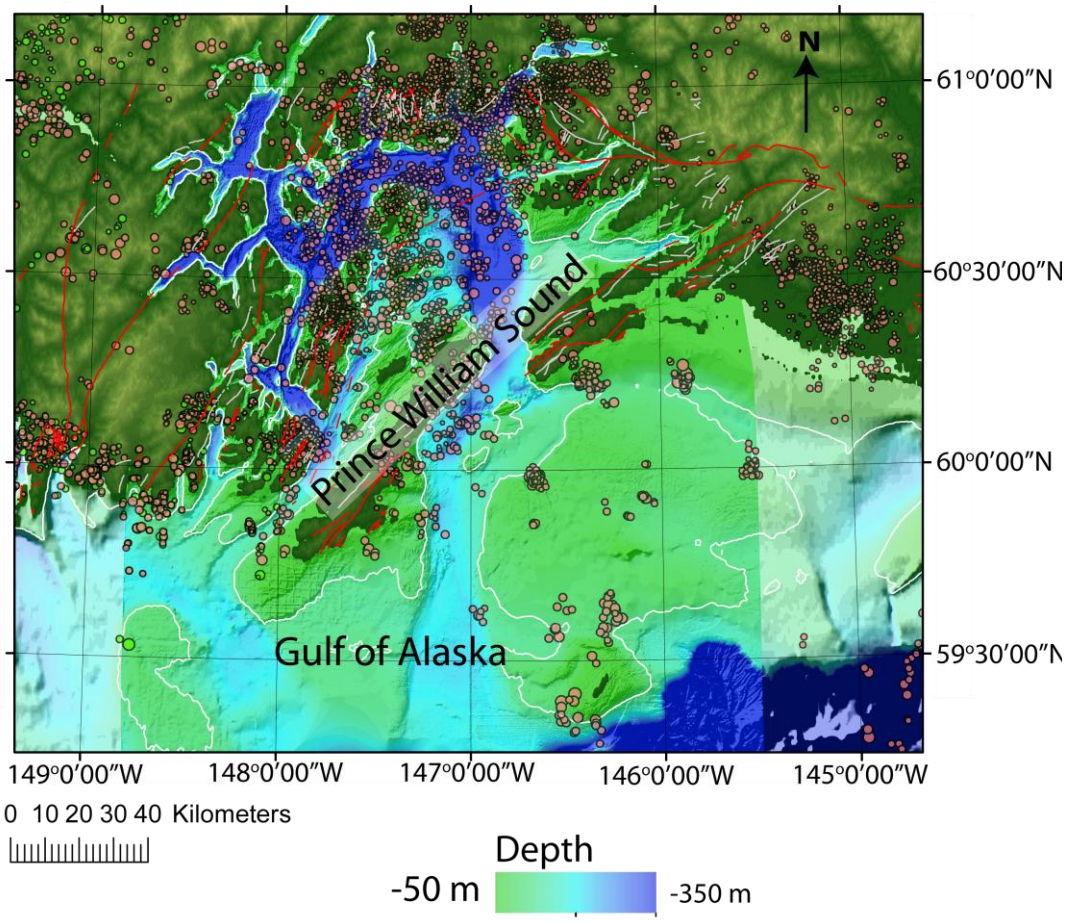

Figure 7: Map of PWS overlaid with relocated earthquakes from 1971-2001 (modified from Doser et al., 2008), faults are shown in red (modified from Wilson and Hults, 2008) . Shallow earthquakes, less than 20km depth, are shown in pink. Deeper earthquakes, greater than 20km, are shown in green. Locations of towns around PWS are shown and labeled.

Paleoseismicity

The 1964 earthquake was not a unique event; similar magnitude earthquakes have a recurrence interval of 650-900 years for PWS (Carver and Plafker, 2008). Large subduction zone related earthquakes such as the 1964 event are interpreted to have occurred within this region as evidenced by widespread faulting with significant vertical slip, paleo-tsunami deposits, and exposed modern or fossilized biota (Plafker, 1969; Carver and Plafker, 2008). Carver and Plafker [2008] developed a timeline of seismic events using paleoseismic studies of PWS, Kenai Peninsula, and Kodiak Island, with the most complete record of seismic events for PWS near the Copper River. Within the last 5,500 years as many as 10 earthquakes of similar or larger size are thought to have occurred within PWS as recorded by terrace and flooded marsh deposits (Carver and Plafker, 2008; Shennan et al., 2008). Sediments from the Valdez Arm record reoccurring "varve-like" turbidites sequences recording the past tsunami events generated by large earthquakes and show a consistent recurrence pattern (Ryan et al., 2010).

CHAPTER TWO

SEISMIC DATA ACQUISITION

Overview

A Boise State University and US Geological Survey science team acquired more than 300 km of high resolution marine seismic data between August 23, 2009-August 31, 2009 on the 15 m long USGS Research Vessel Alaskan Gyre. We averaged 36 km of active acquisition per twelve-hour day. Transit time was minimized as our crew of four plus captain remained on the boat for the eight days of acquisition. Using bathymetry and structure maps, we narrowed our survey to four areas to determine whether water bottom lineaments are related to active faulting. These areas include Hinchinbrook Entrance, Orca Bay, Gravina Bay, and Montague Strait. Utilizing the small vessel, we mapped faults to within a few meters of land to tie surface outcrop exposures subbottom stratigraphy (Condon and Cass, 1958; von Huene et al., 1975; Carlson et al., 1985; Fuis et al., 2008).

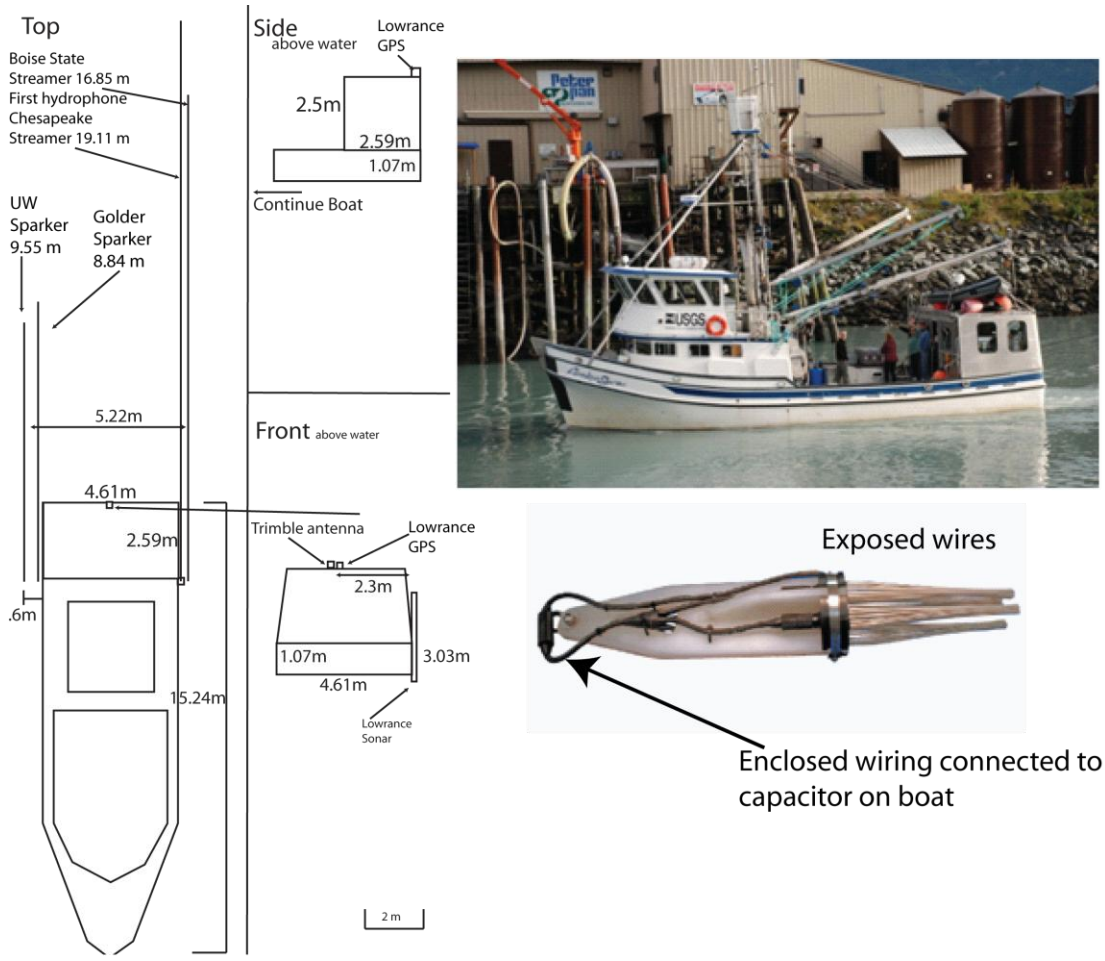

Figure 8: Left: Schematic of the RV Alaskan Gyre with positions for field equipment. Upper Right: 15m USGS Alaskan Gyre research seismic acquisition vessel. Lower right image of a sparker source (Alliance Coastal Technologies, 2011) (not same as used during this acquisition, though same principle). Exposed wires are electrified while the sparker is in the water. Similar to a spark plug of a car, the sparker arcs electricity and generates acoustic energy.

Seismic Data

Seismic source equipment for data acquisition included a primary and backup sparker source power supply pulsing at 200 or 300 joules. A sparker source provides seismic signal by discharging a short burst of electricity. The sparker source provides meter-scale resolution to depths that match the complete Holocene sedimentary record in PWS (von Huene et al., 1967). A seismic source comparison between a sparker source and other common marine seismic sources is shown in Figure 8. We rented the sparker

systems from the University Washington (UW) and Golder Associates. The Golder Sparker system included a CSP 1500™ Seismic Energy Source from Applied Acoustic Engineering (Applied Acoustic, 2012). The UW sparker was towed 9.55 meters behind the boat stern and the Golder sparker was towed 8.84 meters behind the boat's stern (Figure 8). The sparker power supply and recording equipment were placed port and starboard sides of the boat respectively to avoid electrical interference.

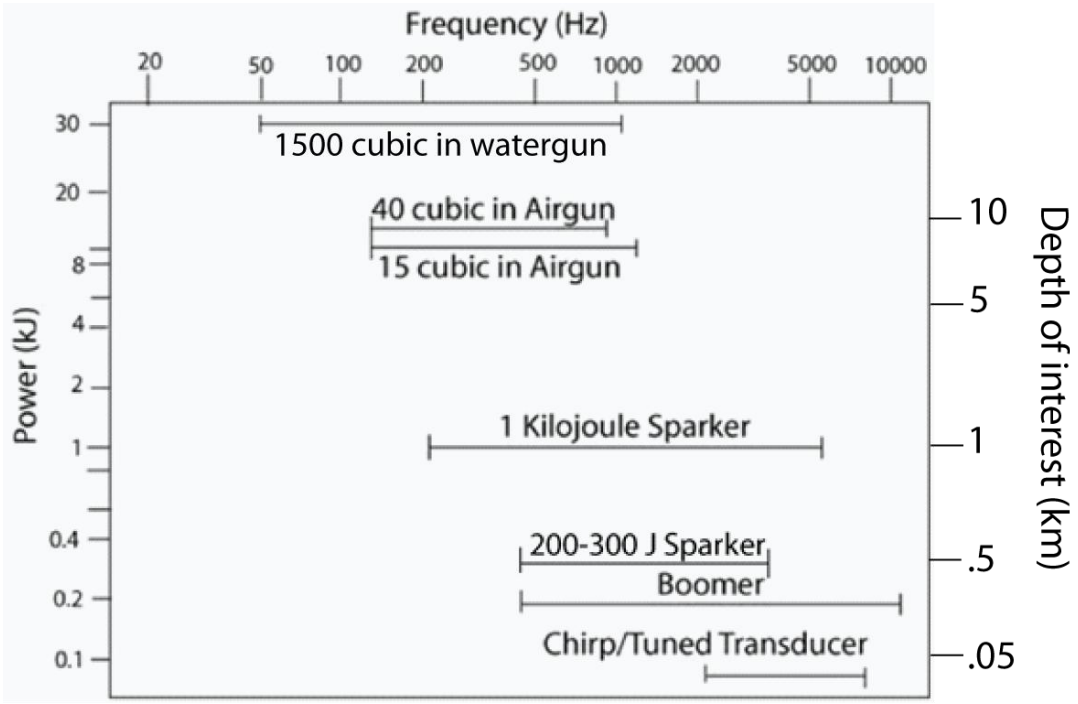

Figure 9: A comparison of the power and frequency of several marine seismic acquisition sources. Lower frequency sources generally produce higher power with higher frequency sources generally produce lower power and less signal penetration. Generally power and frequency change signal penetration or observable depth for reflection data. (modified from Trabant, 1984).

A Geometrics ™ Stratavisor seismograph recorded the seismic response from the sparker source. We recorded nominally for 0.85 sec each second with a sampling rate of 0.25 ms to record signals up to 1,500 Hz (Figure 9). The data were recorded in SEG2 format and converted to SEGY format after acquisition was complete (Barry et al., 1975;

Pullan, 1990). We deployed an Innovative Transducers™ solid state, 12-channel single element hydrophone streamer, with 3 meter spacing between receivers. The solid state hydrophones have improved signal to noise compared to single channel oil-filled streamers (Hoogeveen et al., 2005). We positioned the first hydrophone 16.59 meters from boat's stern (Figure 8). The single channel multi-element fluid filled streamer from Golder Associates was towed 19.11 meters behind the boat's stern. Audacity software ® was used to record the single channel streamer (Audacity, 2009).

We experienced acquisition problems including power fluctuations, shutdown related to the presence of marine mammals, sparker and recording equipment malfunctions, and weather limitations. On-board power failure resulted in a premature ending of the cruise on August 31. When backup inverter power was activated during acquisition, cyclic noise appeared on recorded data that was not completely removed during data processing. We shut down acquisition when marine mammals approached within 100 m of the boat or streamer to allow the animals to pass (National Marine Fisheries guidelines); these rare occurrences caused data gaps that were usually recovered by circling the boat. Sparker equipment issues plagued the first several days of acquisition. When a sparker triggered inconsistently or with low energy, we removed the unit from the water for repair. The sparker repairs shut down operations for 5-30 min and we would circle the boat to avoid data gaps. Computer issues during the first two days of our survey allowed only .5-.6 sec record lengths; this was later extended to .85 sec. To improve signal to noise ratio, we maintained a boat speed between 800-1,000 revolutions per minute. Finally, a half day was lost on August 28 due to inclement weather; however, this allowed time to repair the sparker systems.

Our seismic resolution was adequate to record meter-scale stratigraphy and structures. At water velocity of 1,480 m/s and a center frequency of 800 Hz, the resulting wavelength is 1.85 m. Using a quarter wavelength criteria (Widess, 1973), we can resolve features as small as 0.46 m. The horizontal resolution based on the Fresnel zone at 200 m water depth and 800 Hz is 20 m (Sheriff 104). Therefore, offsets similar to the Great Alaska 1964 earthquake, between 2 and 12 m, may be resolvable with our seismic data (Plafker, 1969).

Sonar Data

We acquired data from a sonar unit for depth comparison to seismic data and as a backup to our primary GPS. The sonar unit Lowrance™ LCX-26C HD housed a 50 kHz and 250 kHz transducer and was mounted on the port side near the hydrophone cable storage (Figure 8). The sonar unit measures temperature and bathymetric depth. The unit was lowered to a depth of about one meter below the water surface. Data collection started about 20 minutes earlier than seismic data acquisition to ensure adequate coverage for all hydrophones behind the boat position.

GPS Data

The Lowrance™ LCX-26C HD and a Trimble GPS system were mounted on the roof of the back central area of the lab (Figure 8). Both the Lowrance GPS and the Trimble GPS systems were used for geometry files applied to the seismic data. The Trimble system recorded positions every one second and the Lowrance system recorded every two seconds.

Orca Bay Acquisition

Importance

Several water bottom lineaments appear in Orca Bay (Figure 10) (NOAA, 2012). Plafker [1969] estimated between two and four meters of regional uplift within Orca Bay during the 1964 earthquake, however no faults with recent movement were identified on nearby islands or main land or previous marine seismic surveys (Condon and Cass, 1958; Plafker, 1969; Carlson and Molnia, 1978). We tested the hypothesis that lineaments on land and on the seafloor may be related to active faults that extend into Orca Bay (Condon and Cass, 1958). New reflection seismic lines help characterize the Holocene sediment deposition history and tectonic deformation. Again, Orca Bay is near economically important shipping channels for areas of Valdez and Cordova and faults are a potential risk for tsunamis or local ground shaking (Plafker, 1969; Arno and McKinney, 1973). I identified two lineations, L1 and L2, on National Oceanic and Atmospheric Administration, NOAA, bathymetric dataset. These lineations trend east and west through central Orca Bay and may point to a hazard if they are related to active faulting (Figure 10) (NOAA, 2012).

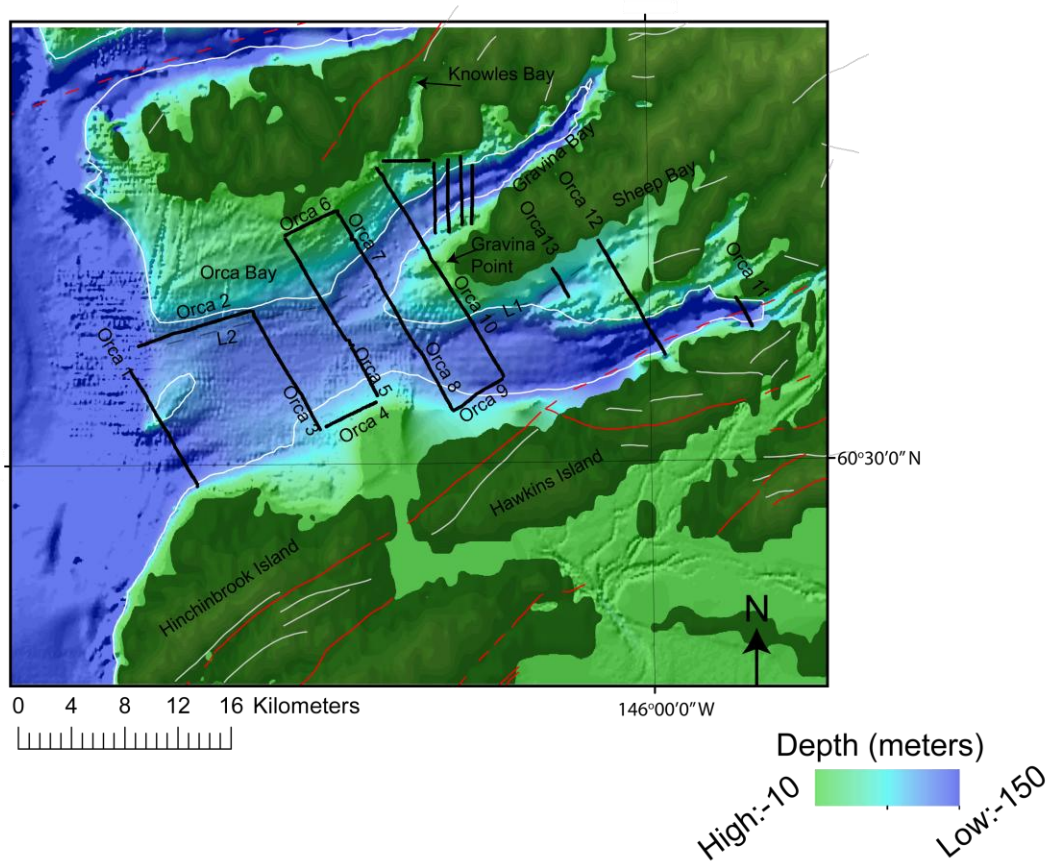

Figure 10: Bathymetric derivative map of Orca Bay with the 13 collected reflection seismic data (Orca 1 through Orca 13). Lineations are highlighted within figure by northeast lighting angle, lineations L1 and L2 continue >30 km through Orca Bay.

Procedure

Approximately 150 km of data were acquired in Orca Bay along 13 seismic profiles between August 23, 2009 and August 28, 2009 (Figure 10). Water depth ranged from 30-300 m with an average 100 m water depth. The sparker output was set at 200 J for the majority of the survey. A record length of 0.85 sec was used with sampling rate of 0.25 ms. A half a day acquisition loss on August 28 was due to poor weather. This downtime allowed us to repair sparker equipment to provide an improved acquisition data quality on Orca 11-13.

Gravina Bay Acquisition:

Importance

We identified a west-east lineament, L3, in Gravina Bay on a NOAA bathymetry that may be related to active faulting (Figure 11) (Andring, 2006). Similar to Orca Bay, several mapped faults do not extend offshore from adjacent land (Figure 11). Our objective was to determine whether identified lineations are related to active faulting and whether they connect to mapped faults or lineations on shorelines (Condon, 1966; Wilson and Hults, 2008).

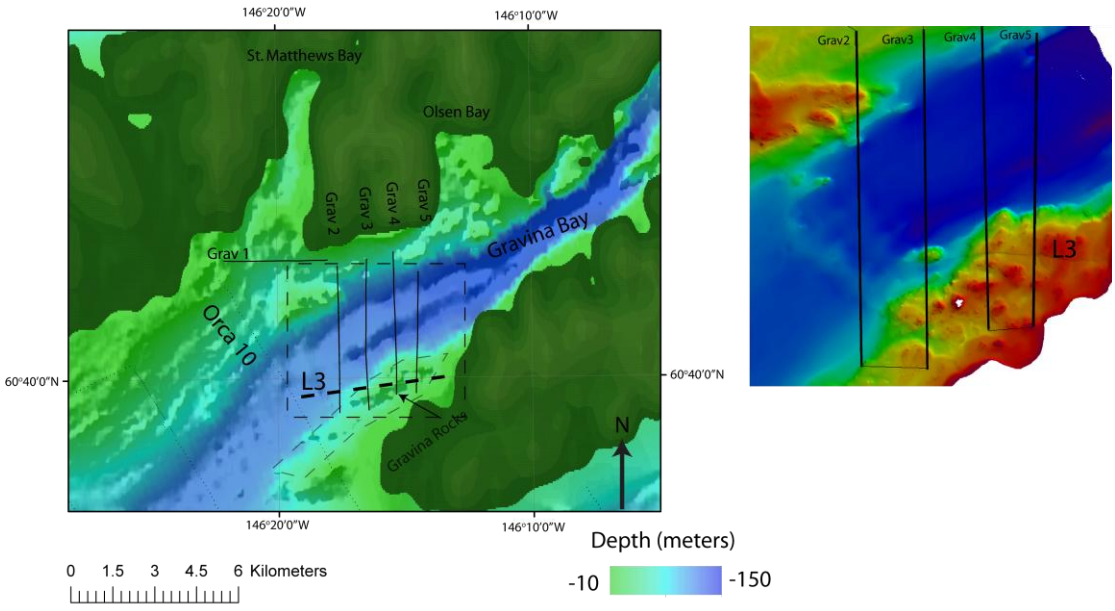

Figure 11: (left) Bathymetric derivative map of Gravina Bay with the five collected reflection seismic data (Grav1 through Grav5). Lineations are highlighted within figure by alighting angle from the northeast. (right) Enhanced view of lineation L3 that is intersected by seismic profiles Grav 3, 4 and 5.

Procedure

Approximately 30 km of data were acquired in Gravina Bay along five profiles on August 27, 2009 (Figure 11). Water depth ranged from 40-200 m with an average depth of 150 m. The power output from the sparker source maintained an output of 300 J.

Hinchinbrook Entrance Acquisition

Importance

A seismic survey in Hinchinbrook Entrance was conducted to test the hypothesis that splay faults that surface on Montague Island connect to similarly oriented faults mapped on Hinchinbrook Island (Wilson and Hults, 2008) (Figure 4; Figure 12). West of Hinchinbrook Entrance along southern Montague Island, along the Patton Bay fault there was approximately ten meters of regional uplift during the 1964 earthquake (Plafker, 1969). Patton Bay fault may extend beneath the southeast shore of Montague Island and extend across or steps over Hinchinbrook Entrance (Plafker, 1969; Nelson et al., 1985; Wilson and Hults, 2008). Seismic profiles along the southeastern shoreline of Montague Island may constrain the presence and position of the Patton Bay fault beneath Hinchinbrook Entrance. Several water bottom lineaments are interpreted to extend offshore from Hinchinbrook Island (Winkler and Plafker, 1981). For example, Seal Rock is the southwest extension of a linear bathymetric high that defines the southern boundary of Hinchinbrook Island (Figure 12). New seismic data between Hinchinbrook and Montague Island help to identify and characterize possible active faults. Finally, a

potential tsunami risk for shipping lanes through the Hinchinbrook Entrance may be present where nearby faults may rupture (Plafker, 1969).

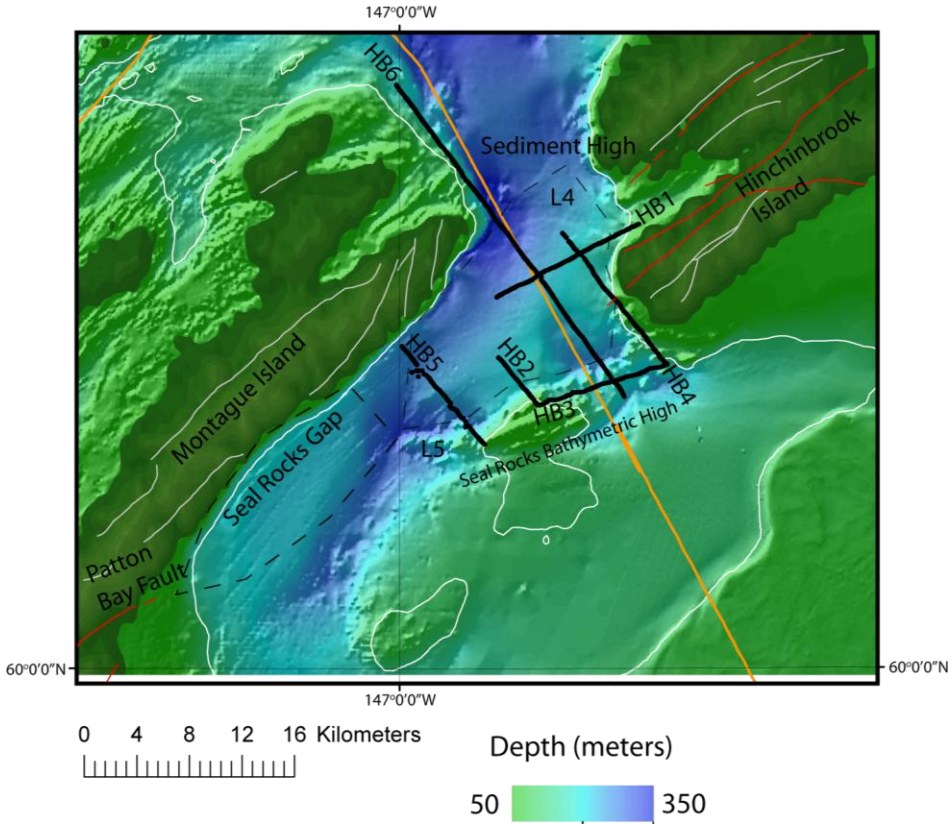

Figure 12: Bathymetric map of Hinchinbrook Entrance with the six reflection seismic profile locations (HB1 through HB6) and TACT profiles (bright orange), faults (dark red). Lineations are highlighted within figure by northeast lighting angle.

Procedure

We acquired approximately 100 km of seismic data near Hinchinbrook Entrance along six profiles between August 24, 2009 and August 25, 2009. Water depth for the survey ranged from 40-350 m with an average depth of 150 m. Inconsistency with sparker electrical output required running the system at a lower power output of 200 J.

Along these profiles, computer issues also required a record length of between .5 and .6 sec.

Montague Strait Acquisition

Importance

NOAA bathymetry provided targets for regionally continuous lineations in Montague Strait (Figure 13). Along west and central Montague Strait, a 50 m scarp, L6, was identified that may be tectonically significant (Deodato et al., 2000). Bathymetric lineation L6 is offset in an en echelon pattern from lineation L7 similar to the Patton Bay fault on Montague Island (Figure 13). Along the northern shore of Montague Island and along the southern boundary of Montague Strait, the Hanning Bay fault recorded nearly five meters of slip during the 1964 Great Alaska earthquake. We investigated whether splay faults were north of Montague Island and documented the Holocene uplift history of these faults.

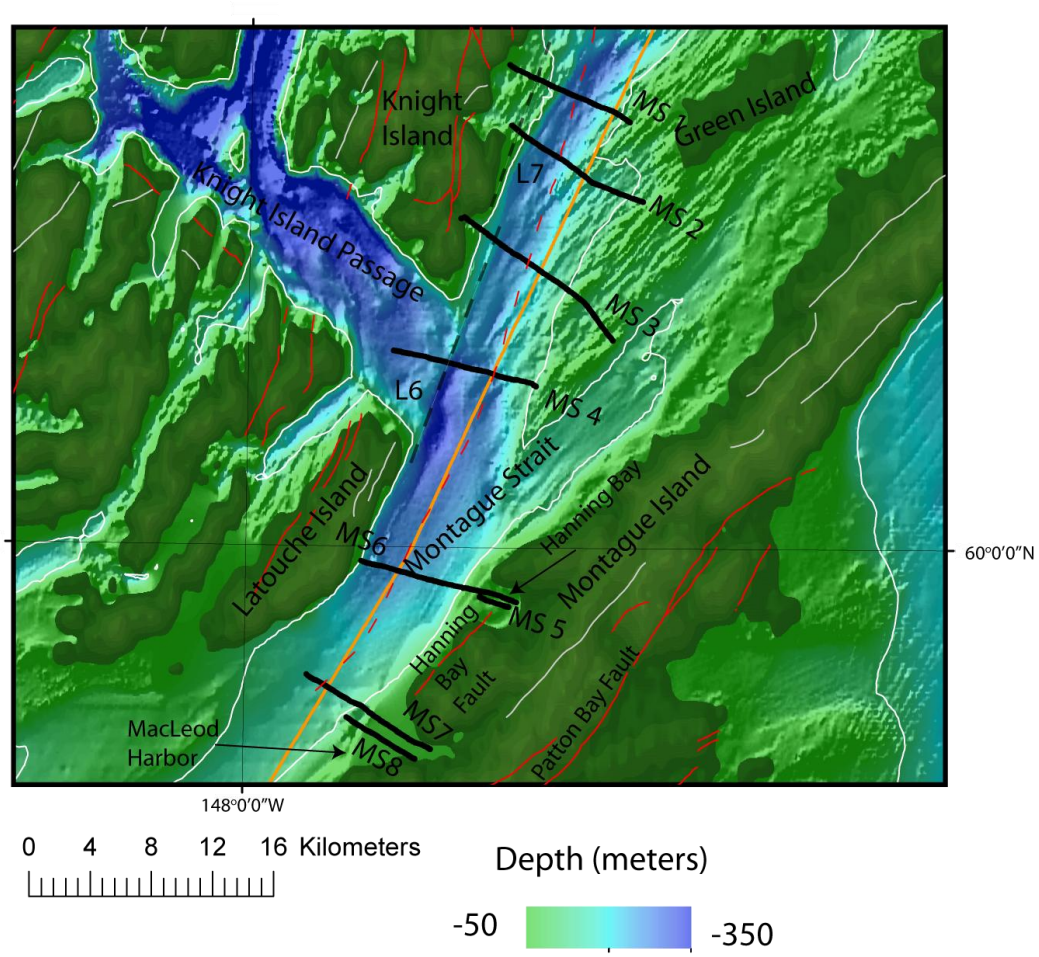

Figure 13: Bathymetric map of Montague Strait with the location of eight new reflection seismic profiles (black) (MS1 through MS8)(Red lines are mapped faults, orange line is TACT profile, dashed red line is interpreted fault, grey lines are regional lineations, white line is 110 m water depth contour). Lineations are highlighted within figure by northeast lighting angle.

Procedure

Approximately 70 km of seismic data were acquired in Montague Strait along eight profiles between August 29, 2009 and August 31, 2009 (Figure 13). Water depth ranged from 30-400 m with an average depth of 200 m. The sparker source was set at a power of 300 J for much of the survey, but some profiles were acquired at 200 J. Boat power issues occurred on August 30, which required switching from the boat generator to

inverter power, and added electrical noise to the seismic signal. Boat power failure on August 31 resulted in the termination of our survey.

CHAPTER THREE: DATA PROCESSING

Reflection Processing

Review of Reflection Processing

I processed the seismic data to produce an image for interpretation. I generated a pseudo-geologic cross-section called a stack by sorting shot gathers into common midpoint (CMP) gathers, applying proper velocity corrections and simple processing steps (Yilmaz, 2001). Shot gathers are time series of amplitude values at a variety of source-receiver offsets. The data are recorded for a fixed record length and sampling frequency. In a marine environment, an acoustic source releases seismic energy into the water column and reflected signals are recorded at the range of the source-receiver offsets. In our case, a sparker source provides an acoustic impulse in the water column that is recorded on hydrophones along a streamer pulled behind a boat. Each shot gather is processed to attenuate undesired signal and depth converted to create a pseudo cross-section that can be geologically interpreted.

Procedure Overview

Initially, we recorded seismic data in SEG2 format and converted it using SeismicUNIX to SEGY format (Barry et al., 1975; Pullan, 1990; Cohen and Stockwell, 2011). The seismic data processing procedures are outlined in Figure 14. I processed all seismic data using the Landmark software PROMAX ®. Final images for display were

created using SeismicUNIX. PROMAX includes several modules for processing. The processing steps that I used included velocity analysis, normal moveout (NMO) corrections, CMP sorting, CMP stacking, filtering, migration and deconvolution (Yilmaz, 2001). The first step in processing field data includes assigning the correct geometry to each source-receiver pair from using GPS positioning and field notes.

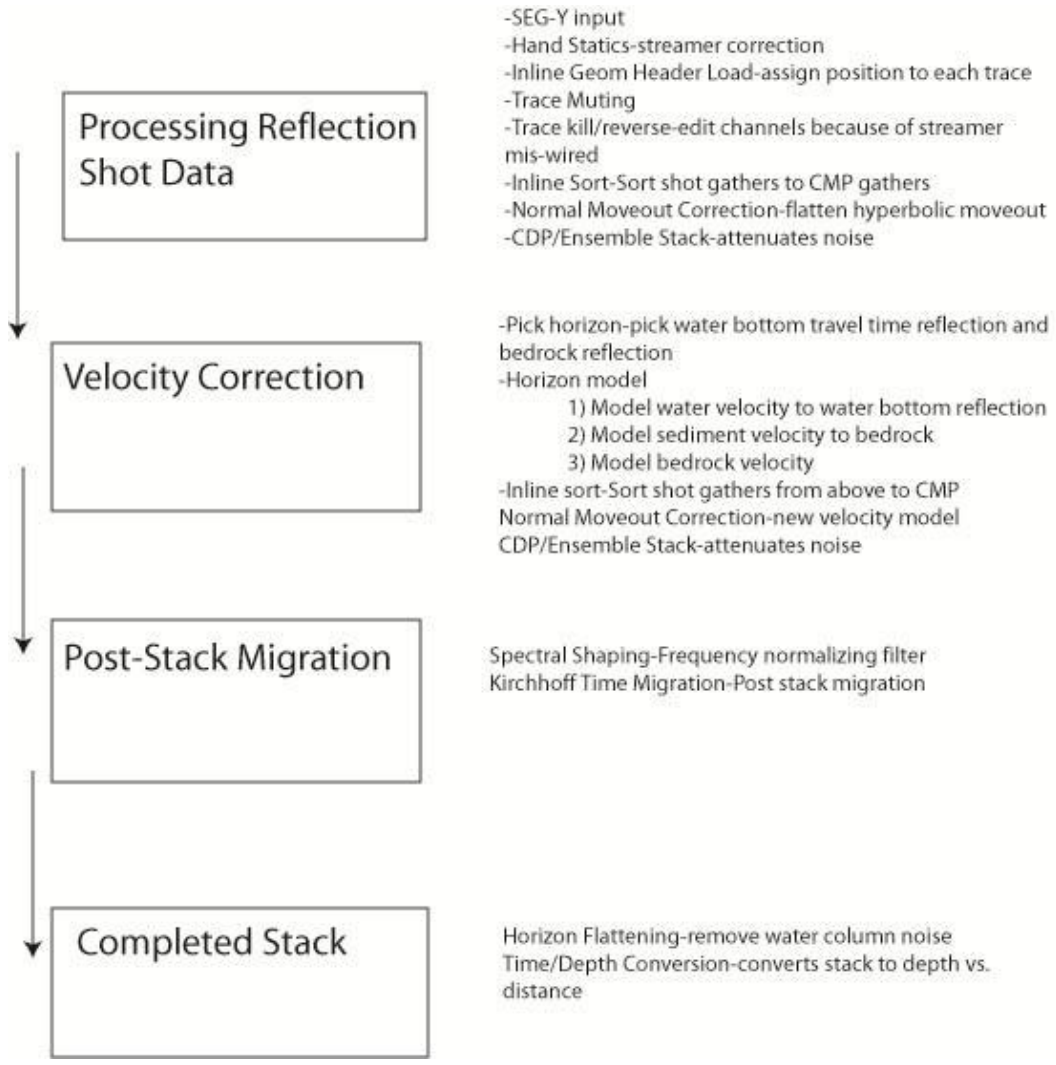

Figure 14: Processing flow diagram showing general flow processes (left) and detailed flow list (right).

Geometry

The geometry used for seismic processing requires GPS data for shot and receiver positions. GPS field files were imported into EXCEL™. The GPS files record time, latitude, and longitude for each source/receiver position. I converted source-receiver positions to Universal Transverse Mercator (UTM) using Matlab™ code. A GPS-seismograph time sync allowed accurate position information to match exact source receiver positions. The values for each source and receiver position was corrected to account for the position of the boat relative to the sensors.

Preprocessing and CMP Sort

Once geometry was applied to each seismic trace, I sorted each time series trace from near to far offsets and applied a streamer geometry time correction. I removed misfired shots, reversed select channels due to streamer miswiring, and sorted to CMP. A spectral shaping filter of 250 to 1000 Hz was applied to the data to attenuate low frequency streamer strum and high frequency random noises. The spectral shaping filter normalizes the amplitude for the range of passed frequencies.

Velocity Model

I created a velocity model by using a simple layer model. The first layer accounted for the water column velocities. An empirical equation for the speed of sound in water is known (Figure 15) (Sheriff 270).To accurately calculate the velocity of sound in water, temperature, salinity, and depth is required. Surface temperature was measured from the Lowrance sonar unit and using a general temperature curve with depth (Xiong

and Royer, 1984), I interpolated temperature with water depth. I assumed salinity was constant for all of Prince William Sound (Klein, 1983). I calculated water depth by picking the travel time from the first prominent reflector. The initial velocity of the water column was approximately 1,482 m/s with a gradient of about -0.18 m/s per meter (Figure 15).

$$Vel = 1449.2 + 4.6T - .055T^2 + .0003T^3 + (1.34 - .010T) * (S - 35) + .016Z$$

Equation 1: Shows water velocity (Vel) as determined using temperature (T), Salinity (S), and depth (Z).

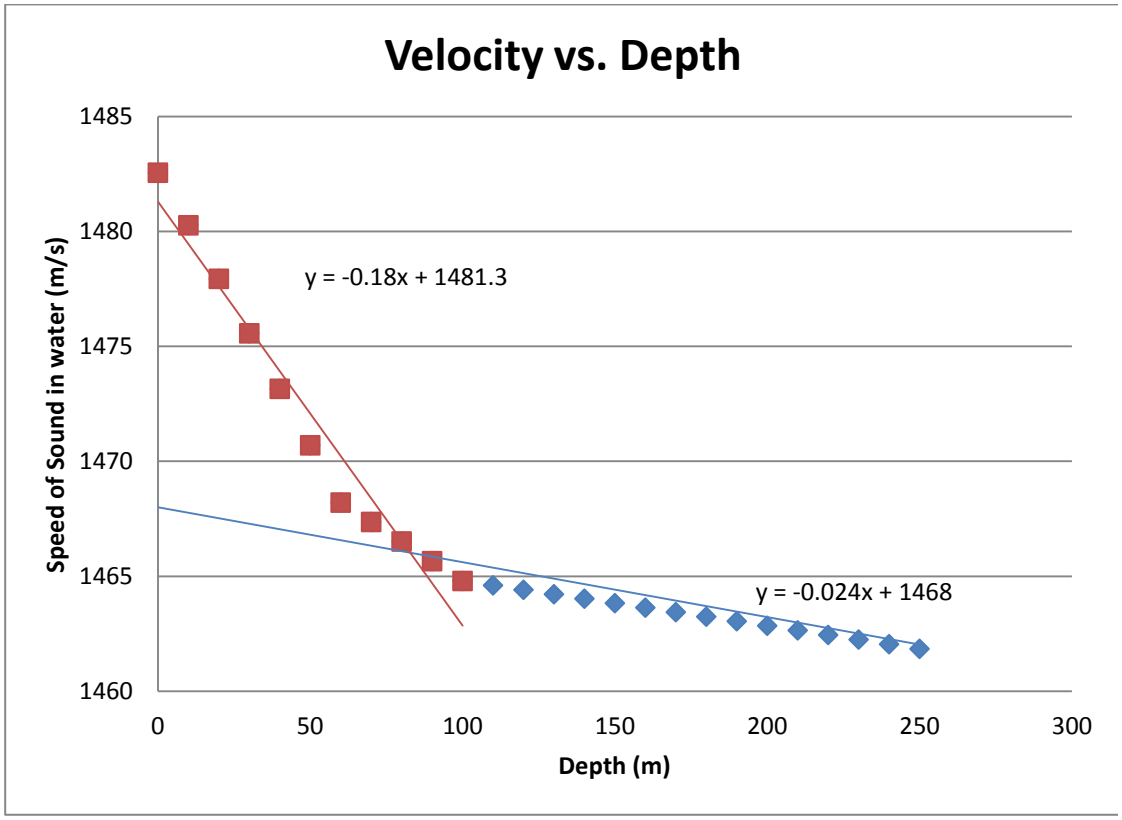

Figure 15: Points calculated from equation 1. Values for temperature with depth were from surveys in central PWS (Vaughan et al., 2001). A decrease in speed of sound in water with depth is observed to 250 m with constant salinity. Slope ranges from .0239 m/s/m and .1844 m/s/m.

From well drilling tests in the Gulf of Alaska and from nearby refraction profiles, I estimate the velocity of Holocene unconsolidated sediments at 1,600 m/s and a gradient of 1.5 m/s per meter to account for sediment compaction (Le Douran and Parsons, 1982; Brocher et al., 1994). I estimate the velocity of Orca group rocks at approximately 2,200 m/s with a gradient of 1 m/s per meter (Brocher et al., 1994). Older meta-sedimentary rocks are assigned a velocity of 4,000 m/s (Brocher et al., 1994). Interval velocities for all layers were converted to stacking velocities using Dix formula, Equation 2.

$$V_n = sqrt\left(\frac{[\overline{V}_n t_n - \overline{V}_{n-1} t_{n-1})}{t_n - t_{n-1}}\right)$$

Equation 2: Dix formula solves for the stacking velocity from interval velocities of n layers.

Velocity Correction

NMO corrections account for the difference of the reflection time as a function of offset between source and receiver (Sheriff 169). The NMO correction removes the hyperbolic moveout to provide an equal travel time for each source receiver pair at each CMP location.

$$T = x^2 * \frac{1}{Vrms^2} + to^2$$

Equation 3: Travel time equation used for NMO in seismic data processing.

An additional static correction was also needed to account for streamer geometry that was balanced for fresh water (Figure 15). The added time shift was 0.063 ms per meter of hydrophone offset to account for the greater hydrophone depths at the far channels. After NMO corrections, the water bottom reflectors appear at the same travel time for each source-receiver pair, assuming a flat water bottom surface topography.

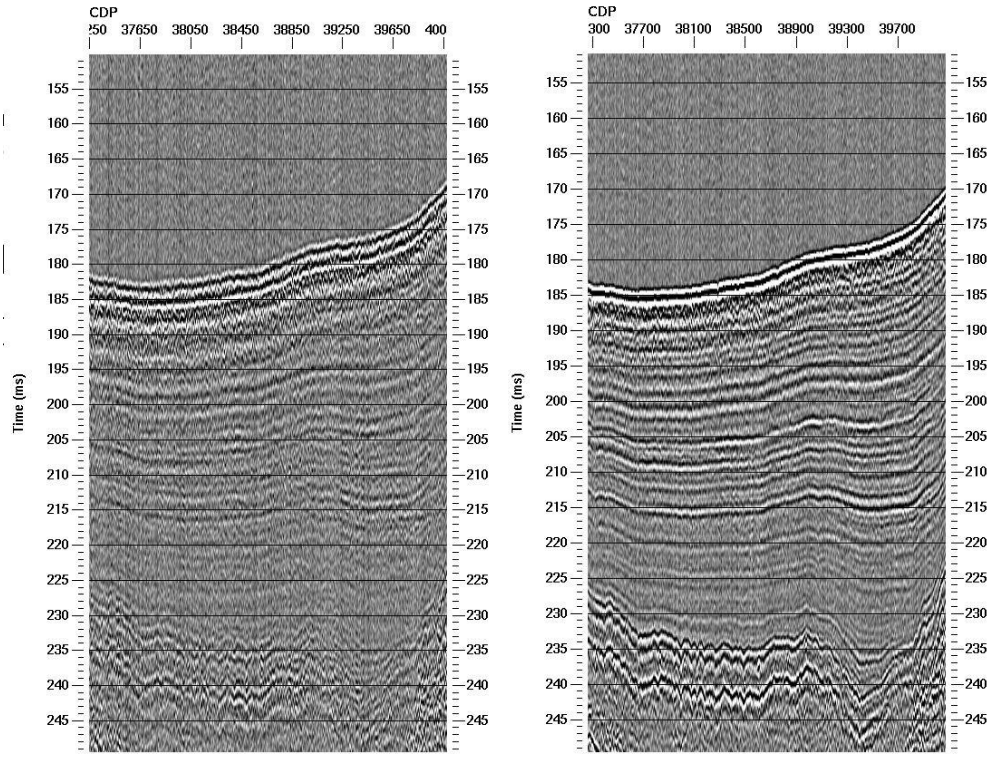

Figure 16: Initial uncorrected curved streamer geometry, left. Corrected streamer geometry, right. Identical processing steps were applied to each panel. Improved signal quality resulted from proper geometry correction.

Migration and Final Stack

Seismic migration is the process to correct reflected arrivals to their imaging point instead of source-receiver midpoint (Sheriff 157). The filtered, NMO corrected, stacked data were then post-stack migrated using a Kirchhoff time migration. The Kirchhoff time migration was chosen because the algorithm uses an integral form of the wave equation to collapse hyperbolic arrivals to a point (Sheriff 157). Finally, the migrated stack in time is converted to depth by using the estimated velocities previously described.

Limitations and Assumptions

Processing errors in the seismic reflection data result from a first-order geometry assignment and a simplified velocity model. During the geometry assignment, I assume that the distance between source and the receivers remains constant, however with slight boat course corrections from a straight line this source-receiver distance would change. In addition, I assume the location for the source was directly behind to the stern of the boat, in actuality the source was 6 m off the starboard side of the stern. I created a velocity model using a three layer model, when the actual earth model is likely more complex. Interfaces between layers of the velocity model were picked with a previously more simplified velocity model, one that assumes a linear increasing velocity. The water layer of the model assumes a linear decrease of water velocity with depth (Figure 15); the real model can be more complex given by salinity or temperature variations that are common in large water ways (Sheriff 270) (Equation 1). Another assumption in the velocity model that I made is that sediment velocities are identical throughout PWS, whereas localized differences in lithology and seismic velocity are based on grain size, sediment sorting, and compaction (Carlson and Molnia, 1978; Brocher et al. 1994). In addition, I assumed the basal reflector is from competent rock or bedrock with an interval velocity estimated by Brocher et al. [1994]. The velocity model is used in the NMO correction, migration, and time to depth conversion processes so any errors will result in lower data quality.

Bathymetry Data

The bathymetry datasets allow a view of the water bottom topography. As part of our cruise plan, bathymetry data were used to determine focus areas for our seismic survey. Two datasets of bathymetry were used. The first bathymetry file, a multi-beam

NOAA dataset was collected and processed by NOAA (NOAA, 2012). The second dataset included digital sounding data throughout PWS collected by NOAA between 1920 and 2004 (NOAA, 2012).

CHAPTER FOUR: INTERPRETATIONS

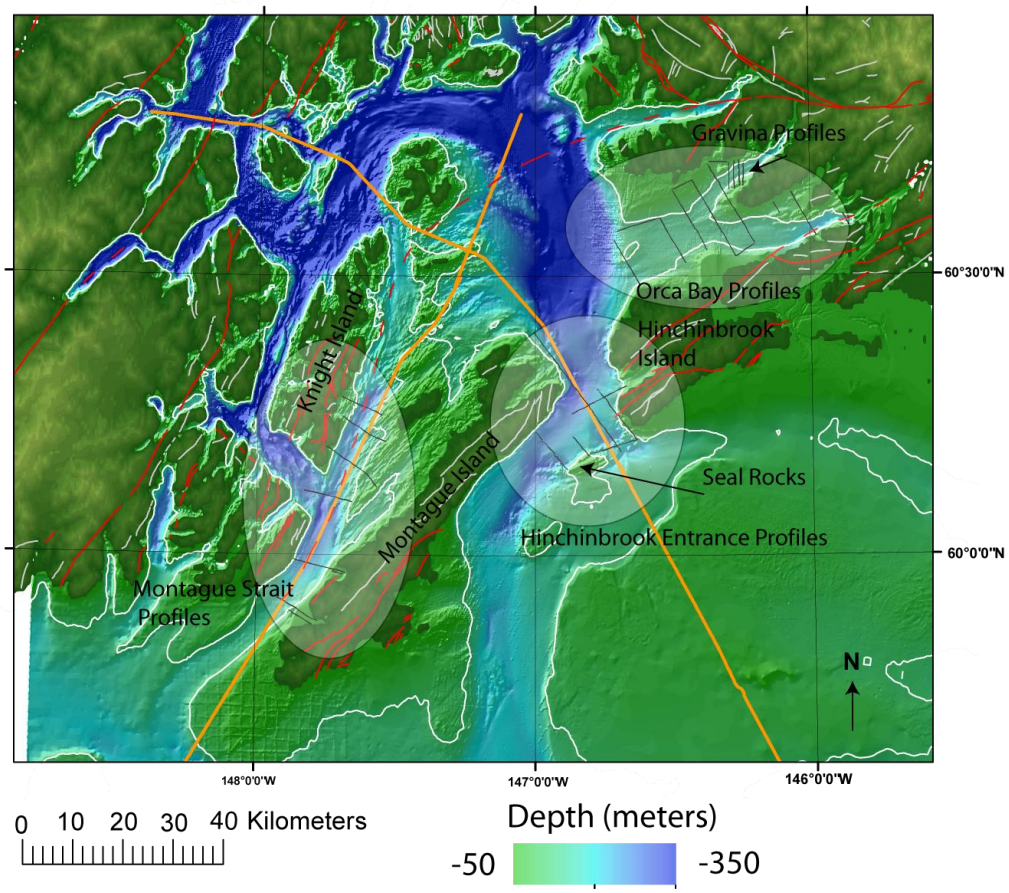

Figure 17: PWS overview map with bathymetry. Orange line shows USGS TACT lines while black lines show Boise State University seismic profiles collected in August 2009, red lines show faults (modified Wilson and Hults, 2008). Three areas of seismic surveys are circled.

Orca Bay Interpretations

Bathymetry

Orca Bay is located in eastern PWS, north of Hinchinbrook Island (Figure 17), where land and bathymetric lineations trend between N50˚E and N80˚E (Wilson and Hults, 2008; NOAA, 2012). Lineations within Orca Bay are most prominent in areas shallower than 110 m and several lineations continue on land (Condon, 1966). Within the northern and central portion of Orca Bay, the sea floor increases in depth to the south. Few bathymetric lineations appear in southern Orca Bay along the north shore of Hinchinbrook and Hawkins Islands compared to areas to the north and east. Within eastern Orca Bay, lineations average trend N80˚E (Figure 18).

Bathymetric lineations in southern Orca Bay tend to parallel the adjacent shoreline while lineations in northern Orca Bay are independent of the adjacent shoreline trend or offshore extension of mainland Alaska (Figure 18). Lineation L1 in central Orca Bay trends parallel to the shoreline and extends 30 km from Sheep Bay to central PWS. Lineation L2 trends approximately east to west in west-central Orca Bay and bends sharply northward, trending northeast to southwest, near seismic profile Orca 5. Lineation L1 strikes E-W and is regionally continuous from Orca 12 to Orca 5. L1 may intersect L2 near Orca 5; bathymetric expression of L1 is reduced between Orca 8 and Orca 5.

Seismic Profile Orca Bay 1 (Orca 1)

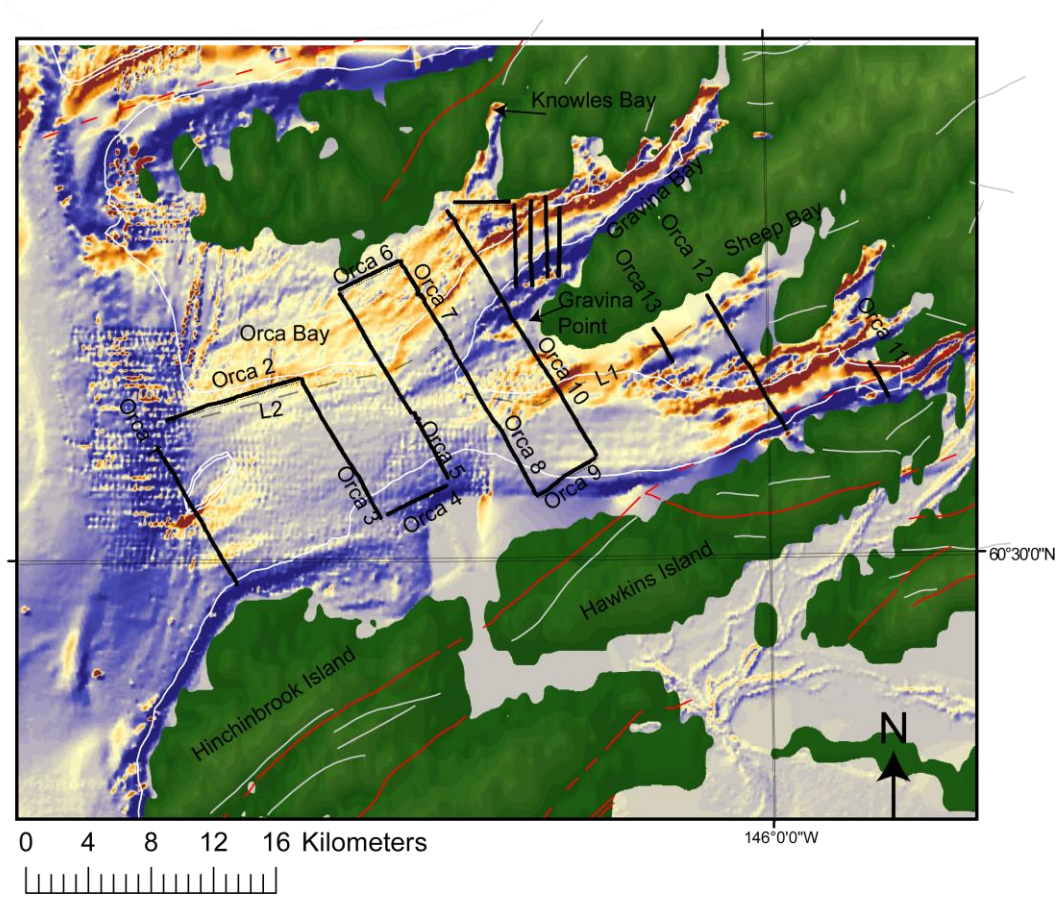

Figure 18: Bathymetric derivative map (NOAA, 2012) of Orca Bay (Red lineations dip southward, blue lineations dip northward) with the 13 collected reflection seismic data (Orca 1 through Orca 13). Red lines denote mapped faults, white lines are lineations (Wilson and Hults, 2008).

The 10.1 km south-north Orca 1 seismic profile is located near the intersection of Orca Bay and central PWS and extends south to Hinchinbrook Island (Figure 18). The water depth ranges from 100 m to 230 m (Figure 19). An asymmetric bathymetric high is centered at CMP 24,200 with a steep sided south slope. The profile was acquired between 9:06 AM and 10:05 AM local time with an average boat speed of 2.9 m/s, shot spacing of 3.8 m, and binned CMP spacing of 1.5 m.

The Orca 1 unmigrated seismic section reveals reflections to more than 0.1 s two-way travel time below the water bottom reflector (Figure 19). On the migrated/depth converted image, I interpret three layers below water bottom that represent the Holocene, undifferentiated Quaternary, and Tertiary strata. Unit O1 represents the shallowest strata, varies in thickness from 0-100 m, and is characterized by distinctive parallel to subparallel reflectivity. Given local sedimentation rates of .3 cm/year (Klein, 1983), this shallow unit likely contains post-glacial (<12,000 years) marine sediments transported by local streams and from the Gulf of Alaska current (Figure 17) (Carlson and Molnia, 1978). I interpret lateral variations of sediment thickness and an asymmetric water bottom to imply active faulting, submarine landslides, water bottom currents, and/or local sediment sources that have influenced sediment deposition and erosion.

Unit O2 stratigraphically underlies Unit O1 and is most clearly imaged between CMP 21,000 and 23,000 (Figure 19). This unit is characterized by a seismically transparent zone with clear unconformities both above and below the layer. I interpret the overlying unconformity to represent the last glacial maxima, where shallower global sea levels and regional glaciations exposed portions of Orca Bay (Hamilton, 1994). Unit O2 could span any portion of Quaternary time record or O2 could represent an early phase of post-glacial Holocene deposition. However, given the maximum thickness of 90 m and assuming modern sedimentation rates, Unit O2 likely represents only a small portion of the Quaternary history. I interpret the Unit O2 as containing coarse-grained sediments based on the lack of internal reflectivity (e.g., Hofmann et al., 2006; Cowan et al., 2010).

Unit O3 underlies the O1 and O2 sequences (Figure 19). The unit is characterized by little to no reflectivity and projects to outcrop exposures of undivided Tertiary aged Orca Group sedimentary rocks at Gravina Point (Wilson and Hults, 2008).

Two water bottom offsets along Orca 1 tie to lineations on the bathymetric map (Figure 18). These offsets are located at CMP locations 24,000 and 25,500 (Figure 19). The 50 m water bottom offset at CMP 24,000 is part of a down to the south lineation, ~30˚ slope, that continues at least 7 km to the northeast and southwest. I interpret this lineation as a fault related to the PWS megathrust fault system that separates Tertiary bedrock in the hanging wall from younger strata in the footwall (Figure 19). I interpret this fault as near vertical with water bottom slope shaped by erosion and differential deposition. At CMP 23,400, offsets of Unit O2 strata suggest a fault may control the margin of an older basin to the south. While the absence of a water bottom offset suggests this fault is not active, there is broad warping of water bottom that may represent drape over an older fault. A lineation at CMP 25,500 shows distinctive change in water bottom slope with a thinning of Units O1 and O2. This lineation is spatially continuous for at least 3 km.

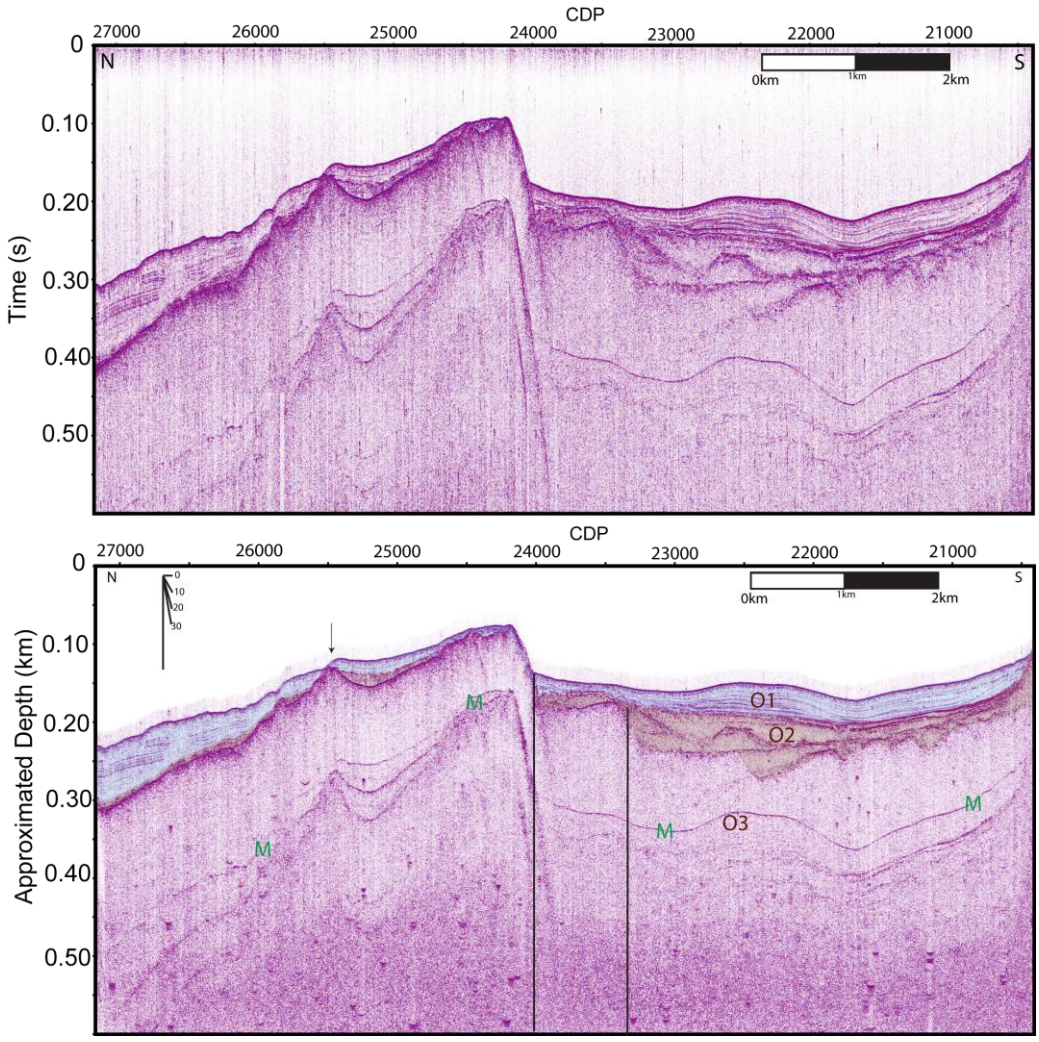

Figure 19: (top) Unmigrated travel time stack for Orca 1. (bottom) Migrated depth converted stack of Orca 1. Seismic multiple displayed on profile with green "M." The arrow represents a water bottom lineation without evidence for offset on deeper reflectors. Dip meter in top right shows angle of reflectors or faults on profile.

Seismic Profile Orca Bay 2 (Orca 2)

The 11.5 km west-east seismic profile Orca 2 obliquely crosses a bathymetric lineation L2 in water depth that ranges from 120 m to 200 m (Figure 18; Figure 20). The deepest portion of bathymetric low is centered at CMP 27,300 with a gradual west sloping water bottom. The water bottom is flat lying east from CMP 28,500. The profile

was acquired between 10:24 AM and 12:33 PM local time with an average boat speed of 1.5 m/s, shot spacing of 2.4 m, and binned CMP spacing of 1.5 m.

The unmigrated seismic section of Orca 2 reveals reflections to more than 0.06 s two-way travel time below the water bottom reflector (Figure 20). I interpret three layers below the water bottom representing the Holocene (Unit O1), undifferentiated Quaternary (Unit O2), and Tertiary strata (Unit O3). Unit O1 is the shallowest strata, with a thickness up to 25 m, and characterized by a subhorizontal reflectivity. Unit O1 is continuous along the profile except between CMP 27,500 and 28,000. Unit O2 stratigraphically underlies unit O1, can be characterized by hummocky reflectivity, and is most clearly imaged between CMP 32,000 and 33,000. Unit O3 is the basal Orca Group strata that contain transparent to chaotic reflectivity. The change of bathymetric baseline across along the seismic profile reflects the out of plane representation of bathymetric lineation L2.

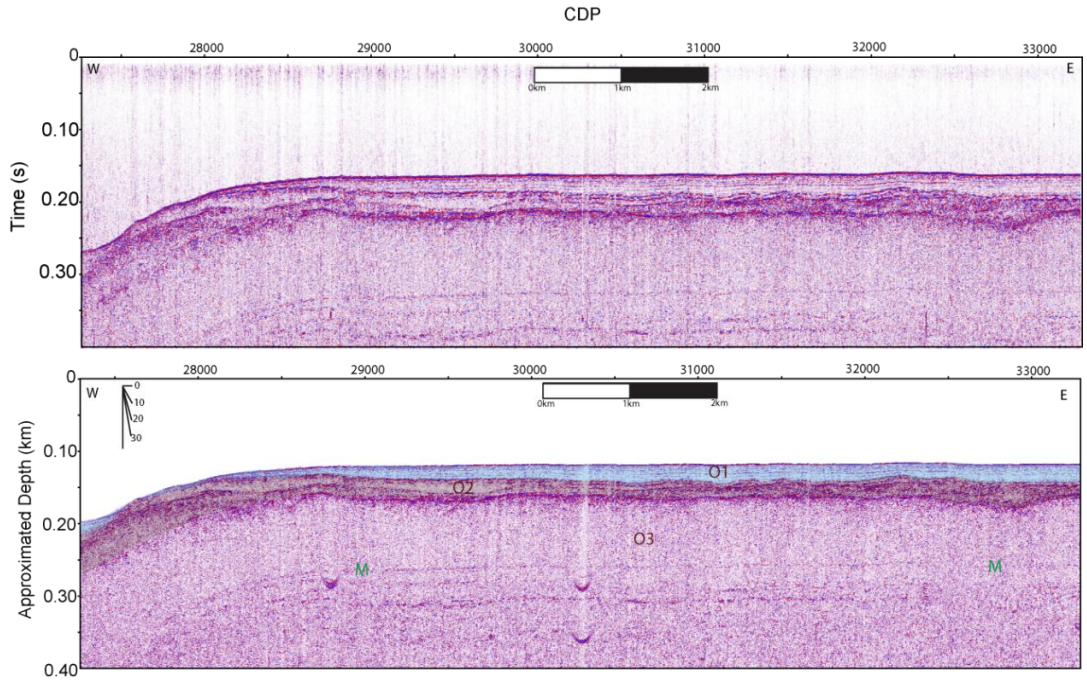

Figure 20: (top) Unmigrated travel time stack for Orca 2. (bottom) Migrated depth converted stack of Orca 2. Migrated depth converted stack of Orca 1. Seismic multiple displayed on profile with green "M." Dip meter in top right shows angle of reflectors or faults on profile.

Seismic Profile Orca Bay 3 (Orca 3)

Seismic profile Orca 3 is located in central Orca Bay (Figure 18). This 10.3 km north-south profile extends from bathymetric lineation L2 and crosses a bathymetric low that extends throughout central Orca Bay in water depth that range from 150 m to 200 m (Figure 21). The greatest water depth is centered between CMP 38,000 and CMP 39,000 with a gentle slope to the north and south. The profile was acquired between 12:41 PM and 2:12 PM local time with an average boat speed of 1.9 m/s, an average shot spacing of 2.5 m, and binned CMP spacing of 1.5 m.

The unmigrated seismic section for Orca 3 reveals reflections to more than 0.2 s two-way travel time below the sea floor (Figure 21). I interpret three geologic layers that I interpret to represent the Holocene (Unit O1), undifferentiated Quaternary (Unit O2),

and Tertiary strata (Unit O3). Unit O1 represents the shallowest strata and is characterized by upwards of 45 m of sub-horizontal continuous reflectors. Unit O2 stratigraphically underlies Unit O1, is upwards of 120 m thick, and is most clearly imaged between CMP 36,000 and 39,000. I observe reflectors within Unit O2 between CMP 39,000 and 40,000. I observe south-dipping reflectors upwards of 10 degrees between CMP 39,000 and 39,400 with a change of dip to 5 degrees until CMP 40,000. I interpret these reflectors to represent the margin of a relic basin while the modern depocenter is located near CMP 38,000. The basal seismic unit that I interpret is Unit O3 composed of Tertiary aged strata.

I interpret distinct water bottom and deeper strata offsets to represent active faulting at CMP 36,700 (Figure 21). Older faults that do not offset modern water bottom but offset older strata are located at 37,050 and 39,000. I observe an inflection in the slope angle of the water bottom at CMP 35,800 identified as a water bottom lineation that might be fault related. Furthermore, strata are offset in Unit O2 at CMP 35,800 by as much as 20 m. The fault at CMP 36,700 offsets the water bottom, unit O2, and the boundary between unit O2 and O3 by 10, 30, and 50 m respectively. I interpret an inactive fault at CMP 37,050 that offsets the boundary between Unit O2 and O3 by at least 20 m. I interpret another inactive fault is located at CMP 39,000 that offsets Unit O2 and O3 by as much as 50 m. A bathymetric lineation at CMP 41,000 represents a 15 m water bottom and sediment drape.

I suggest a northward depocenter migration may result from normal faults in Orca Bay such as at CMP 36,700 (Figure 21). I identify three remnant depocenters (CMP 38,000; 38,700; and 41,000) each with proximity to faulting. I suggest depocenters

migrated northward at least 3 km since deposition of unit O2 to accommodate upper crustal shortening. Furthermore, I suggest deeper sediment zones have merged into a broader, ~10 km, basin due perhaps from increased sedimentation following the end of the last glacial period.

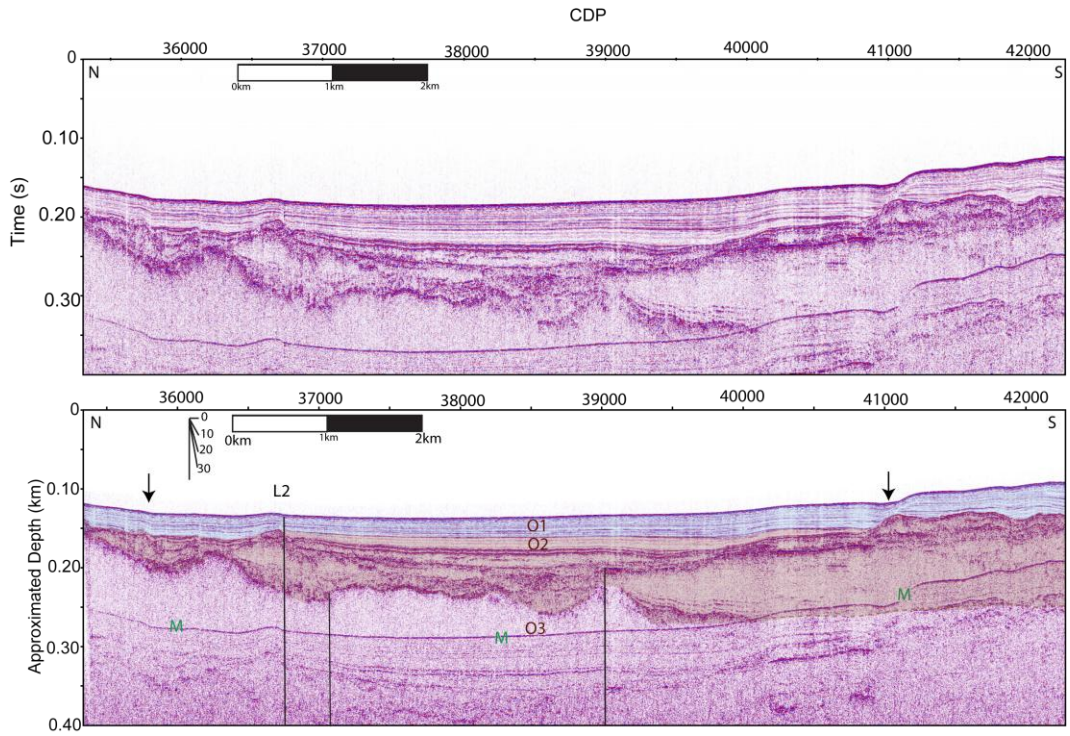

Figure 21: (top) Unmigrated travel time stack for Orca 3. (bottom) Migrated depth converted stack of Orca 3. Migrated depth converted stack of Orca 1. Seismic multiple displayed on profile with green "M." The arrow represents a water bottom lineation without evidence for offset on deeper reflectors. Dip meter in top right shows angle of reflectors or faults on profile.

Seismic Profile Orca Bay 4 (Orca 4)

Seismic profile Orca 4 is located in central Orca Bay (Figure 18). This 4.8 km west-east profile crosses a bathymetric high at CMP 46,000 that extends north of Hinchinbrook Island in water depth that range from 50 m to 90 m (Figure 22). The profile was acquired between 2:12 PM and 2:51 PM local time with an average boat speed of 2.12 m/s, shot spacing of 3.3 m, and binned CMP spacing of 1.5 m.

The unmigrated seismic section for Orca 4 reveals reflections to more than 0.1 s two-way travel time below the water bottom reflector (Figure 22). I interpret three layers below the water bottom to represent the Holocene (Unit O1), undifferentiated Quaternary (Unit O2), and Tertiary strata (Unit O3). Unit O1 represents the shallowest strata and varies in thickness to a maximum of 50 m. A modern erosional channel appears at CMP 44,900 based on reflector truncations on the seafloor. The thickest strata of unit O1 occupy a bedrock low between CMP 43,800 and 44,500, west of the channel feature. Unit O2 stratigraphically underlies Unit O1 and is most clearly imaged between CMP 44,000 and 46,700. The basal seismic unit that I interpret is Unit O3, representing older Tertiary strata.

I interpret a growth fault at CMP 45,800 based on increased strata offsets with depth (Figure 22). The fault offsets the water bottom by 15 m and the base of O1 by 70 m. As a result of faulting, Unit O3 shallows to the east. I identify other faults at CMP 43,800; 45,900; and 46,600. The fault at 43,800 offsets Unit O1 strata drape over a 20 m offset at the Unit O1-O2 boundary. The fault at 45,900 offsets the boundary between Unit O2 and O3 by 20 m. The fault at 46,600 also offsets Unit O2 and O3 by 10 m. I interpret undulating water bottom east of CMP 45,800 as localized zone of smaller offset and active faulting.

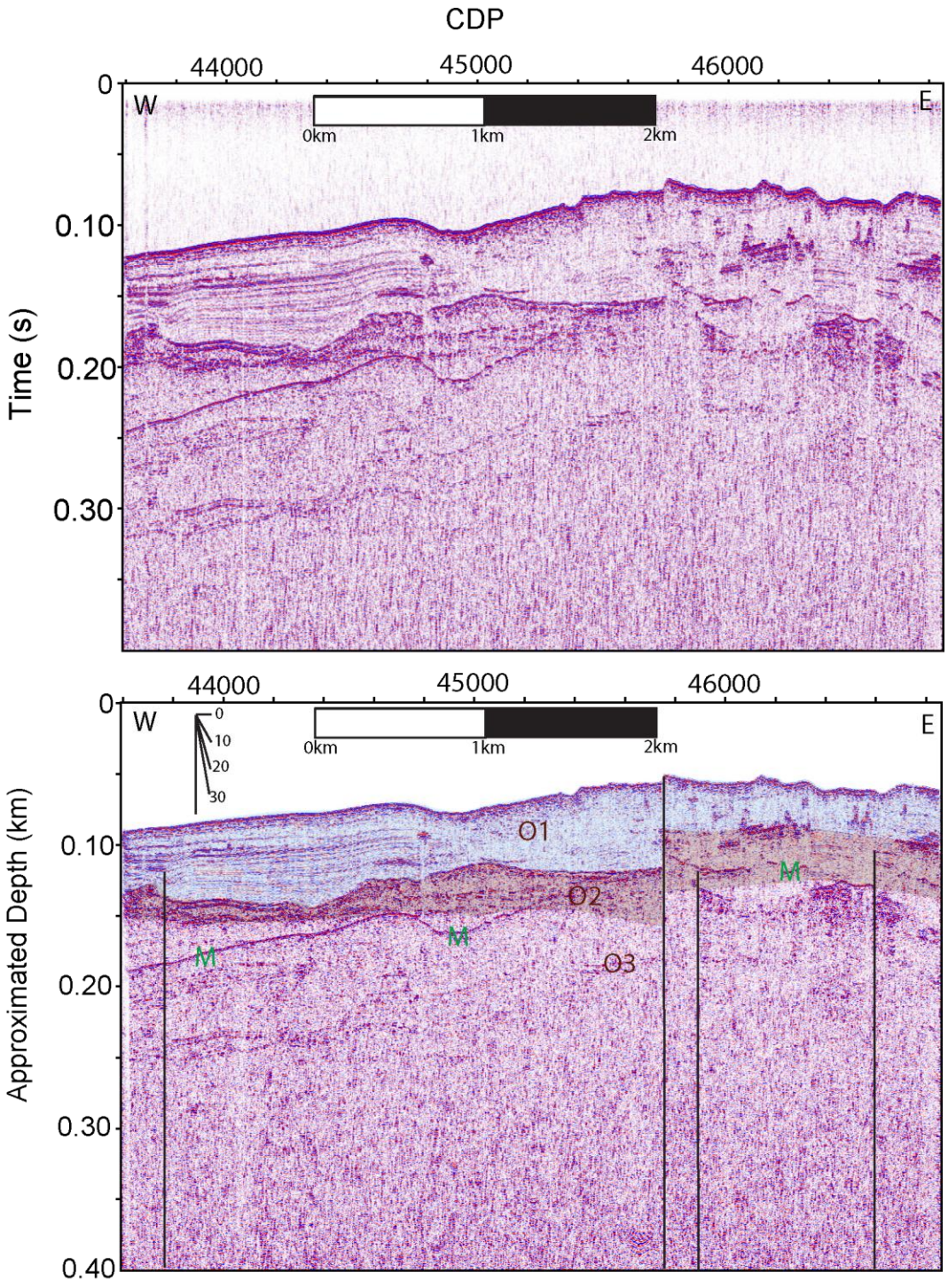

Figure 22: (top) Unmigrated travel time stack for Orca 4. (bottom) Migrated depth converted stack of Orca 4. Migrated depth converted stack of Orca 1. Seismic multiple displayed on profile with green "M." Dip meter in top right shows angle of reflectors or faults on profile.

Seismic Profile Orca Bay 5 (Orca 5)

The central Orca Bay profile Orca 5 in (Figure 18) is a 13.9 km north-south profile that crosses the bathymetric high L2 in water depth that range from 40 m to 150 m (Figure 23; Figure 32). The profile was acquired between 2:52 PM and 5:22 PM local time with an average boat speed of 1.54 m/s, shot spacing of 2.5 m, and binned CMP spacing of 1.5 m.

The unmigrated seismic section Orca 5 reveals reflections to more than 0.2 s two-way travel time below the water bottom reflector (Figure 23). I interpret three layers on the migrated/depth converted image that I interpret to represent the Holocene (Unit O1), undifferentiated Quaternary (Unit O2), and Tertiary strata (Unit O3). Unit O1 represents the shallowest strata and varies in thickness to a maximum of 90 m. Unit O2 stratigraphically underlies Unit O1 and is most clearly imaged between CMP 48,000 and 50,000. The basal seismic unit that I interpret is Unit O3.

The greatest O1 thickness is located south of CMP 49,000 in an area with several landslides (Figure 23) (NOAA, 2012). I interpret these landslides based on transparent seismic zones related to slope failures along northern Hinchinbrook Island that can occur at low angles <10 degrees. Landslide deposits laterally extend for at least one kilometer for individual flow while the larger length of landslides may be greater than five kilometers (Figure 32).

I identify six faults along the profile based on offset reflectors. Faults at 53,100; 51,950; and 49,100 offset the base of unit O1 (Figure 23). The fault at CMP 49,000 offsets Unit O1 by ~15 and defines the northern extent of recent submarine landslides. At CMP 52,000 the water bottom and deeper strata are offset by 15 m and 50 m, respectively

and represent the L1 lineation. The fault at CMP 52,900 offsets Unit O1 by 20 m and offsets the base of Unit O2 by 35 m. Faults at 50,000; 50,400; and 50,750 offset only unit O2 and unit O3 suggesting older activity of faults. The faults at 50,000; 50,400; and 50,750 offset the boundary of unit O2 and O3 by 20 m, 30 m, and 30 m, respectively. The fault at 55,300 offsets internal reflectors of unit O3 near the multiple by approximately 10 m.

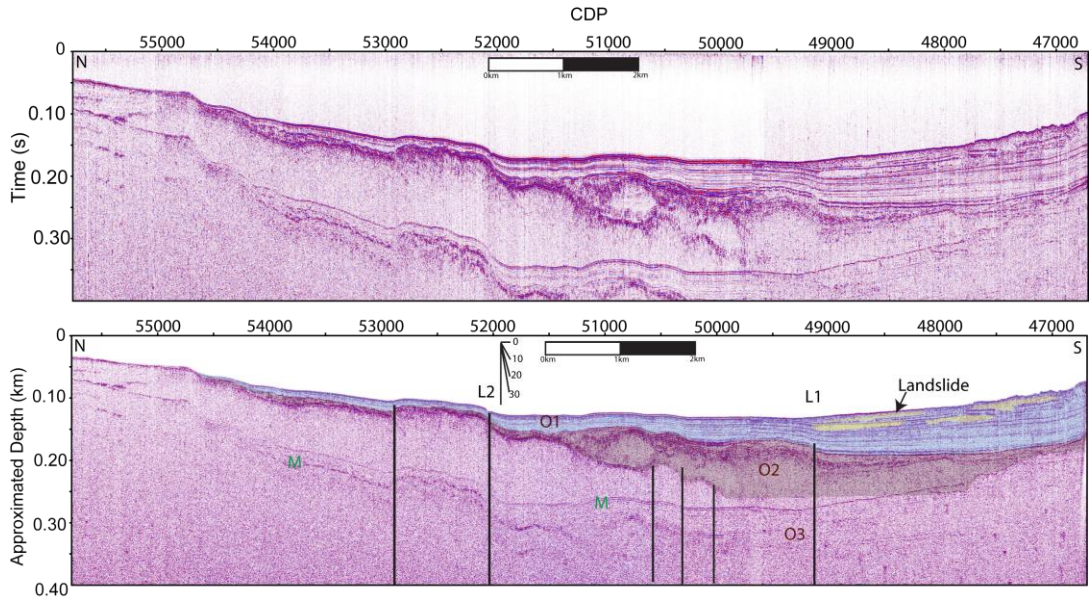

Figure 23: (top) Unmigrated travel time stack for Orca 5. (bottom) Migrated depth converted stack of Orca 5. Migrated depth converted stack of Orca 1. Seismic multiple displayed on profile with green "M." Dip meter in top right shows angle of reflectors or faults on profile.

Seismic Profile Orca Bay 6 (Orca 6)

The 4.2 km west-east Orca 6 seismic profile crosses a bathymetric high that extends from Knowles Bay in water depth that range from 20 m to 50 m (Figure 18; Figure 24). An asymmetric bathymetric high is centered at CMP 60,700 with a gradual west trending slope. The profile was acquired between 5:24 AM and 5:53 AM local time

with an average boat speed of 2.42 m/s, shot spacing of 3.2 m, and binned CMP spacing of 1.5 m.

The unmigrated seismic section for Orca 6 reveals reflections to more than 0.05 s two-way travel time below the water bottom reflector (Figure 24). I interpret two layers below the water bottom to represent the Holocene (Unit O1) and Tertiary strata (Unit O3). Unit O1 represents the shallowest strata and varies in thickness to a maximum of 20 m. The basal seismic unit that I interpret is Unit O3. The undulating water bottom along the profile represents recent strata draping over shallow Tertiary strata. I see no reflector offsets that would represent active faulting.

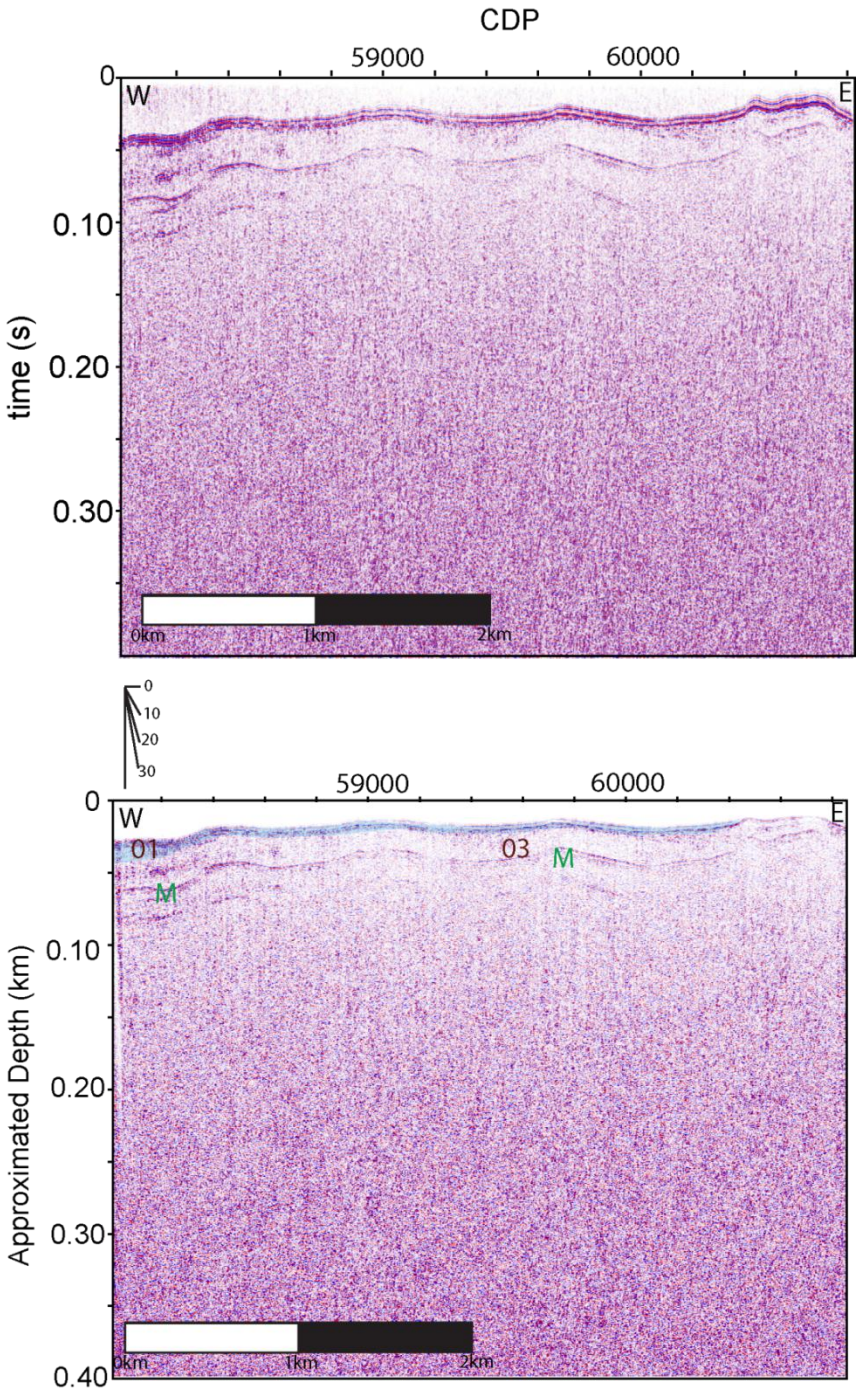

Figure 24: (top) Unmigrated traveltime stack for Orca 6. (bottom) Migrated depth converted stack of Orca 6. Migrated depth converted stack of Orca 1. Seismic multiple displayed on profile with green "M." Dip meter in top right shows angle of reflectors or faults on profile.

Seismic Profile Orca Bay 7 (Orca 7)

The 2.8 km north-south Orca 7 profile was acquired in central Orca Bay and crosses a bathymetric high that extends from Knowles Bay in water depth that range from 20 m to 80 m (Figure 18; Figure 25). A bathymetric high centered at CMP 60,700 gradually dips to the south. The profile was acquired between 5:54 PM and 6:32 PM local time with an average boat speed of 1.2 m/s, average shot spacing of 2.55 m, and binned CMP spacing of 1.5 m.

The unmigrated seismic section for Orca 7 reveals reflections to more than 0.075 s two-way travel time below the water bottom (Figure 25). On the migrated and depth converted image, I interpret three layers below the water bottom to represent the Holocene (Unit O1), undifferentiated Quaternary (Unit O2), and Tertiary strata (Unit O3). Unit O1 represents the shallowest strata and varies in thickness to a maximum of 50 m. Unit O2 stratigraphically underlies Unit O1 between CMP 62,000 and 62,600, but is absent along the northern portions of the profile. The basal seismic unit that I interpret is Unit O3.

I interpret two water bottom offsets at CMP 61,500 and 62,150. At CMP 61,400, offsets of the water bottom by 20 m may imply active faulting, however offsets of older strata are not clear (Figure 25). At 62,100, offset of the water bottom is 30 m and the increased thickness of O1 and O2 strata to the south provides strong evidence for active faulting. Both of these water bottom offsets extend along the sea floor for at least 14 km, thus providing further evidence that these offsets represent active faults (Figure 18).

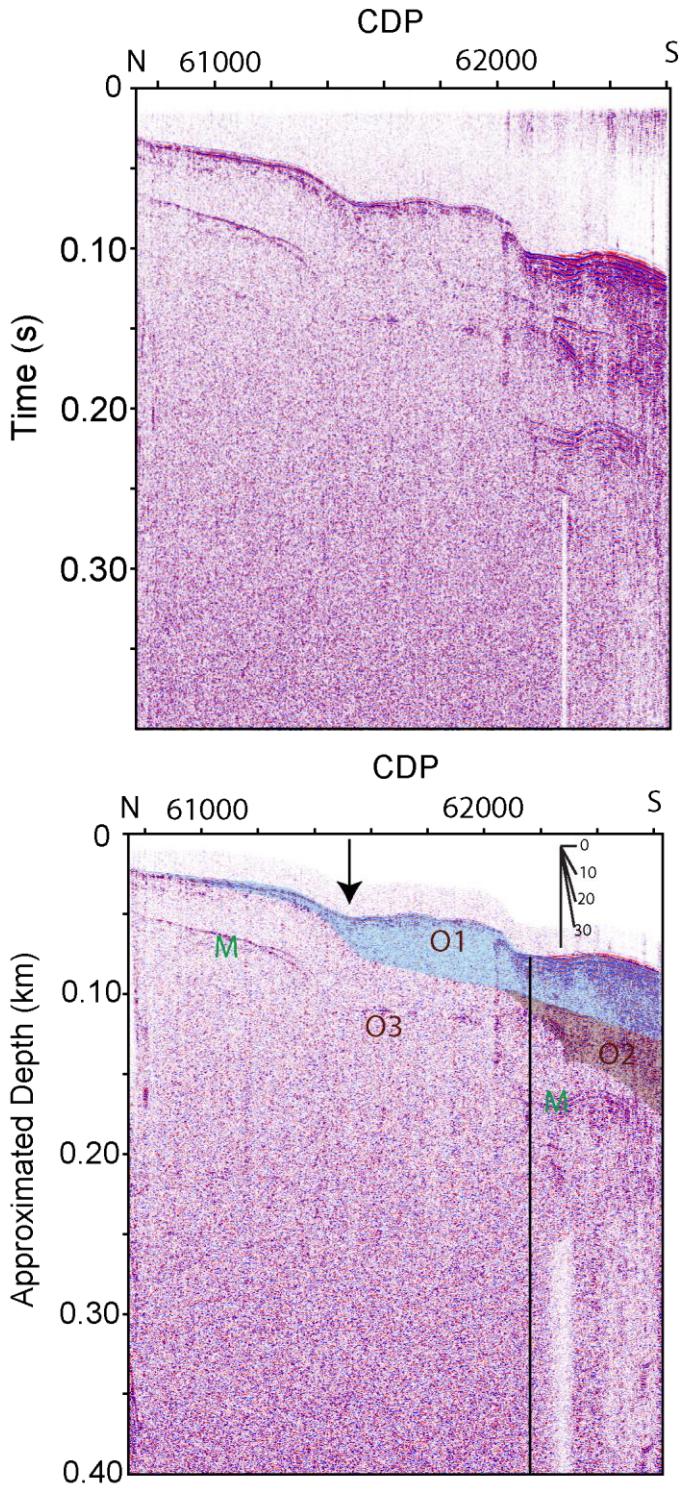

Figure 25: (top) Unmigrated traveltime stack for Orca 7. (bottom) Migrated depth converted stack of Orca 7. Migrated depth converted stack of Orca 1. Seismic multiple displayed on profile with green "M." The arrow represents a water bottom lineation without evidence for offset on deeper reflectors. Dip meter in top right shows angle of reflectors or faults on profile.

Seismic Profile Orca Bay 8 (Orca 8)

The 14.3 km north-south Orca 8 profile in central Orca Bay crosses the bathymetric high centered at CMP 66,500 that extends from Gravina Point in water depth that range from 80 m to 150 m (Figure 18; Figure 26). An asymmetric bathymetric high is centered at CMP 66,500 has a steep sided north slope and a gradual south slope. The profile was acquired between 9:12 AM and 11:52 AM local time with an average boat speed of 1.5 m/s, shot spacing of 2.9 m and binned CMP spacing of 1.5 m.

The unmigrated seismic section for Orca 8 reveals reflections to more than 0.2 s two-way travel time below the water bottom reflector (Figure 26). On the migrated and depth converted image, I interpret three layers below the water bottom to represent the Holocene (Unit O1), undifferentiated Quaternary (Unit O2), and Tertiary strata (Unit O3). Unit O1 represents the shallowest strata and varies in thickness to a maximum of 75 m. Unit O2 stratigraphically underlies Unit O1 and is most clearly imaged near the northern and southern portions of the profile. The basal seismic unit that I interpret is Unit O3. I interpret two ancestral basins, as defined by a >100 m of unit O2 thickness, centered at CMP 66,000 and 69,500. Two modern basins , as defined by the >50 m O1 unit, are centered at CMP 65,500 and 70,500. A Tertiary high, located between CMP 67,000 and 68,500, separates the ancestral basins. The northern most basin exhibits a northward shift in basin center from the ancestral basin to the modern basin. In the southern basin, the location of maximum thickness for unit O1 and unit O2 suggests a slight southward direction of basin shift. However, the modern deepest location of the basin is between CMP 68,500 and 69,000. The unit O3 high that separates two

depocenters is covered by 50 m of O1 and O2 strata, suggesting continuous Holocene deposition along the length of the profile.

I interpret three faults as defined by stratigraphic offsets along the profile. Faults at 65,400; 68,000; and 68,500 offset O1 and water-bottom reflectors (Figure 26). A fault at CMP 65,400 offsets the boundary between Unit O2 and Unit O3 by 50 m. The bathymetric lineation at CMP 66,000 offsets the water bottom by 20 m and offsets the base of O1 by 50 m. However, there is no offset of the base of O2 suggesting this is not a fault. The fault at CMP 68,000, L2, offsets the water-bottom by 10 m and offsets the base of unit O1 by 30 m. Furthermore, this fault has approximately 25 m of offset on the base of O2. I suggest erosion may account for the larger apparent offset at the base of O1. The fault at CMP 68,500 offsets the water bottom by 10 near surface and 70 m at the base of unit O2. I suggest the modern southern basin is controlled by faults L1 and L2 with the deepest area of the basin south these faults. Furthermore, after removing the thickness of the landslides along southern margin of this profile, the modern depocenter would occur between CMP 68,500 and 69,000.

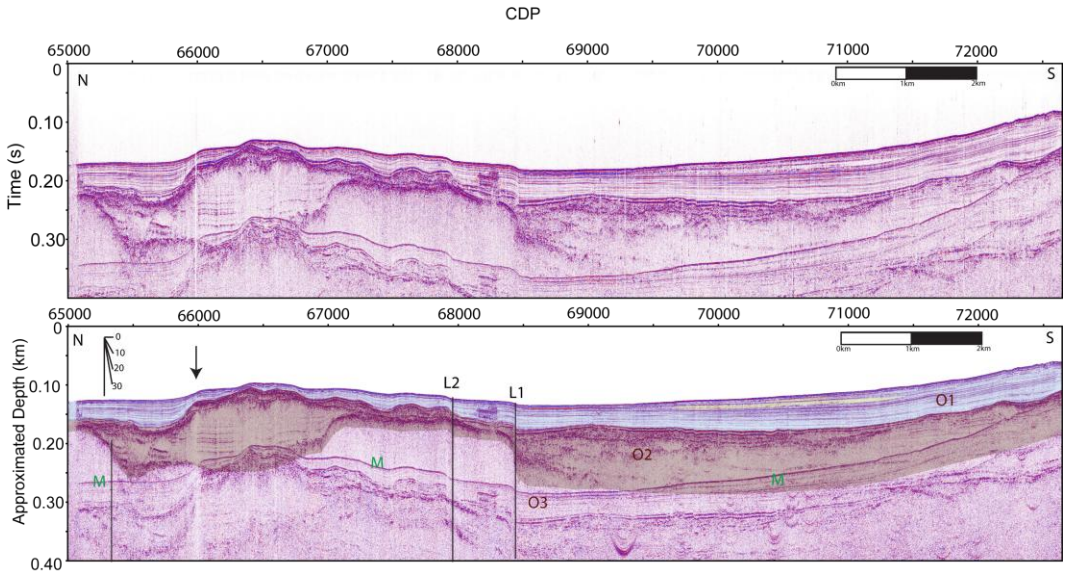

Figure 26: (top) Unmigrated traveltime stack for Orca 8. (bottom) Migrated depth converted stack of Orca 8. Seismic multiple displayed on profile with green "M." The arrow represents a water bottom lineation without evidence for offset on deeper reflectors. Dip meter in top right shows angle of reflectors or faults on profile.

Seismic Profile Orca Bay 9 (Orca 9)

The 4.5 km west-east Orca 9 profile crosses the bathymetric high that extends from Hinchinbrook Island in water depth that range from 80 m to 200 m (Figure 18; Figure 27). The sea floor slopes gradually to the east. The profile was acquired between 11:52 AM and 12:29 PM local time with an average boat speed of 2.01 m/s, shot spacing of 3.06 m, and binned CMP spacing of 1.5 m.

The unmigrated seismic section for Orca 9 reveals reflections to more than 0.2 s two-way travel time below the water bottom reflector (Figure 27). On the migrated and depth converted image, I interpret three layers below the water bottom to represent the Holocene (Unit O1), undifferentiated Quaternary (Unit O2), and Tertiary strata (Unit O3). Unit O1 represents the shallowest strata and varies in thickness to a maximum of 80 m near CMP 76,000. Unit O2 stratigraphically underlies Unit O1 along the profile. The

basal seismic unit that I interpret is Unit O3. This basal reflector is relatively flat lying along the profile at about 250 m depth.

I identify a single lineation at CMP 75,300 (Figure 27). The lineation coincides with offsets Unit O1 and O2. The water-bottom is offset less 2 m while the top of unit O2 is offset by 40 m. The offset is located along a 40 km long water bottom lineation (Figure 27). I suggest the lineation at CMP 75,300 bounds the Orca Bay basin on the south. This lineation is not a fault because of the lack of offset along the unit O2-O3 contact.

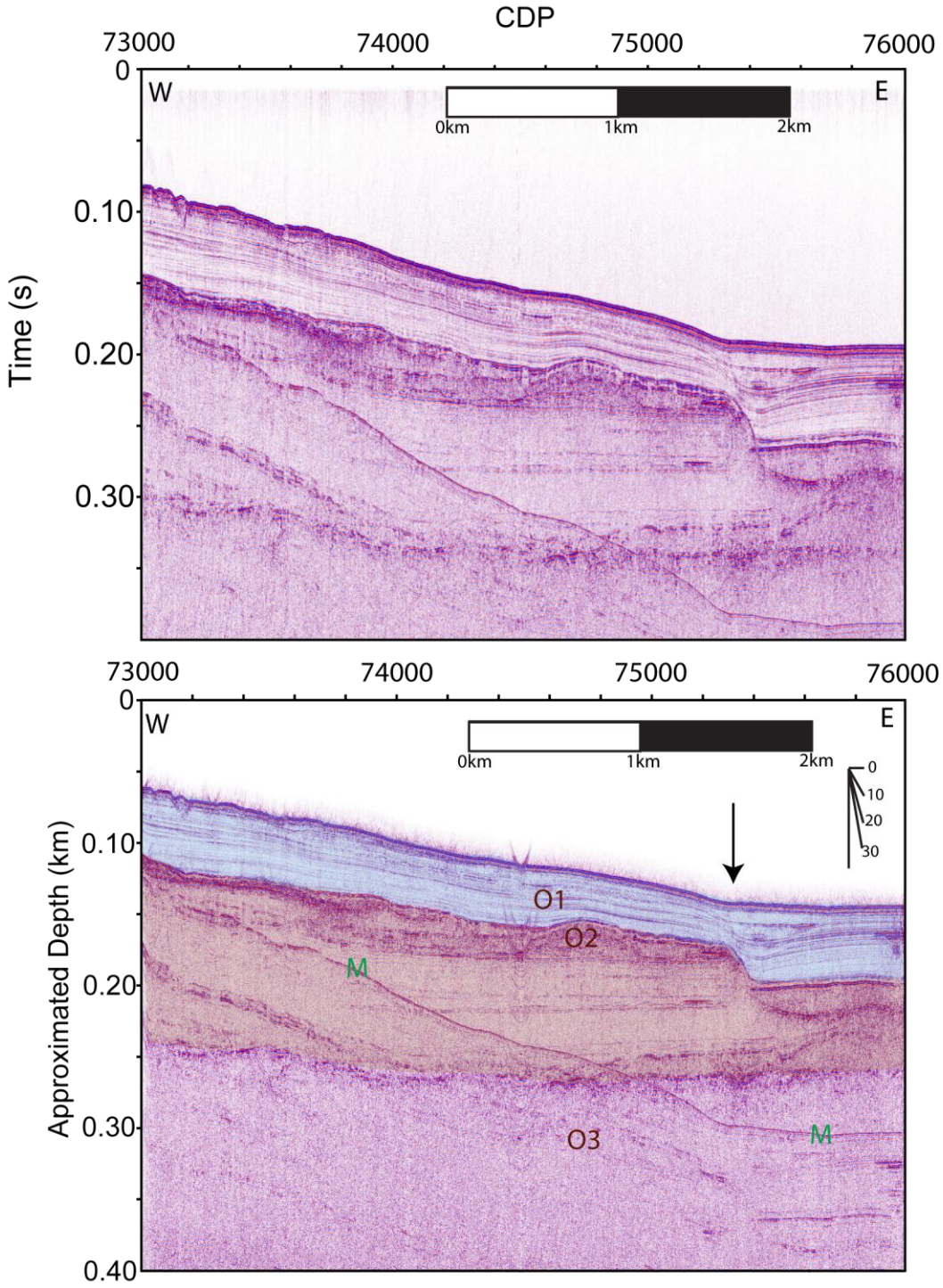

Figure 27: (top) Unmigrated traveltime stack for Orca 9. (bottom) Migrated depth converted stack of Orca 9. Seismic multiple displayed on profile with green "M." Dip meter in top left shows angle of reflectors or faults on profile.

Seismic Profile Orca Bay 10 (Orca 10)

The 18.4 km north-south Orca 10 profile in central Orca Bay (Figure 17) crosses two bathymetric highs that extend from Gravina Point toward central Orca Bay and two bathymetric lows that extend from Gravina Bay and Sheep Bay in water depth that range from 25 m to 160 m (Figure 18; Figure 28). An asymmetric bathymetric high that is centered at CMP 82,000 has a steep sided north slope and mostly gradual south slope. The profile was acquired between 12:31 PM and 2:45 PM local time with an average boat speed of 2.3 m/s, shot spacing of 3.06 m, and binned CMP spacing of 1.5 m.

The unmigrated seismic section for Orca 10 reveals reflections to more than 0.2 s two-way travel time below the water bottom reflector (Figure 28). On the migrated and depth converted image, I interpret three layers below the water bottom to represent the Holocene (Unit O1), undifferentiated Quaternary (Unit O2), and Tertiary strata (Unit O3). Unit O1 represents the shallowest strata and varies in thickness to a maximum of 70 m. Unit O2 stratigraphically underlies Unit O1 and is most clearly imaged between CMP 77,000 and 80,000. The basal seismic unit that I interpret is Unit O3. I have identified an ancestral basin within unit O2 at CMP 78,000. The modern depocenters are at 79,500 and 85,000. I suggest the depocenter at CMP 79,500 has migrated to the north.

I identify seven faults as defined by offsets of stratigraphic units along the Orca 10 profile (Figure 28). The faults at CMP 80,000 and 84,100 offset the water-bottom by 10 m and 20 m, respectively, and the top of O2 by 30 m and 30 m. The fault at CMP 80,000 offsets stratigraphic layers within Unit O1 by as much as 50 m. Faults at 78,800; 85,000; and 86,200 offset Unit O1 strata by 20 m, 20 m, and 40 m, respectively. I suggest

the fault at CMP 80,000 is the northern bounding fault of southeastern Orca Bay with the Gravina Point as the footwall.

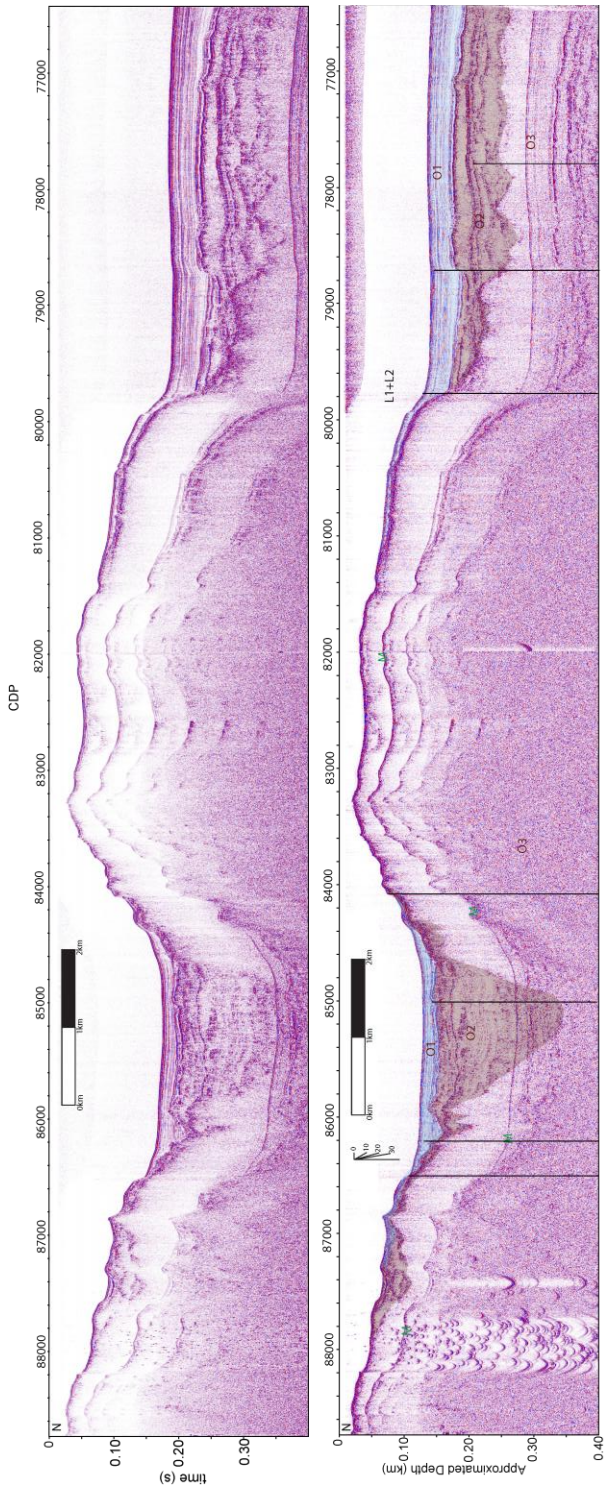

Figure 28: (top) Unmigrated traveltime stack for Orca 10. (bottom) Migrated depth converted stack of Orca 10. Seismic multiple displayed on profile with green "M." Dip meter in top right shows angle of reflectors or faults on profile.

Seismic Profile Orca Bay 11 (Orca 11)

The 2.53 km north-south Orca 11 profile crosses the bathymetric low that extends from Gravina Point (Figure 18) in water depth that range from 40 m to 155 m (Figure 29). An asymmetric bathymetric low is centered at CMP 21,500 with a steep sided north slope. The profile was acquired between 5:05 PM and 5:45 PM local time with an average boat speed of 2.5 m/s, shot spacing of 3.3 m, and binned CMP spacing of 1.5 m.

The unmigrated seismic section for Orca 11 reveals reflections to more than 0.2 s two-way travel time below the water bottom reflector (Figure 29). On the migrated and depth converted image, I interpret three layers below the water bottom to represent the Holocene (Unit O1), undifferentiated Quaternary (Unit O2), and Tertiary strata (Unit O3). Unit O1 represents the shallowest and varies in thickness to a maximum of 100 m. Unit O2 stratigraphically underlies Unit O1 and is most clearly imaged between CMP 21,000 and 22,000. The basal seismic unit that I interpret is Unit O3.

Based on stratigraphic offsets, I interpret three faults at CMP 20,950; 21,000; and 21,950. The fault at CMP 20,950 offsets the base of unit O1 by 20 m (Figure 29). The fault at CMP 21,000 offsets unit O1 strata by 30 m. The fault at CMP 21,950 offset the water bottom by 50 m and unit O1 by at least 70 m. Furthermore this fault is identified by folding of Holocene sediments within the hanging wall. A water bottom expression related to this fault extends laterally for at least 10 km (Figure 18).

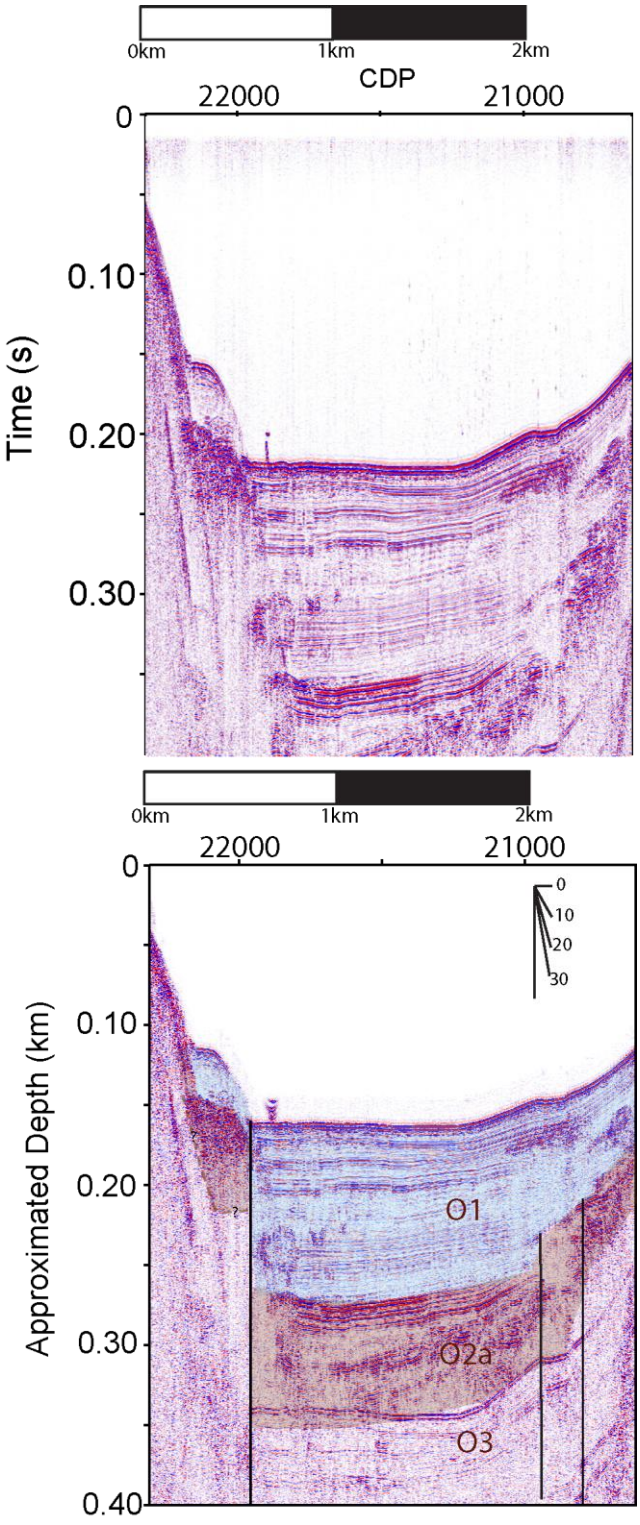

Figure 29: (top) Unmigrated traveltime stack for Orca 11. (bottom) Migrated depth converted stack of Orca 11. Seismic multiple displayed on profile with green "M." Dip meter in top right shows angle of reflectors or faults on profile.

Seismic Profile Orca Bay 12 (Orca 12)

Seismic Profile Orca 12 was acquired from Hawkins Island north to Sheep Bay (Figure 18). This 9.9 km north-south profile crosses a bathymetric high in water depth that range from 50 m to 225 m (Figure 30). The asymmetric bathymetric high is centered at CMP 28,500 with a steep sided south slope. The profile was acquired between 5:57PM and 7:09PM local time with an average boat speed of 2.3 m/s, an average shot spacing of 3.1 m, and binned CMP spacing of 1.5 m.

The unmigrated seismic section for Orca 12 reveals reflections to more than 0.2 s two-way travel time below the water bottom reflector (Figure 30). I interpret three layers below the water bottom that I interpret to represent the Holocene (Unit O1), undifferentiated Quaternary (Unit O2), and Tertiary strata (Unit O3). Unit O1 represents the shallowest reflector and varies in thickness to a maximum of 60 m. Unit O2 stratigraphically underlies Unit O1 and is most clearly imaged between CMP 25,500 and 27,000. The basal seismic unit that I interpret is Unit O3.

Five faults, as defined by offset reflectors, are located at CMP 25,700; 26,200; 30,200; 31,200; and 31,300. The fault at CMP 25,700 offsets reflectors within unit O2 by 10 m (Figure 30). The fault at CMP 26,200 offsets the water bottom by 30 m. The contact between unit O1-O2 is offset by this fault by at least 60 m. The fault at CMP 30,200 offset the unit O1 strata by 10 m and unit O1-O2 boundary by at least 30 m. At CMP 31,200, the fault offsets the unit O1-O3 contact by 25 m. A change in depth of 15 m occurs at the water bottom and the fault scarp appears highly eroded and draped onto surrounding strata. The fault at 31,300 shows a well-defined offset of 20 m. I interpret the

faults at 31,200 and 31,300 to be components of the bathymetric lineation L1 the intercepts profiles Orca 3, 5, 8, and 10 (Figure 32).

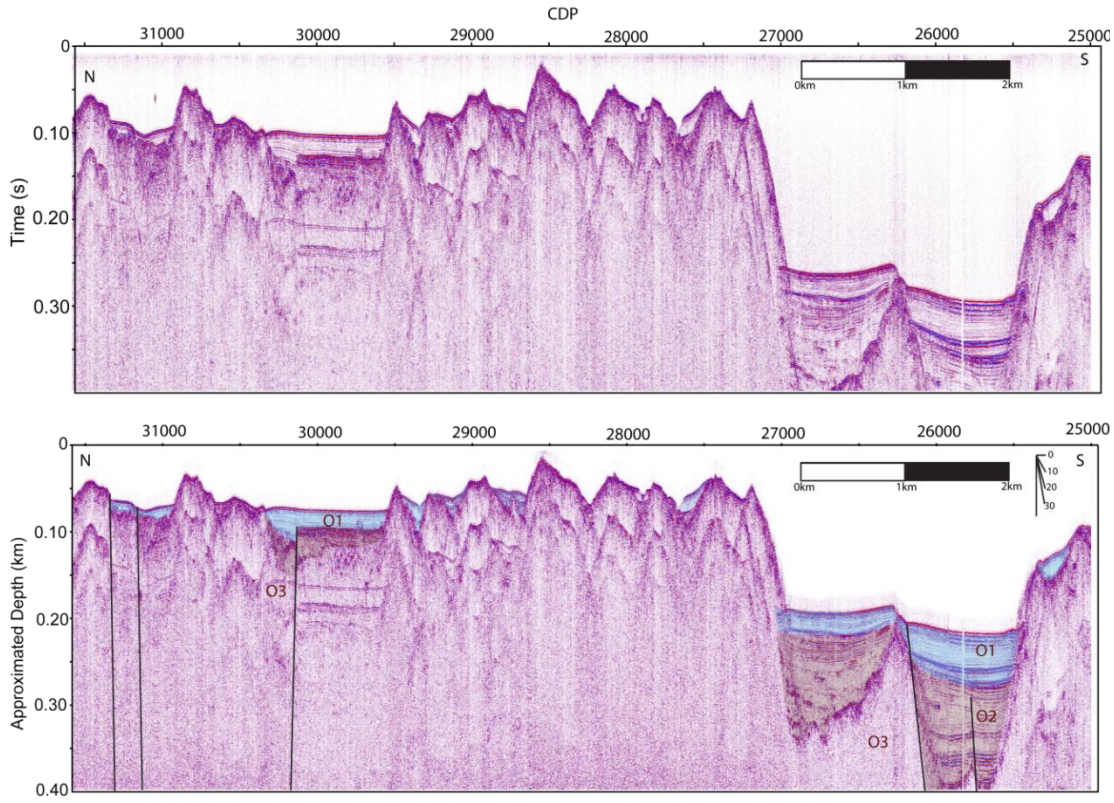

Figure 30: (top) Unmigrated traveltime stack for Orca 12. (bottom) Migrated depth converted stack of Orca 12. Seismic multiple displayed on profile with green "M." Dip meter in top right shows angle of reflectors or faults on profile.

Seismic Profile Orca Bay 13 (Orca 13)

Orca 13 was acquired from central Gravina Point south toward Hawkins Island (Figure 18). This 2.6 km north-south profile crosses the bathymetric low that extends from Sheep Bay toward Hinchinbrook Island in water depth that range from 50 m to 90 m (Figure 31). The asymmetric bathymetric high is centered at CMP 35,000 with a steep sided south slope. The profile was acquired between 7:37PM and 7:58PM local time with an average boat speed of 2.1 m/s, an average shot spacing of 2.8 m, and binned CMP spacing 1.5 m.

The unmigrated seismic section for Orca 13 reveals reflections to more than 0.1 s two-way travel time below the water bottom reflector (Figure 31). I interpret three layers below the water bottom that I interpret to represent the Holocene (Unit O1), undifferentiated Quaternary (Unit O2), and Tertiary strata (Unit O3). Unit O1 is the shallowest strata and varies in thickness to a maximum of 50 m. Unit O2 stratigraphically underlies Unit O1 and is most clearly imaged between CMP 34,500 and 35,400. The basal seismic unit that I interpret is Unit O3.

Three faults, as defined by reflector offsets, are located at CMP 34,550; 35,000; and 35,400. The fault at CMP 34,550 offsets unit O1-O2 contact by 20 m and the unit O2-O3 boundary by 50 m (Figure 31). At CMP 34,550, there is a distinct slope change of unit O1 strata. Also at CMP 35,000, there is a distinct slope change and unit O1-O2 boundary is offset by at least 10 m. At CMP 35,400, there is basin bounding fault with water bottom offset of 50 m. I interpret the faults at 34,550 and 35,000 to be components of the bathymetric lineation L1 on the intercepts profiles Orca 3, 5, 8, and 10 (Figure 18).

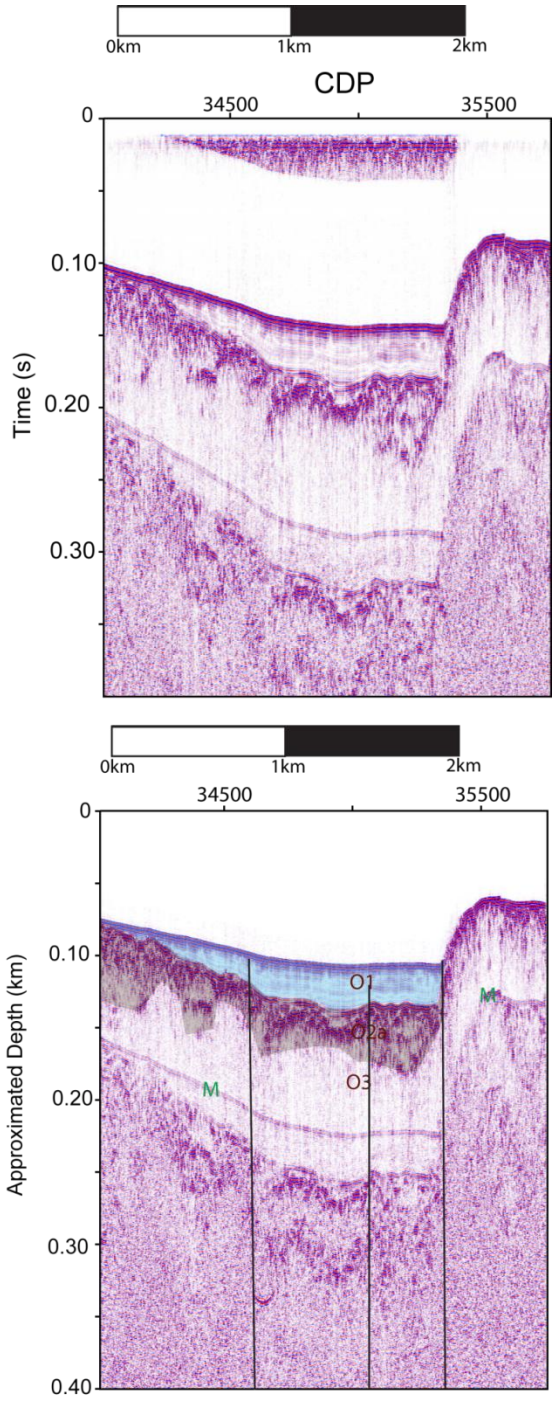

Figure 31: (top) Unmigrated traveltime stack for Orca 13. (bottom) Migrated depth converted stack of Orca 13. Seismic multiple displayed on profile with green "M." Dip meter in top right shows angle of reflectors or faults on profile.

Summary

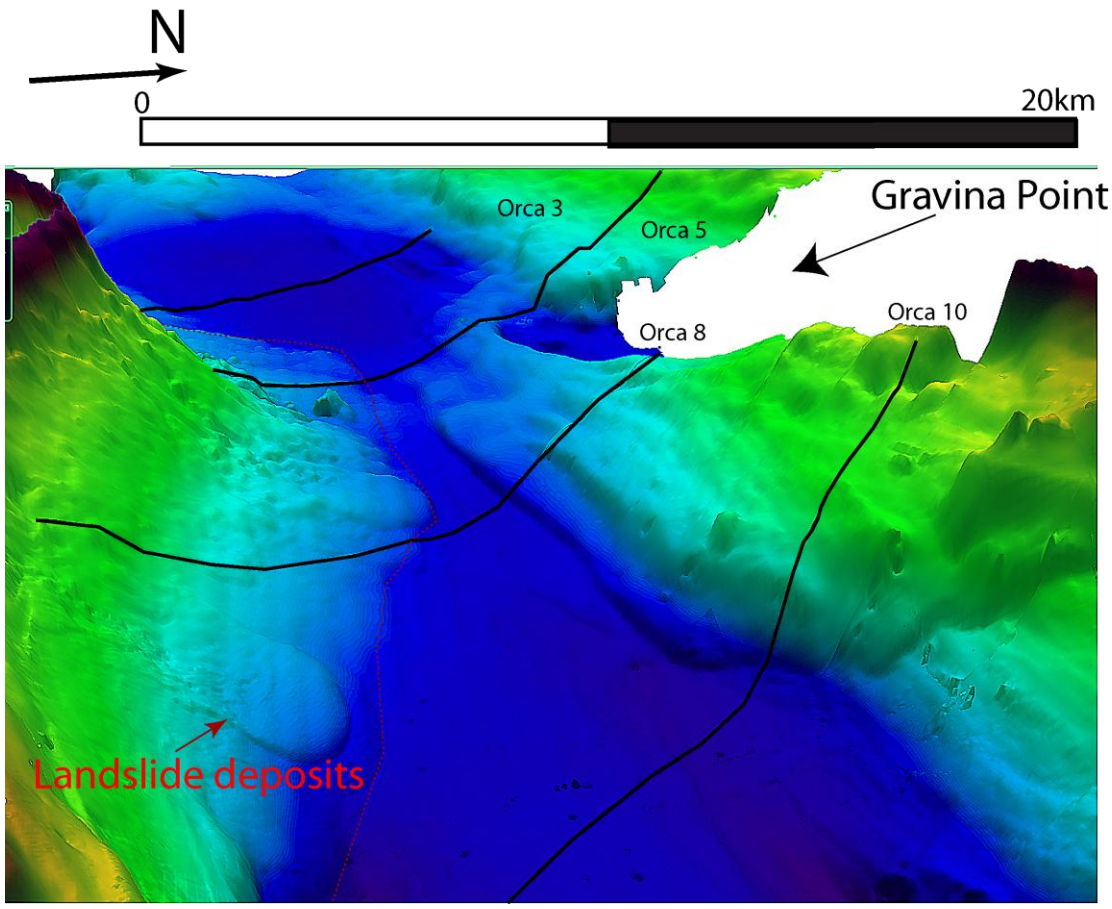

Figure 32: Perspective bathymetry of Orca Bay (NOAA, 2012) (green to blue represents increased water depth), with seismic profiles (black lines). Shows landslide deposits along the southern margin of Orca Bay.

Seismic data from Orca Bay reveal Holocene sediment thicknesses (unit O1) upwards of 70 m and late Quaternary (unit O2) sediment thicknesses upwards of 150 m. I interpret two regionally significant subparallel faults L1 and L2 that predominantly strike east-west. Because many of the faults bound small sedimentary basins, I interpret the majority of faults as high angle faults that extend across Orca Bay and connect to on shore lineations (Wilson and Hults, 2008). If these faults represent basin formation and extension within Orca Bay, they are likely rooted into a deeper megathrust splay fault

related to the subduction of the Pacific plate and Yakutat terrane beneath the North America plate. Based on a continuous lineations throughout Orca Bay and variable offset along strike of those lineations, I interpret the faults imaged on Orca 3, 5, 8, and 10 as related to lineation L1 and L2. These faults to be tectonically driven and not related to sediment drape (Figure 21;Figure 23; Figure 26; Figure 28). L1 and L2 extend for at least 50 km within Orca Bay. L1 parallels faults mapped on land in eastern Orca Bay, toward Sheep Bay.

I observe sediments along the northern Hinchinbrook Island to have slumped or collapsed by marine landslide into Orca Bay. I suggest the collapse of these sediments by marine landslide may be related to sediment accumulation creating instability causing collapse. A moderate or shallow earthquake may be responsible for the slope failure.

Gravina Bay Interpretations

Bathymetry

Within Gravina Bay, surface and bathymetric lineations trend predominantly northeast-southwest and are located primarily at depths less than 110 m (Figure 33) (Condon, 1966). Investigation in Gravina Bay was focused toward a lineations, L3, that trends east-west and cross-cuts the more dominate northeast-southwest trending lineations. Lineations mapped on land in northern portion of Port Gravina trend offshore in a southwest direction (Wilson and Hults, 2008) with the water bottom stepping down toward central Bay channel. In central Port Gravina, a north facing scarp appears at a depth greater than 110 m. I interpret lineations to appear more predominantly at shallower depths due to glacial processes and Tertiary bedrock exposures.

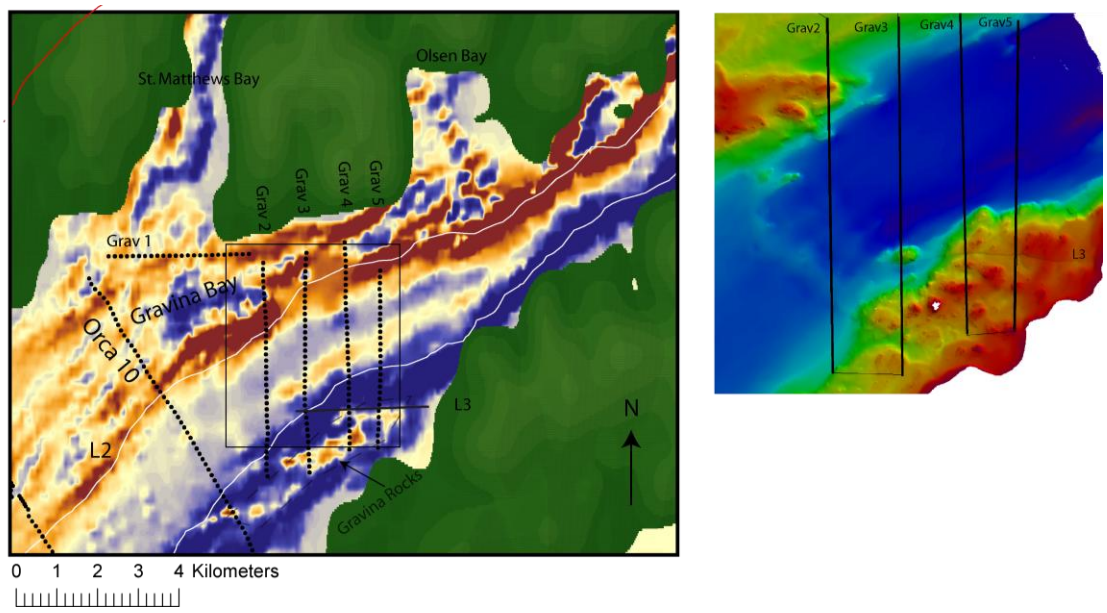

Figure 33: (left) Bathymetric derivative map of Gravina Bay (Red lineations dip southward, blue lineations dip northward) with the five collected reflection seismic data (G1 through G5) (NOAA). Red lines mark faults (Wilson and Hults, 2008). (right) Enhanced image of bathymetry showing lineation L3 that is intersected by seismic profiles Gravina 3,4, and 5.

Seismic Profile Gravina 1 (Grav 1)

The 3.53 km west-east Grav 1 profile is located between St. Matthews Bay and Gravina Bay (Figure 33) and ranges in water depths of 25 m to 60 m (Figure 34). The profile was acquired between 2:53PM and 3:15PM local time with an average boat speed of 2.64 m/s, an average shot spacing of 3.52 m, and binned CMP spacing of 1.5 m.

The unmigrated seismic section for profile Gravina 1 reveals reflections to more than 0.03 s two-way travel time below the water bottom reflector (Figure 34). On the migrated and depth converted image, I interpret three layers below the water bottom to represent the Holocene, undifferentiated Quaternary, and Tertiary strata. Unit G1 represents Holocene strata with a maximum of 20 m sediment thickness between CMP 89,800 and 90,400. Unit G2 stratigraphically underlies Unit G1 and clearly imaged

between CMP 90,800 and 91,000. This unit is characterized by a less acoustically reflective internal layering with clear unconformities both above and below. Based on nearby sedimentation rates estimated by Klein [1983], I interpret the overlying unconformity to represent the last glacial maxima (<10,000 years). I interpret Unit G2 to be composed of coarse to fine grained layered strata. The basal seismic unit is Unit G3. This unit contains little to no internal reflectors and projects to outcrop exposures of older undifferentiated Tertiary strata to the north and west of the profile (Figure 34).

Based on offsets along the boundary between G1 and G3, I interpret two faults along Grav 1 profile (Figure 34). Three lineations that coincide with water bottom offsets are also identified: CMP 89,100; CMP 89,800; and CMP 90,800. CMP 89,300; CMP 89,900; and CMP 90,800 have water bottom offsets of 5m, 20 m, and 20 m respectively. Faults at 89,300 and 89,900 are older faults with at least 15 and 25 m of offset respectively.

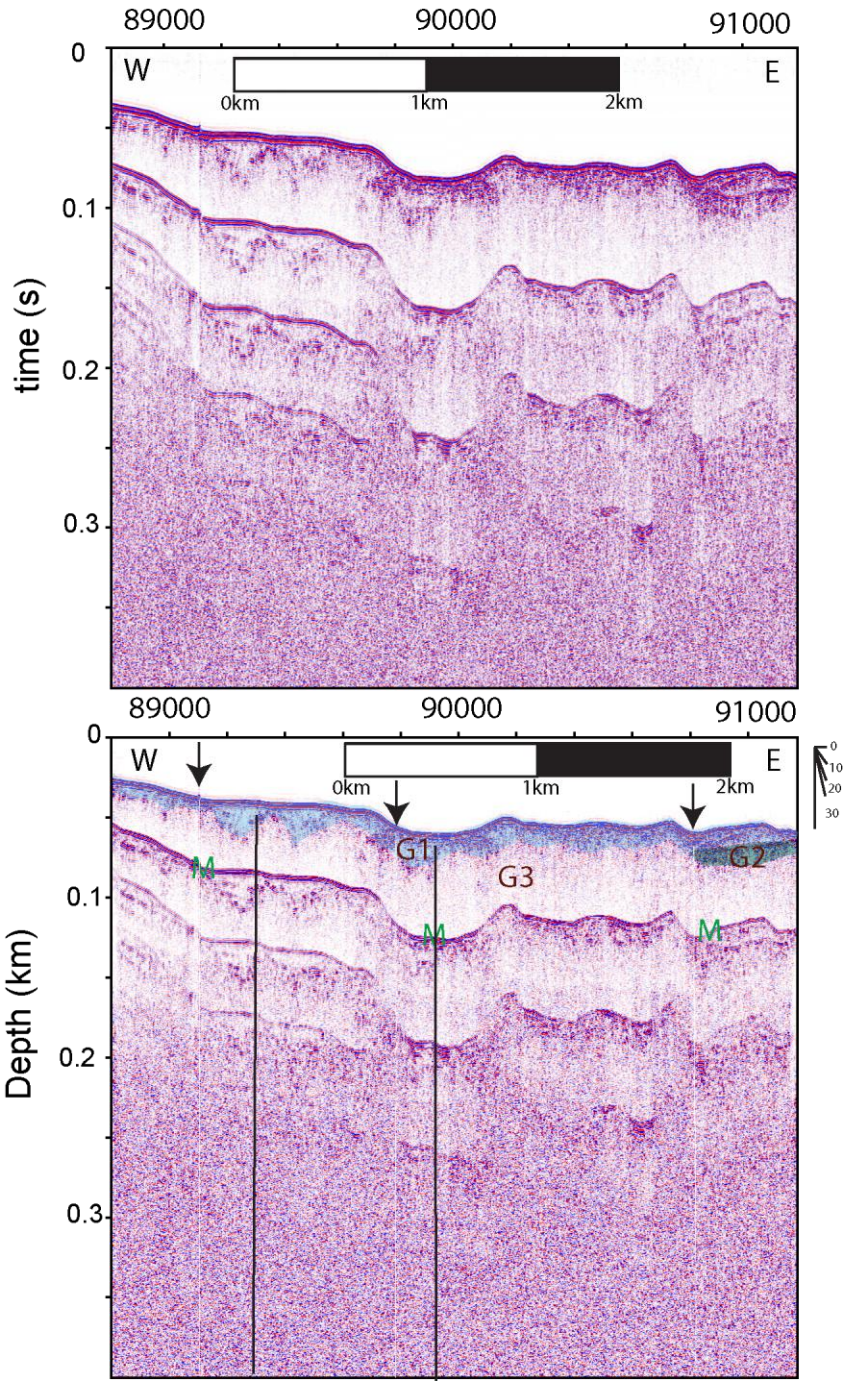

Figure 34: (top) Unmigrated traveltime stack for Gravina 1. (bottom) Migrated depth converted stack of Gravina 1. Seismic multiple displayed on profile with green "M." Dip meter in top right shows angle of reflectors or faults on profile.

Seismic Profile Gravina 2 (Grav 2)

The 5.3 km north-south Grav 2 profile, located in Gravina Bay between St. Matthews Bay and Gravina Point (Figure 33), ranges in depths of 30 m to 180 m (Figure 35). The profile was acquired between 3:36 PM and 4:15 PM local time with an average boat speed of 2.3 m/s, an average shot spacing of 3.03 m, and binned CMP spacing of 1.5 m.

The unmigrated seismic section for profile Grav 2 reveals reflections to more than 0.15 s two-way travel time below the water bottom reflector between CMP 93,000 and 95,000 (Figure 35). From the migrated and depth converted image, I interpret three layers below the water bottom that I interpret to represent the Holocene, differentiated Quaternary, and Tertiary strata. Unit G1 represents Holocene strata with a maximum thickness of 20 m at CMP 92,000. Unit G2 stratigraphically underlies Unit G1 and is imaged between CMP 93,800 and 94,400. With the lack of energy return below Unit G2 and G1-G2 boundary reflection amplitude, I interpret Units G2 to be composed of coarse to fine grained layered sediment. The basal seismic unit is Unit G3. Unit G3 is interpreted to be exposed at CMP 92,400.

Based on water bottom offsets and discontinuities of the boundary between G2 and G3, I identify four faults and one lineation along Gravina 2 profile (Figure 35). From an offset water bottom, I interpret Holocene motion on faults at CMP 92,000 and CMP 93,000 with total water bottom offset of 40 m and 50 m, respectively. Two older, inactive faults bound a depocenter of unit G2. I identify 50 m of offset on G2-G3 boundary across the northern fault at CMP 93,600 whereas I identify 30 m of offset across the southern basin bounding fault at CMP 94,600.

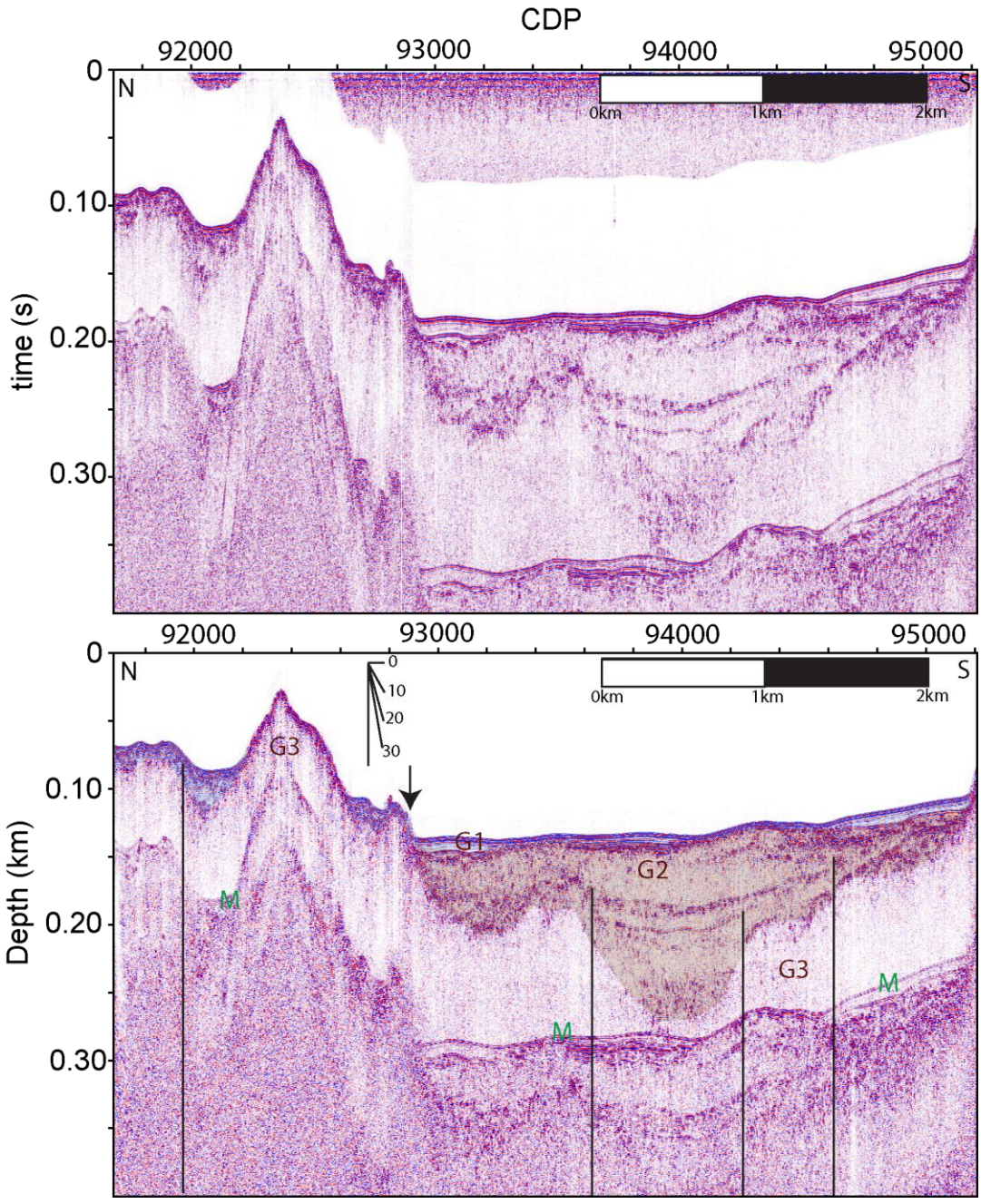

Figure 35: (top) Unmigrated traveltime stack for Gravina 2. (bottom) Migrated depth converted stack of Gravina 2. Seismic multiple displayed on profile with green "M." Dip meter in top right shows angle of reflectors or faults on profile.

Seismic Profile Gravina3 (Grav 3)

The 5.6 km north-south Grav 3 is located between St. Matthews Bay and Olsen Bay (Figure 33) and the profile ranges in water depths from 50 m to 200 m (Figure 36). The profile was acquired between 4:25 PM and 5:02 PM local time with an average boat speed of 2.5 m/s, an average shot spacing of 3.31 m, and binned CMP spacing of 1.5 m.

The unmigrated seismic section for profile Grav 3 reveals reflections to more than 0.1 s two-way travel time below the water bottom reflector between CMP 97,500 and 98,500 (Figure 36). From the migrated and depth converted image, I interpret three layers below the water bottom that I interpret to represent the Holocene, differentiated Quaternary, and Tertiary strata. Unit G1 represents Holocene strata with a maximum of 40 m sediment thickness at CMP 97,800. Unit G2 stratigraphically underlies Unit G1 and is most clearly imaged between CMP 97,200 and 98,400. The basal seismic unit is Unit G3. I interpret Unit G3 to have water bottom exposure between CMP 99,000 and end of profile.

Based on water bottom and G1-G2 or G2-G3 offsets, I interpret four faults and three lineations along the Gravina 3 profile (Figure 36). Based on water bottom offsets across faults at CMP 97,300, I interpret Holocene fault motion. I interpret the fault at CMP 97,300 to have 10 m of water bottom offset and the boundary between Unit G2 and G1 is offset by 20 m. I interpret 40 m of offset at CMP 98,800 (L3), resulting in a local bathymetric high. The lineations at CMP 99,400 and CMP 99,700 have water bottom offsets of 30 m each. The lack of Holocene sediment at lineations at CMP 98,800, CMP 99,400, and CMP 99,700 limits the ability to determine recent slip. Three faults offset older strata but lack water bottom offsets: CMP 96,800; CMP 97,600; and CMP 97,900.

The fault at CMP 96,800 has a 15 m offset across the boundary between G1 and G3. The fault at CMP 96,800 is the northern bound of unit G2. A fault at 97,600 has 15 m of offset along boundary between G1 and G2 as well as an offset of 25 m between G2 and G3. A fault at CMP 97,000 has an offset of 25 m between G2 and G4 with a minimum offset of G3 of 40 m.

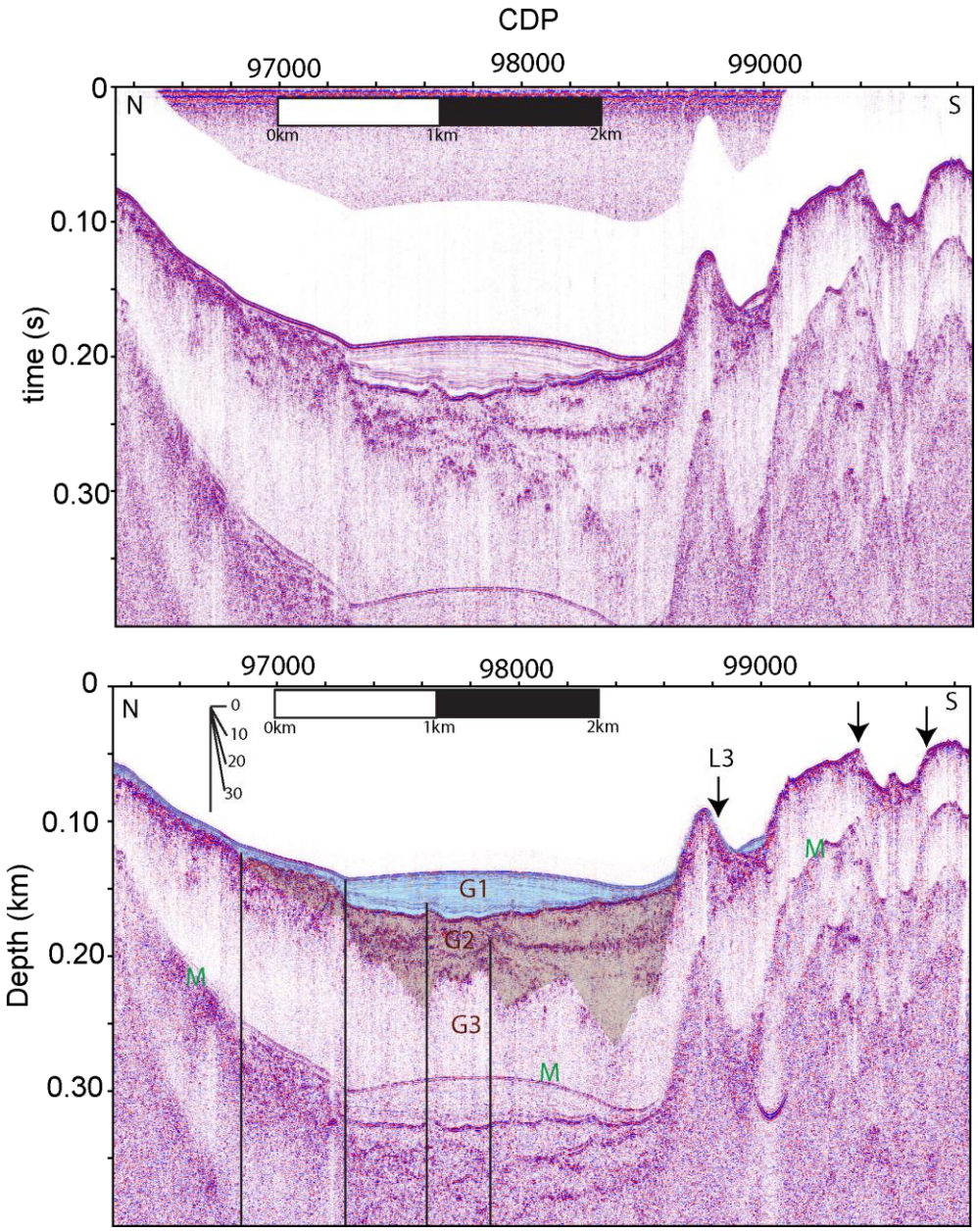

Figure 36: (top) Unmigrated traveltime stack for Grav 3. (bottom) Migrated depth converted stack of Grav 3. Seismic multiple displayed on profile with green "M." Lineation L3 (Figure 33) is at CMP 98,800. Dip meter in top right shows angle of reflectors or faults on profile.

Seismic Profile Gravina4 (Grav 4)

This 5.3 km north-south Grav 4 profile is located between Olsen Bay and Gravina Point and ranges in depths of 25 m to 200 m (Figure 33; Figure 37). The profile

was acquired between 5:09 PM and 5:45 PM local time with an average boat speed of 2.5 m/s, an average shot spacing of 3.3 m, and binned CMP spacing of 1.5 m.

The unmigrated seismic section for profile Grav 4 reveals reflections to more than 0.1 s two-way travel time below the water bottom reflector between CMP 101,500 and 102,200 (Figure 37). From the migrated and depth converted image, I interpret three layers below the water bottom to represent the Holocene, undifferentiated Quaternary, and Tertiary strata. Unit G1 represents Holocene strata with a maximum of 50 m sediment thickness at CMP 101,600. Unit G2a lies below Unit G1 and is most clearly imaged between CMP 100,800 and 102,400. The basal seismic unit G3 is exposed between CMP 102,800 and 103,400.

I interpret four faults along Grav 4 profile (Figure 37). Recent slip as defined by water bottom offset occurred on faults at CMP 102,200. The fault at CMP 101,200 is interpreted to have an offset of 20 m on the boundary between G2 and G1 and 40 m of offset on the boundary between G3 and G2. The lineation at CMP 100,800 is the northern terminus of unit G2. Older basin opening related faults are located at CMP 101,700; 102,000; and 102,200. The fault at CMP 101,800 has 20 m of offset on the G2-G1 boundary.

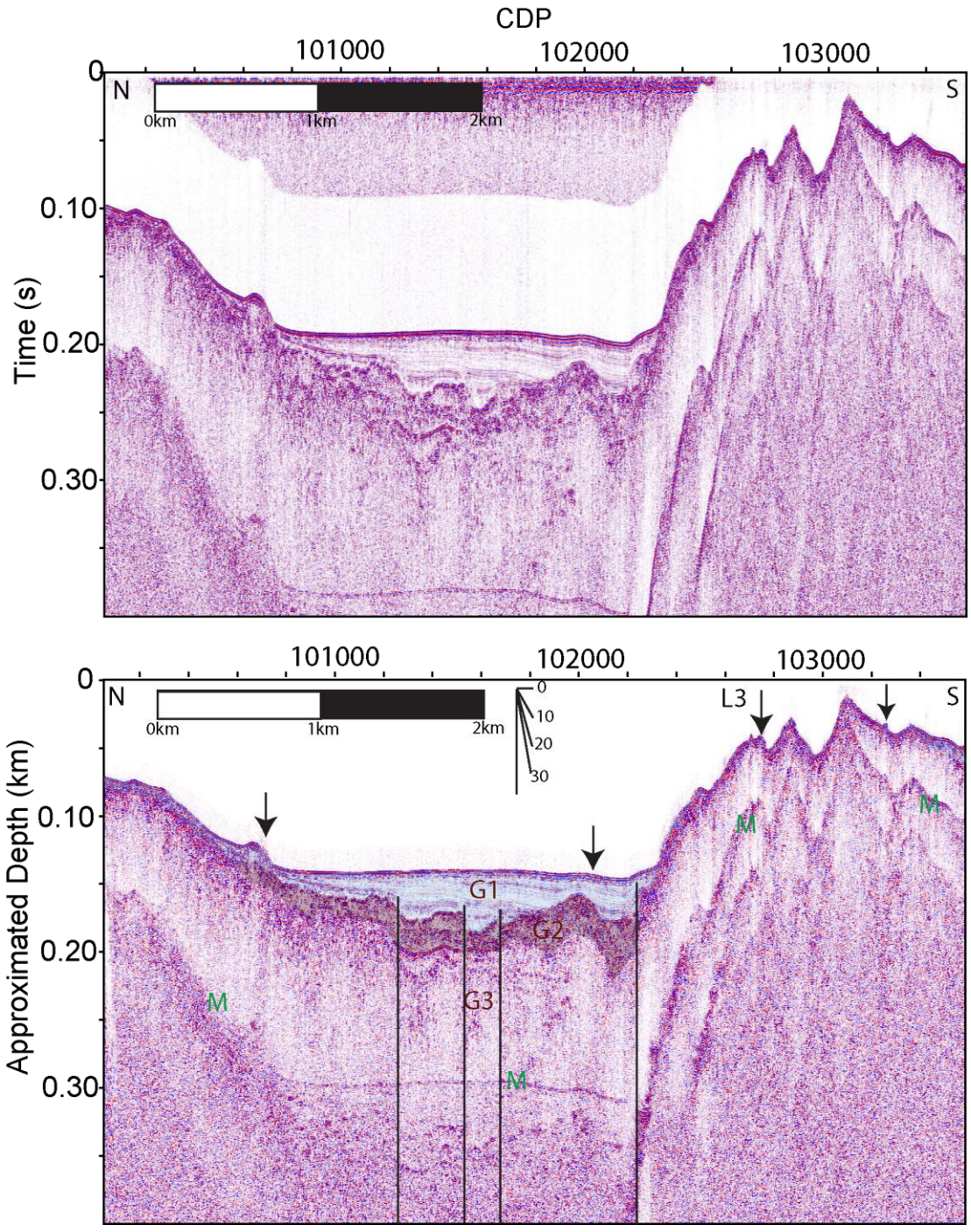

Figure 37: (top) Unmigrated traveltime stack for Grav 4. (bottom) Migrated depth converted stack of Gravina 4. Seismic multiple displayed on profile with green "M." Lineation L3 is located 102,800. Dip meter in top right shows angle of reflectors or faults on profile.

Seismic Profile Gravina5 (Grav 5)

Seismic profile Grav 5 was acquired from central Port Gravina north to Olsen Bay (Figure 33). This 4.5 km north-south profile ranges in depths of 15 m to 200 m (Figure 38). The profile was acquired between 5:50 PM and 6:25 PM local time with an average boat speed of 2.2 m/s, an average shot spacing of 3.3 m, and binned CMP spacing of 1.5 m.

The unmigrated seismic section for profile Grav 5 reveals reflections to more than 0.1 s two-way travel time below the water bottom reflector between CMP 105,000 and 106,400 (Figure 38). I interpret three layers below the water bottom to represent the Holocene, undifferentiated Quaternary, and Tertiary strata. Unit G1 represents Holocene strata with a maximum of 50 m sediment thickness at CMP 105,000. Unit G2a stratigraphically underlies Unit G1 and is most clearly imaged within the depositional basin bounded by CMP 105,000 and 106,400. The basal seismic unit G3 has water bottom exposure between CMP 104,000 and 105,000.

I interpret nine faults along Grav 5 profile (Figure 38). Recent slip as defined by water bottom offset appears on faults at CMP 104,600; CMP 104,400 (L3); and 104,200. The fault at 105,000 is the southern terminus of basin filling sediment units G1 and G2. Older and inactive faults are located at CMP 106,400; 106,000; 105,600; 105,400; and 105,200. The fault at 106,400 has 20 m offset of G1-G2 boundary. Fault at 106,000 has offset of 20 m offset at G1-G2 boundary and minimum of 40 m offset on boundary G2-G3. The fault located at CMP 105,600 is interpreted to have offset of 40 m between G1-G2 boundary and minimum of 60 m offset on G2-G3 boundary. Faults at 104,400 and

104,200 bound a past smaller depocenter or channel. The faults of G1-G2 boundary offset of 20 m.

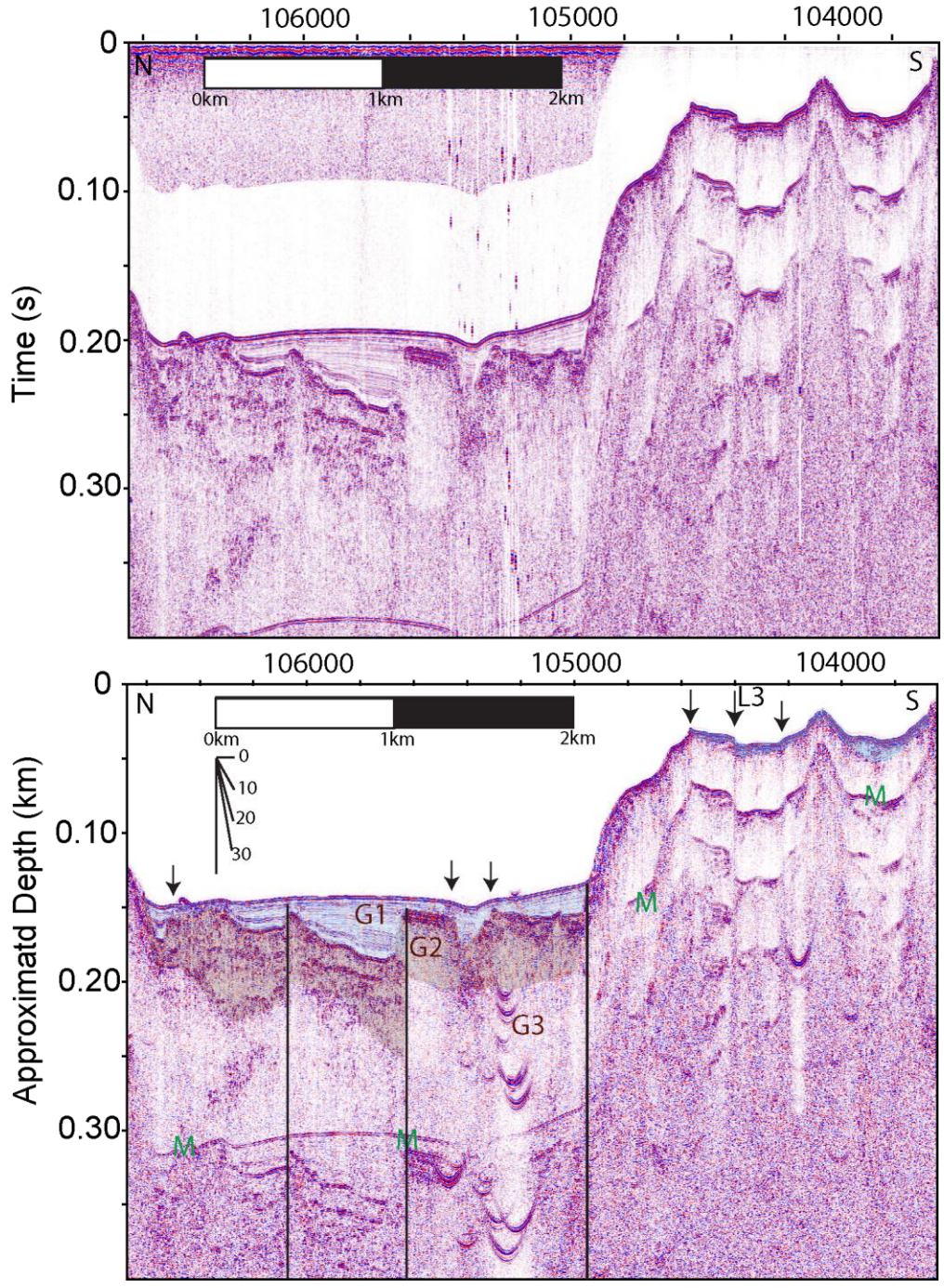

Figure 38: (top) Unmigrated traveltime stack for Grav 5. (bottom) Migrated depth converted stack of Grav 5. Seismic multiple displayed on profile with green "M." Lineation L 3 is exposed at CMP 104,400. Dip meter in top right shows angle of reflectors or faults on profile.

Summary

Within Port Gravina, seismic reflection data show a variation in sedimentation rates perpendicular to the basin axis. Based on the changing thickness of unit G1, I interpret central Port Gravina to have modern sedimentation rates approximately three times greater than the western extent of Port Gravina. Varying thickness of unit G2 show significant fault within Port Gravina. Compared to Orca Bay, central Port Gravina may not have a locally derived sediment source and thus a decrease in sediment rates that is observed on these profiles.

I interpret lineations within the center of Port Gravina to show recent offset and faulting, while along the northern portion of Gravina Point Tertiary units are faulted. The basin is bound by high angle faults that possibly accommodate extension within Port Gravina. Offset that is seen within the basin is along normal faults that predominantly rupture the lower Holocene reflection. I interpret faults within Tertiary rocks to be localized with the greatest expression within the center Gravina Rocks bathymetric high. The east-west lineation L3 is observed on Grav 3, 4 and 5 as a bedrock offset (Figure 33; Figure 36; Figure 37; Figure 38).

Hinchinbrook Entrance

Bathymetry

Hinchinbrook Entrance is a waterway and shipping channel between Hinchinbrook Island and Montague Island (Figure 17). The Hinchinbrook Entrance study includes the area around the exposed Tertiary rocks of Seal Rocks to the northern limits of Montague and Hinchinbrook Islands (Figure 39). Seal Rocks is part of a greater than 25 km N60˚E bathymetric lineament extending along the southern margin of Hinchinbrook Island west and offshore of the eastern limits of Montague Island. I term the Seal Rocks gap as the area between Seal Rocks and Montague Island. Northeast-trending lineations dominate the southern portions of the study site while north-south lineations appear north of Hinchinbrook Entrance.

Sediment related to the Alaska coastal current enters PWS from the south through Hinchinbrook Entrance (Klein, 1983; Jaeger et al., 1998). Sediment cores identify an increase rate of sediment deposition to the north through Hinchinbrook Entrance marked by the L4 region and is clearly identified on bathymetry map (Figure 39).

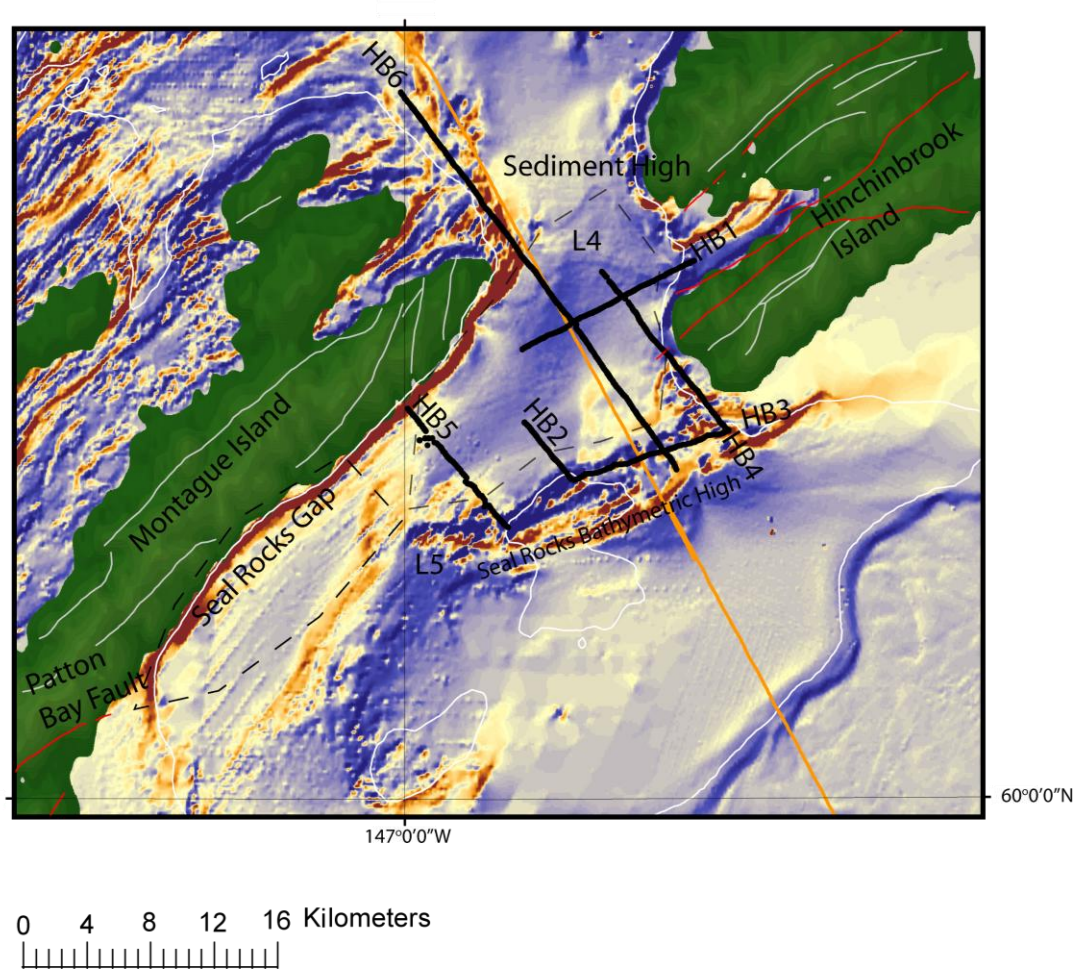

Figure 39: Bathymetric derivative map of Hinchinbrook Entrance (red lineations dip southward, blue lineations dip northward) with the six collected reflection seismic data (H1 through H6) (NOAA bathymetry). Red lines mark lineations (Wilson and Hults, 2008).

Seismic Profile Hinchinbrook Entrance 1 (HB1)

The 15.2 km east-west HB1 profile crosses a bathymetric high sloping from Seal Rocks west to Montague Island (Figure 39). Water depths along this profile range from 75 m to 290 m (Figure 40). Along this profile, a bathymetric high is centered between CMP 43,200 to 43,500 and slopes to the west. The profile crosses a local water bottom high at CMP 45,000. The profile was acquired between 9:48AM and 12:02PM local time

with an average boat speed of 1.89 m/s, an average shot spacing of 1.972 m, and CMP spacing of 1 m.

The unmigrated seismic section for HB 1 reveals reflections to more than 0.1 s two-way travel time below the water bottom reflector (Figure 40). Nearby sediment cores suggest this shallow unit contains post-glacial (<10 kya) sediments shed from local streams and the Copper River delta (Figure 6) (Klein, 1983). On the migrated depth corrected HB1 profile, I interpret three layers below the water bottom that represent the Holocene (H1), undifferentiated Quaternary (H2), and Tertiary strata (H3). Unit H1 represents the shallowest subbottom strata and is characterized by sub-horizontal reflections. Unit H2 stratigraphically underlies Unit H1 and is most clearly imaged between CMP 44,000 and 46,000. This unit is characterized by a seismically transparent zone with angular unconformities defining both the top and bottom of the unit. I interpret the overlying unconformity to represent the last glacial maxima at approximately 12 kA (Hamilton, 1994) and onset of post-glacial sedimentation (Molnia, 1989). Internal reflectivity within Unit H2 may represent any period within the Quaternary record. Given the seismic character with lack of inter-unit reflectors, I interpret the unit as containing mostly coarse-grained sediments (Carlson and Molnia, 1978; Molnia, 1989). The basal seismic unit that I interpret is Unit H3. This unit sits below the lower angular unconformity and shows little to no internal reflectors, projects to outcrop exposures of metasediments, and represents older undifferentiated Tertiary strata.

I interpret the 20 m bathymetry high at CMP 45,000, L4, to represent a fault scarp with the east-facing erosional slope (Figure 40). The related bathymetric lineation extends at least 5 km and crosses seismic profile HB6 (Figure 39). I interpret two water

bottom lineaments at CMP 43,300 and 43,400 that show water bottom expression and offsets the H2-H3 boundary. A fault at 44,400 offsets the H1-H2 contact by 20 m, but does not offset the shallower reflectors, suggesting the fault is inactive. I interpret a fault at 46,000 that offsets reflectors within H1 by at least 7 m but does not offset the water bottom and therefore may not be active.

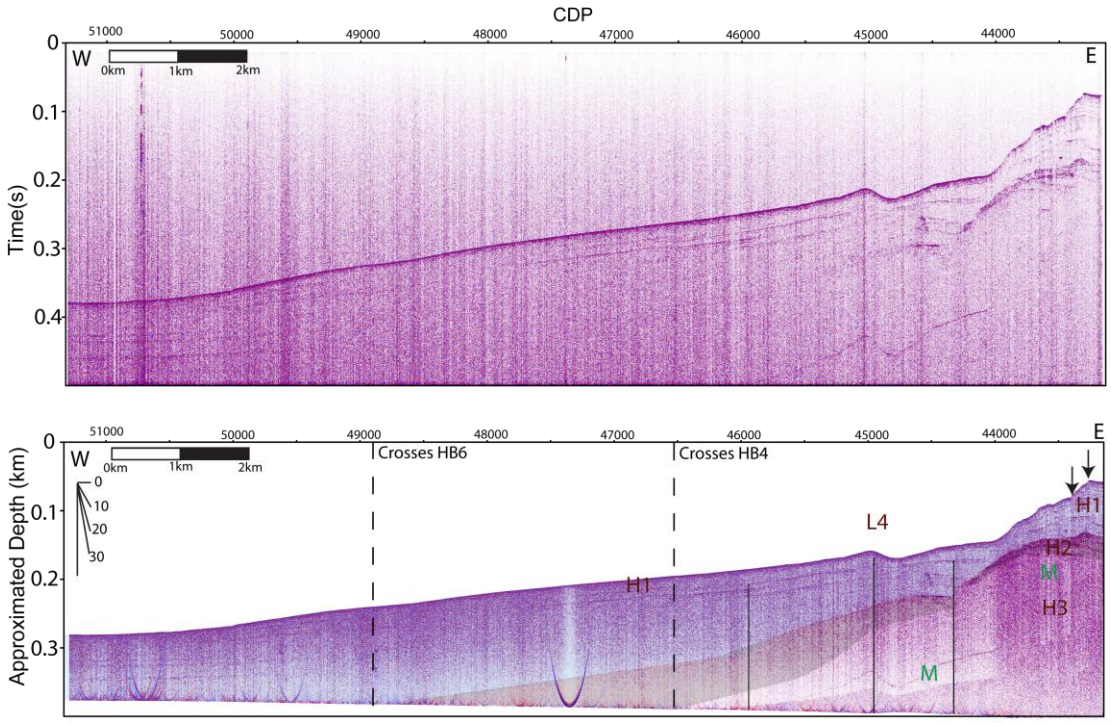

Figure 40: (top) Unmigrated traveltime stack for HB 1. (bottom) Migrated depth converted stack of HB 1. Dashed lines show points of intersection with other seismic profiles as labeled. Seismic multiple displayed on profile with green "M." Dip meter in top right shows angle of reflectors or faults on profile.

Seismic Profile Hinchinbrook Entrance 2 (HB2)

The 8.7 km north-south HB 2 profile crosses the bathymetric high that extends from Seal Rocks in water depth that range from 50 m to 270 m (Figure 39; Figure 41). An asymmetric bathymetric high at CMP 69,100 contains a steep sided north-facing slope. The profile was acquired between 12:45PM and 2:17PM local time with an

average boat speed of 1.57 m/s, an average shot spacing of 1.6 m, and CMP spacing of .8 m.

The unmigrated seismic section for HB 2 reveals reflections to more than 0.2 s two-way travel time below the water bottom reflector (Figure 41). On the migrated and depth converted image, I observe stratigraphic layers H1, H2, and H3 as distinctive units and each layer varies in thickness along the profile. Unit H1contains a maximum of 100 m between CMP 64,000 and CMP 65,000. Unit H2 stratigraphically underlies Unit H1 and is most clearly imaged between CMP 67,000 and 68,000. I interpret an unconformity at the base Unit H1 to represent an erosional surface related to the last glacial maximum. Strong reflectivity within Unit H1 is likely related to alternating fine and coarse-grained strata. Unit H2 contains fewer reflections that Unit H1 and likely contains coarser sediment than Unit H1 (Carlson and Molnia, 1978). The base of Unit H2 was not imaged due to sediment thickness exceeding maximum recorded time. Unit H3 is most clearly imaged between CMP 68,000 and 69,000, projects to the surface at Seal Rocks, and represents Tertiary bedrock.

I interpret reflector offsets at Unit H2 and H3 at CMPs 67,750; and 68,000 to represent faults (Figure 41). Fault offsets vary between several meters and 50 meters. These faults do not cut shallow reflectors, and therefore these faults have no evidence for Holocene motion. A bathymetric lineament is located at CMP 68,100. A bathymetric high of 20 m at CMP 68,400 overlies a 20 m thick paleochannel. The coincident channel and bathymetric high may be related to small marine landslide burying the preexisting channel. A second paleochannel at CMP 67,700 may be related to a meander of the CMP

68,400 channel or may represent channel migration. I interpret the acoustically transparent zone in Unit H1 between 65,500 and 66,500 to be related to gas propagation along a fault (Carlson et al., 1985; Lee and Chough, 2003).

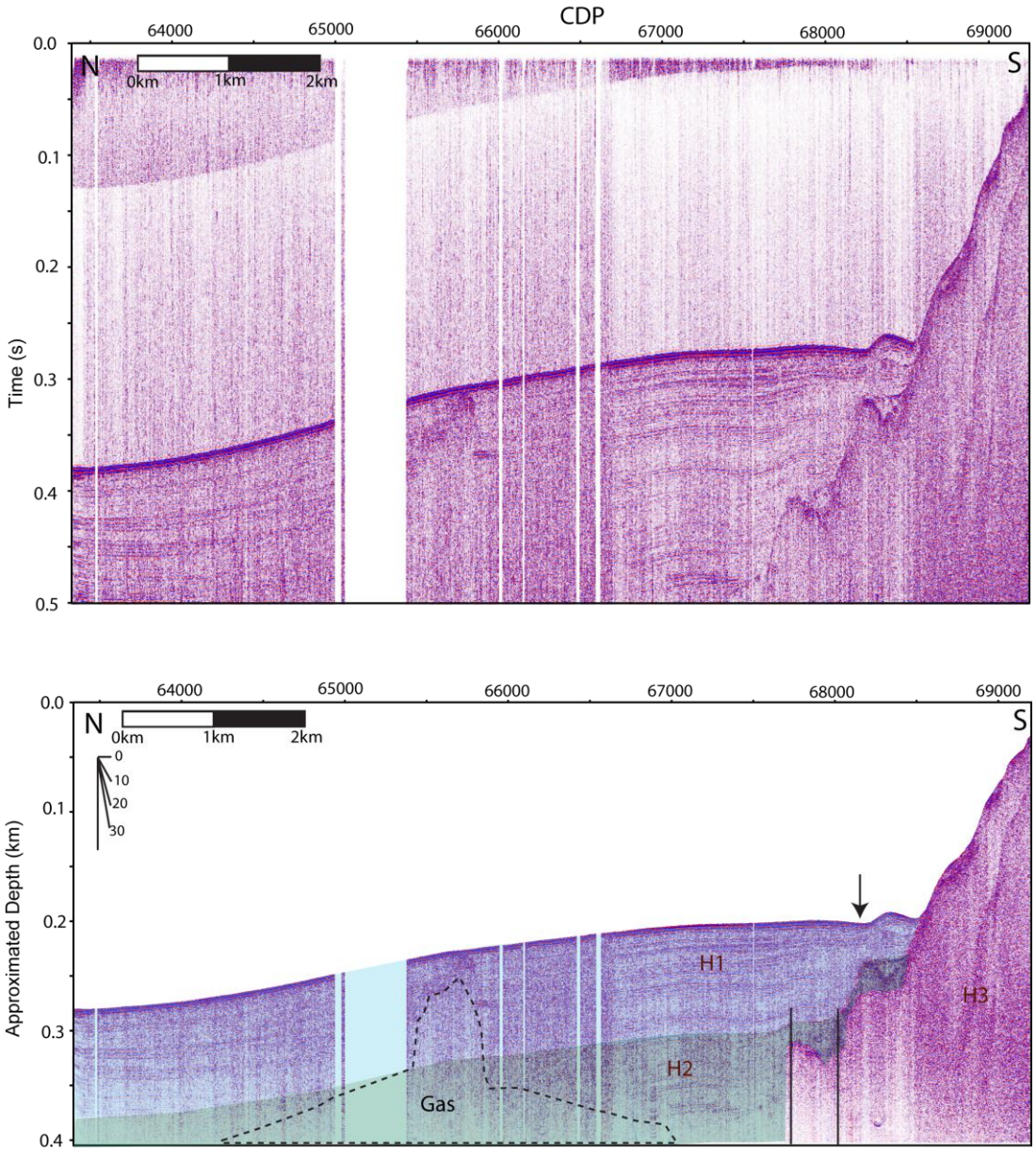

Figure 41: (top) Unmigrated traveltime stack for HB 2. (bottom) Migrated depth converted stack of HB 2. Lower boundary of H2 is not imaged. Seismic multiple displayed on profile with green "M." Dip meter in top right shows angle of reflectors or faults on profile.

Seismic Profile Hinchinbrook Entrance 3 (HB3)

The 10.3 km west-east HB 3 profile is located north of Seal Rocks (Figure 39) and is in water that ranges from 50 m to 210 m depth (Figure 42). The bathymetric high is centered at the beginning of the line with a steep sided east slope. The profile was acquired between 2:18PM and 4:31PM local time with an average boat speed of 1.3 m/s, an average shot spacing of 1.32 m, and CMP spacing of 0.6 m.

The unmigrated seismic section for HB 3 reveals reflections to more than 0.2 s two-way travel time, and 0.05s two-way travel time below water bottom (Figure 42). On the migrated and depth converted image, I observe stratigraphic layers H1 and H3 as distinctive and varying in thickness along the profile. I observe the thickness of Unit H1 up to a maximum of 20 m between CMP 75,000 and CMP 77,000. Unit H3 stratigraphically underlies Unit H1 and is most clearly imaged between CMP 75,000 and 77,000. Unit H3 likely represents the stratigraphy that appears on the Seal Rocks (Figure 42). The seismically transparent Unit H2, observed on profiles HB1 and HB2, is not observed along the profile.

Stratigraphic offsets on unit H3 at CMP 75,100; 75,500; 76,100; and 77,000 may be related to faults that offset strata (Figure 42), however are marked as lineaments because offsets only occur within the single unit. CMP 75,100 and CMP 77,000 also have water bottom offset. CMP 75,100 has a 50 m step down to the east on the H1-H3 boundary and 10 m of offset on the water bottom interface. CMP 75,500 has 10 m of offset on the H1-H3 boundary. CMP 76,100 has 30 m of offset on the H1-H3 boundary.

CMP 77,000 has 50 m of offset of the water bottom with a change in sediment dip on each side of the offset.

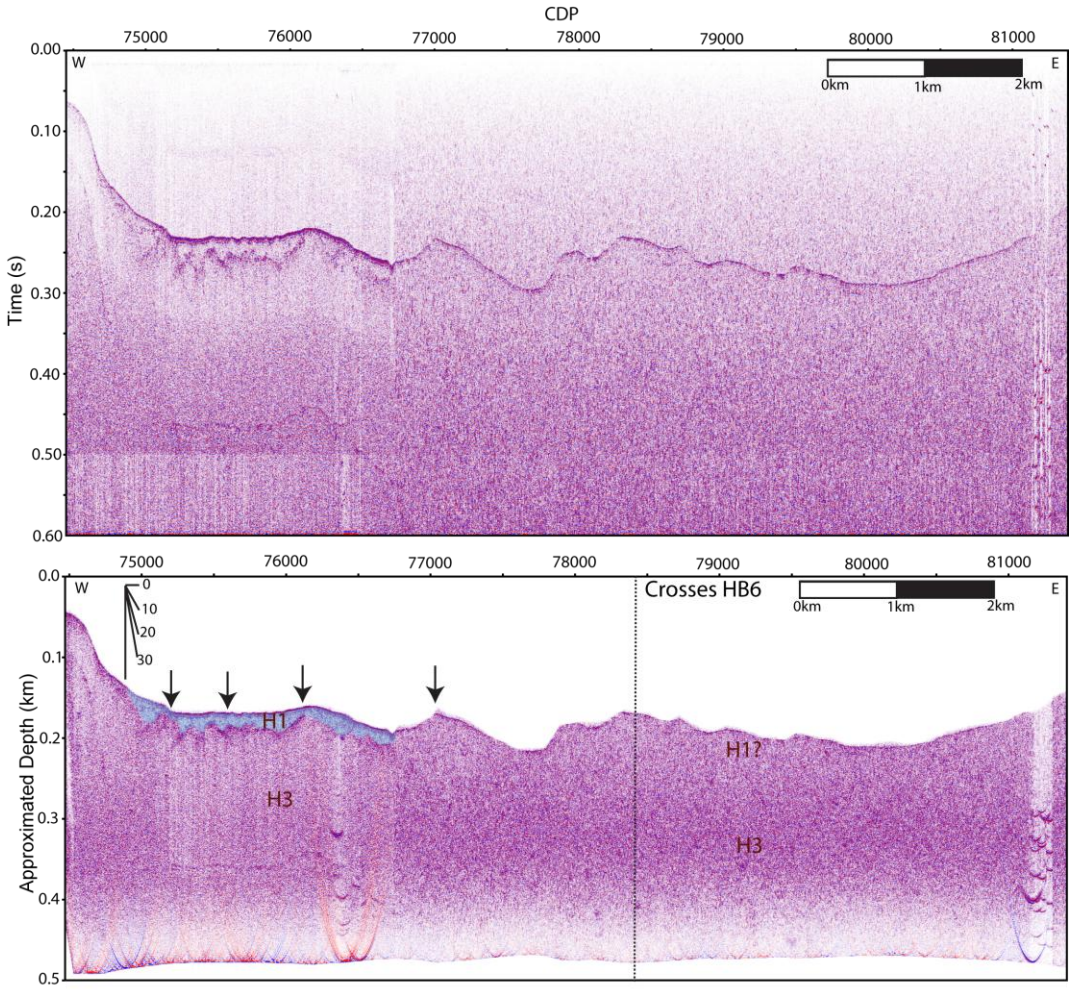

Figure 42: (top) Unmigrated traveltime stack for HB 3. (bottom) Migrated depth converted stack of HB 3. Seismic multiple displayed on profile with green "M." Dip meter in top right shows angle of reflectors or faults on profile.

Seismic Profile Hinchinbrook Entrance 4 (HB4)

Seismic Profile HB 4 was acquired along the west coast of Hinchinbrook Island (Figure 39). The 15.0 km north-south HB 4 profile crosses the bathymetric high that extends west of Seal Rocks (Figure 37) in water depth that range from 40 m to 250 m

(Figure 43). An asymmetric bathymetric high is centered at CMP 93,000 with a steep sided north slope. The profile was acquired between 4:33PM and 6:45AM local time with an average boat speed of 1.89 m/s, an average shot spacing of 2.23 m, and a CMP spacing of 1.1 m.

The unmigrated seismic section for HB 4 reveals reflections to more than 0.2 s two-way travel time below the water bottom reflector (Figure 43). I observe stratigraphic layers H1, H2, and H3 as distinctive and varying in thickness along the profile. I observe the thickness of Unit H1 up to 100 m between CMP 95,000 and CMP 97,000. Unit H2 is present between CMP 94,800-99,400 and is predominantly acoustically opaque. The unconformity between Unit H2 and H3 is likely an erosional surface, similar to the H1-H2 boundary. Unit H3 stratigraphically underlies Unit H2 and is most clearly imaged between CMP 95,000 and 97,000. Unit H3 coincides with the bathymetric high of Seal Rocks (Figure 39).

I interpret an offset of reflectors at the Tertiary-Quaternary as faults in the Tertiary strata at CMP 94,400; CMP 93,900; CMP 92,200; and CMP 91,000 (Figure 43). I identified these locations based on punctuated water bottom slope inflections and significant bathymetric offsets. These faults coincide with bathymetric lineations (Figure 39). I interpret these faults as related to a larger splay fault uplifting the entire bathymetric high with several localized basins. I interpret a fault controlled basin margin at CMP 92,200. I also suggest the depressions along the profile are fault controlled.

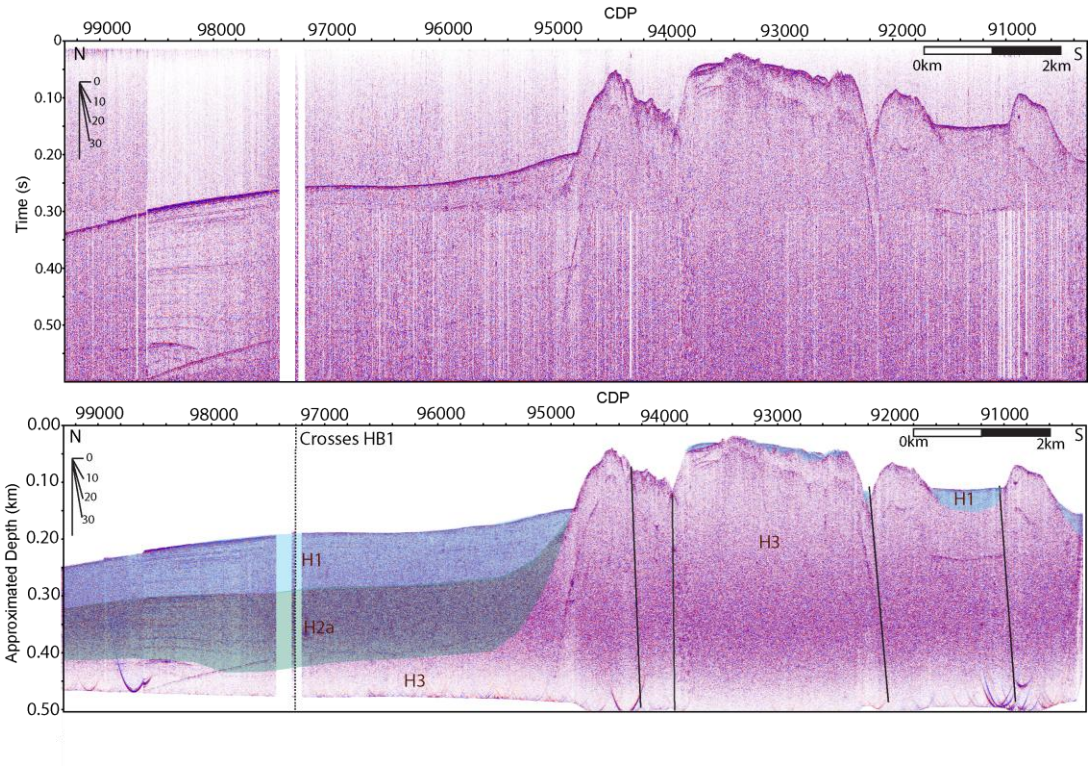

Figure 43: (top) Unmigrated traveltime stack for HB 4. (bottom) Migrated depth converted stack of HB 4. Seismic multiple displayed on profile with green "M." Dip meter in top right shows angle of reflectors or faults on profile.

Seismic Profile Hinchinbrook Entrance 5 (HB5)

The 9.8 km north-south HB5 profile crosses the bathymetric high between CMP 126,000 to CMP 127,000 that extends from Seal Rocks to Montague Island (Figure 39) in water depths that range from 70 m to 270 m (Figure 44). The profile was acquired between 8:54 AM and 2:32PM local time with an average boat speed of 1.5 m/s and an average CMP spacing of 1.53 m.

The unmigrated seismic section for profile HB 5 reveals reflections to more than 0.2 s two-way travel time below the water bottom reflector (Figure 44). On the migrated and depth converted image, I observe stratigraphic layers H1, H2, and H3 as distinctive

and varying in thickness along the profile. Unit H1varies from 0 to a maximum of 150 m thickness at CMP 123,500. Unit H2 stratigraphically underlies Unit H1 and is most clearly imaged between CMP 120,500 and 124,500. Unit H3 surfaces at near the end of the profile at Seal Rocks (Figure 39).

I interpret an antiform centered at 123,500 that overlies a low amplitude reflection zone (Figure 44). The south end of the profile approaches Seal Rock where Tertiary outcrop exposures (Unit H3) are mapped (Wilson and Hults, 2008) (Figure 39). I identify a 50 m offset of the H1-H3 contact at CMP 124,500 and 125,000. H1 is offset by 50 m at CMP 126,000 followed by another offset of 30 m at CMP 126,500. I interpret the acoustically transparent zone in Unit H1 between 122,500 and 124,000 to be related to gas propagation along a fault, with a pull up of seismic reflectors and acoustic attenuation (Carlson et al., 1985; Lee and Chough, 2003).

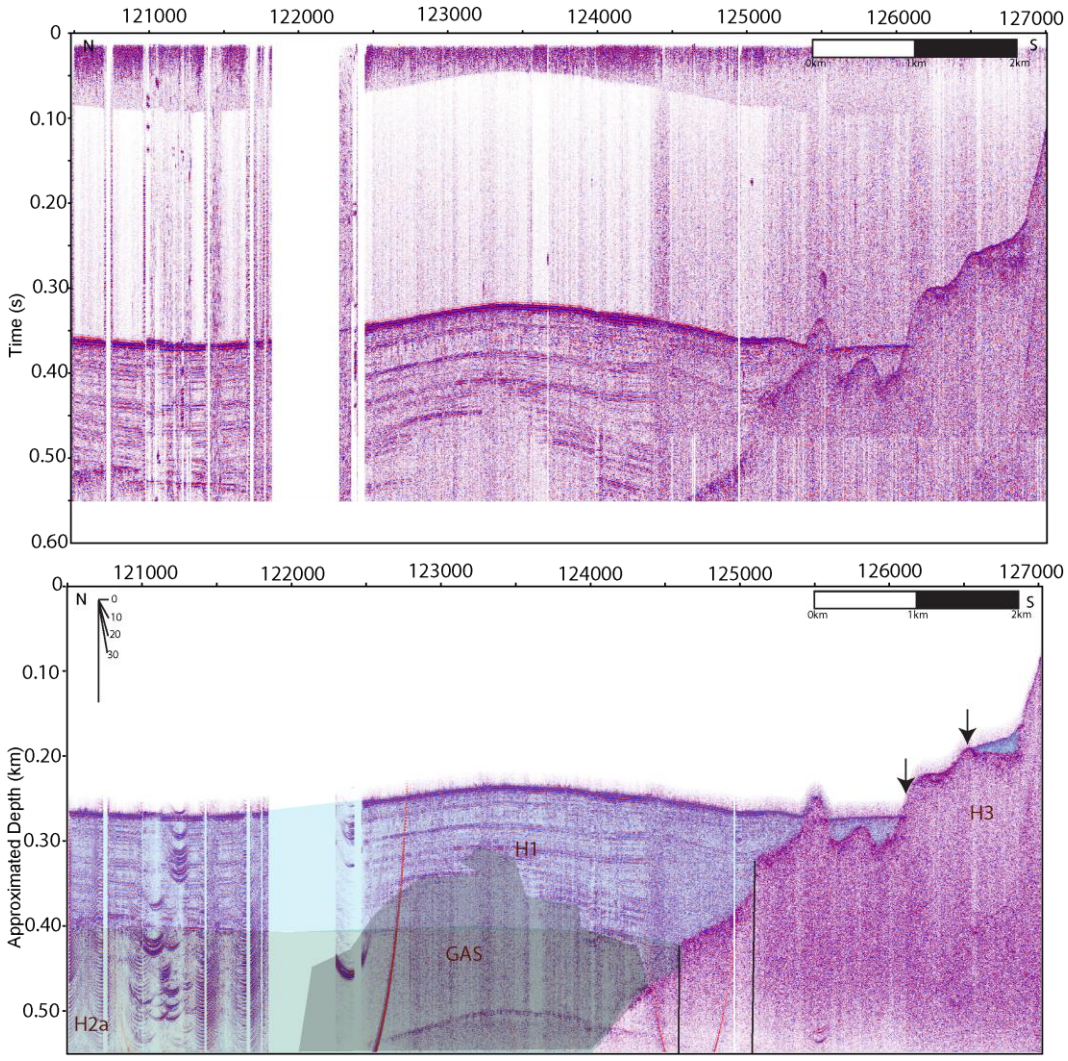

Figure 44: (top) Unmigrated traveltime stack for HB 5. (bottom) Migrated depth converted stack of HB 5. Gas zone observed by opaque seismic reflectance and slight layer "pull-up." Seismic multiple displayed on profile with green "M." Dip meter in top right shows angle of reflectors or faults on profile.

Seismic Profile Hinchinbrook Entrance 6 (HB6)

The 29.5 km north-south HB 6 profile crosses the bathymetric high that extends from Seal Rocks north to central PWS (Figure 39) in water depths that range from 100 m to 225 m (Figure 45). The Seal Rock bathymetric high is centered at CMP 135,000 and with a steep sided north slope. The profile was acquired between 3:40 PM and 7:15 PM local time with an average boat speed of 2.29 m/s and an average CMP spacing of 2.6 m.

The unmigrated seismic section for HB 6 reveals reflections to more than 0.2 s two-way travel time below the water bottom reflector (Figure 45). On the migrated and depth converted image, I observe three stratigraphic layers H1, H2, and H3 as distinctive and varying in thickness along the profile. I observe the thickness of the Holocene unit up to a maximum 200 m at CMP 141,000. Unit H2 stratigraphically underlies Unit H1 and is most clearly imaged between CMP 136,000 and 138,000. Unit H3 is in contact with the water bottom at the northern and southern end of the profile. The southern edge of the profile crosses the lineation related to Seal Rocks (Figure 39). The lack of subbottom reflectivity beneath the northern end of the profile suggests Tertiary rock appears along the sea floor, consistent with Tertiary exposures along northeastern Montague Island (Wilson and Hults, 2008)

I interpret a fault that offsets Unit H1 at CMP 143,500, identified by the 5 m water bottom offset, 10 m Holocene-Quaternary boundary offset, and bounds a paleo-channel. This fault likely ruptured during one of the last few large earthquakes (Figure 45). Faults at 137,500 and 144,500 offset Unit H2 reflectors without offsetting Holocene strata. I interpret faults in the Tertiary basement based on distinctive sharp water bottom relief and lineations that extend more than 20 km on the bathymetry. I interpret the sedimentary basin to be fault bounded at CMP 136,400 and 145,600 based on fault drag deforming H1 strata.

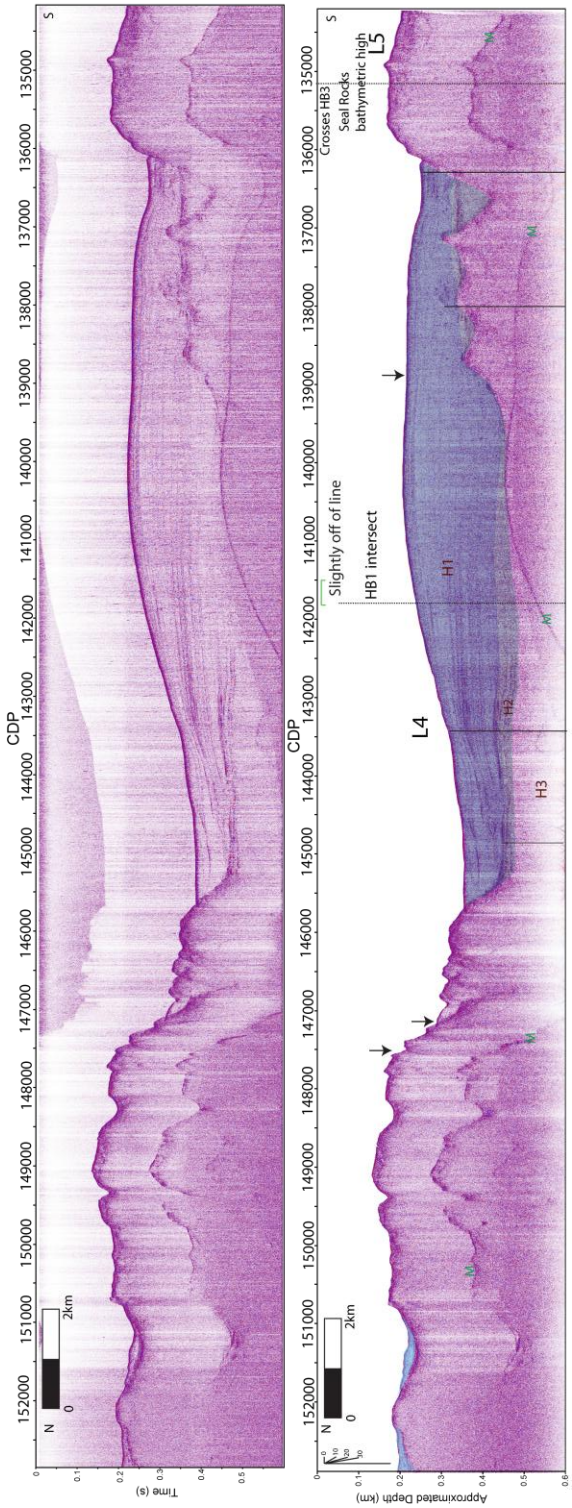

Figure 45: (top) Unmigrated traveltime stack for HB 6. (bottom) Migrated depth converted stack of HB 6. Seismic multiple displayed on profile with green "M." Dip meter in top right shows angle of reflectors or faults on profile.

Summary

The fault controlled Hinchinbrook Entrance represents the along strike expression of the Patton Bay fault system. I interpret lineation L4 that crosses profiles HB1 and HB6 as a fault (Figure 39; Figure 40; Figure 45). Lineation L4 extends from Montague Island to Port Etches of Hinchinbrook Island. I interpret the Lineation L5 extending along Seal Rocks bathymetric high as the surface expression of a fault zone based on reflector offsets and bedrock highs along seismic profiles HB4 and HB6 (Figure 39; Figure 43; Figure 45). Furthermore, water bottom lineation L5 is a narrow 4-km wide zone of Tertiary rock exposed at the water bottom with several exposed rocks related to Seal Rock. I interpret this lineation as a depositional boundary where marine sediments of Copper River are deposited north of the Seal Rocks bathymetric high as water currents are slowed when entering Hinchinbrook Entrance. These sediments are deposited within the glacially enhanced basin that separates Hinchinbrook Island and Montague Island.

I interpret a trapped gas identified on the north slope of Seal Rocks on seismic profiles HB2 and HB5 within Holocene and older Quaternary sediments (Figure 41; Figure 44). The gas zone is a seismically transparent feature, bounded by seemingly continuous stratigraphic layering, and the bounding sediments show a velocity “pull-up” within the gas zone. The gas appears on both HB2 and HB5 and is laterally continuous over at least 5km (Figure 39). There is no gas present on HB6, defining the eastward extent of the gas zone.

Montague Strait Interpretations

Bathymetry

Montague Strait is located in western PWS between Montague Island and the chain of islands consisting of Knight Island and Latouche Island (Figure 17; Figure 46). A portion of the Montague Strait study area includes Knight Island Passage, the channel that separates Latouche Island and Knight Island. Montague Strait trends northeast and Knight Island Passage is nearly a perpendicular bisector.

Northeast-trending bathymetric lineations extend along Montague Strait (Figure 46). A nearly continuous lineation bounds the western Montague Strait shoreline that I interpret as a fault. A water bottom lineation in Hanning Bay represents the Hanning Bay fault that slipped during the 1964 earthquake (Plafker, 1969). Along the shallow water eastern regions of Montague Strait, N45˚E lineations appear (Figure 46). I interpret these lineations to represent glacially scoured rock from glaciers that occupied shallow water portions of Montague Strait.

Lithology

Based on seismic character, I identify three lithologic units within Montague Strait. Unit M1 represents Holocene sediment related to Copper River and smaller source rivers (Klein, 1983). The highly reflective seismic character of Unit M1 suggests fine grained and well sorted strata that are likely not lithified. Unit M1 is distinguished from other strata by its seismic character and an underlying unconformity. Nearby box and gravity core samples suggest modern sedimentation rates of 0.6 cm/yr for central

Montague Strait and 0.3 cm/yr for southern Montague Strait (Klein, 1983; Page et al., 1995).

Unit M2 stratigraphically underlies Unit M1. This unit is characterized by a more acoustically transparent layering with clear unconformities both above and below. I interpret the overlying unconformity to represent the hiatus in sedimentation during the last glacial maxima. I interpret Unit M2 to be composed of coarse to fine grained layered sediment that either represents an early pulse of sediment related to the last glacial maxima or older glacial sediments.

The basal seismic unit that I interpret is Unit M3. This unit contains little to no internal reflectors, projects to outcrop exposures of metasediments, and represents older undifferentiated Tertiary strata.

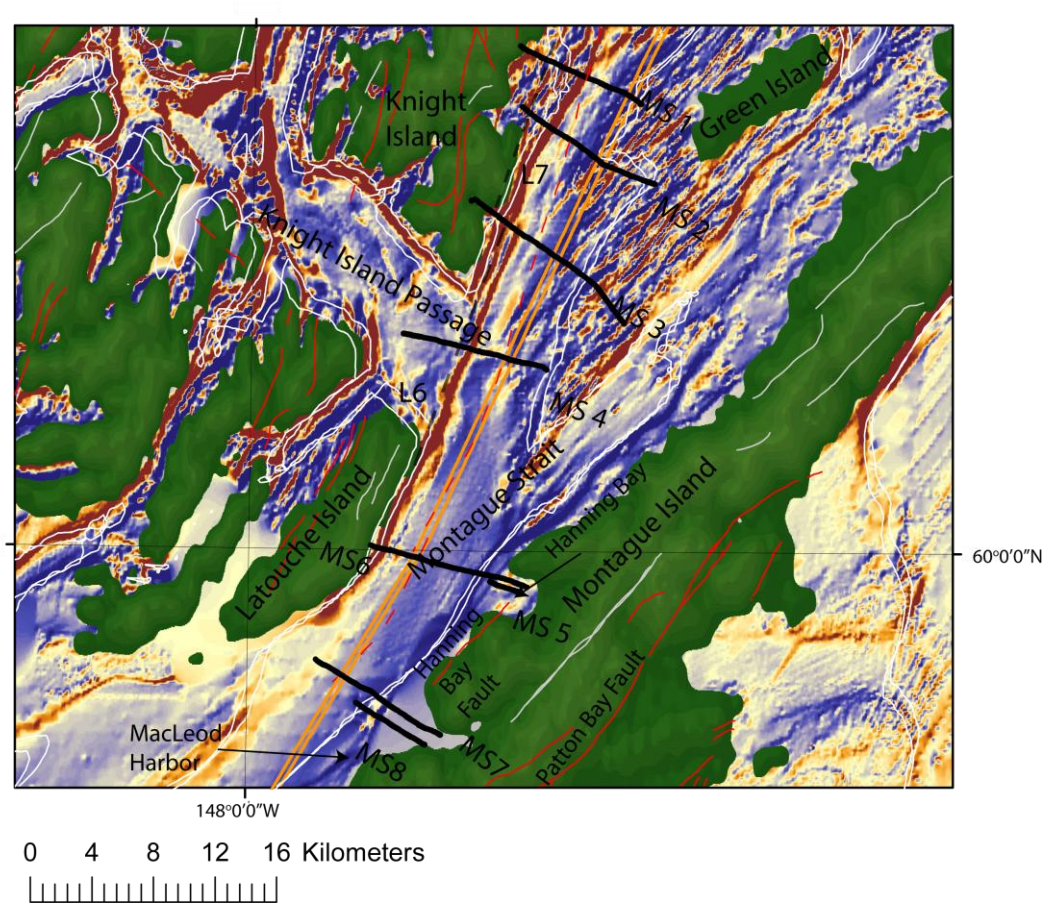

Figure 46: Bathymetric derivative map of Montague Strait (Red lineations dip southward, blue lineations dip northward) with the eight reflection seismic profiles (MS1 through MS8). Red lines mark mapped faults (Condon and Cass, 1958; Wilson and Hults, 2008). Yellow lines mark faults showing motion during 1964 (Plafker, 1969).

Seismic Profile Montague Strait 1 (MS1)

The 8.8 km west-east MS1 seismic profile crosses the bathymetric high that extends from central Montague Strait to Green Island in water depth that ranges from 40 m to 300 m (Figure 47). A bathymetric low extends between CMP 23,000 to 24,700. The seismic profile was acquired between 1:04PM and 2:12PM local time with an average boat speed of 2.16 m/s, an average shot spacing of 2.8 m, and binned CMP spacing of 1.5 m.

The unmigrated seismic section for MS 1 reveals reflections to more than 0.1 s two-way travel time below the water bottom reflector between CMP 23,000 and 24,800 (Figure 47). From the migrated and depth converted image, I interpret three layers below the water bottom to represent the Holocene, undifferentiated Quaternary, and Tertiary strata. Based on nearby cores, Unit M1 represents Holocene strata with a maximum of 80 m sediment thickness between CMP 23,000 and 24,000. Unit M2 stratigraphically underlies Unit M1 and is most clearly imaged between CMP 23,000 and 24,000.

I identify three faults as defined by offsets on water bottom or deeper strata. I interpret water bottom offsets of 20, 15, and 10 m on faults at CMP 23,000; CMP 24,200; and 24,600, respectively. Fault CMP 23,000 separates Tertiary bedrock from modern basin fill strata along the western basin margin. I measure the boundary between unit M2 and M1 across the fault at CMP 23,000 to be offset by 25 m. The fault at 24,200 bounds the deepest portion of the basin. The boundary between M1 and M2 is offset by at least 60 m at CMP 24,200. The boundary of M1-M2 at fault CMP 24,600 has offset of 40 m.

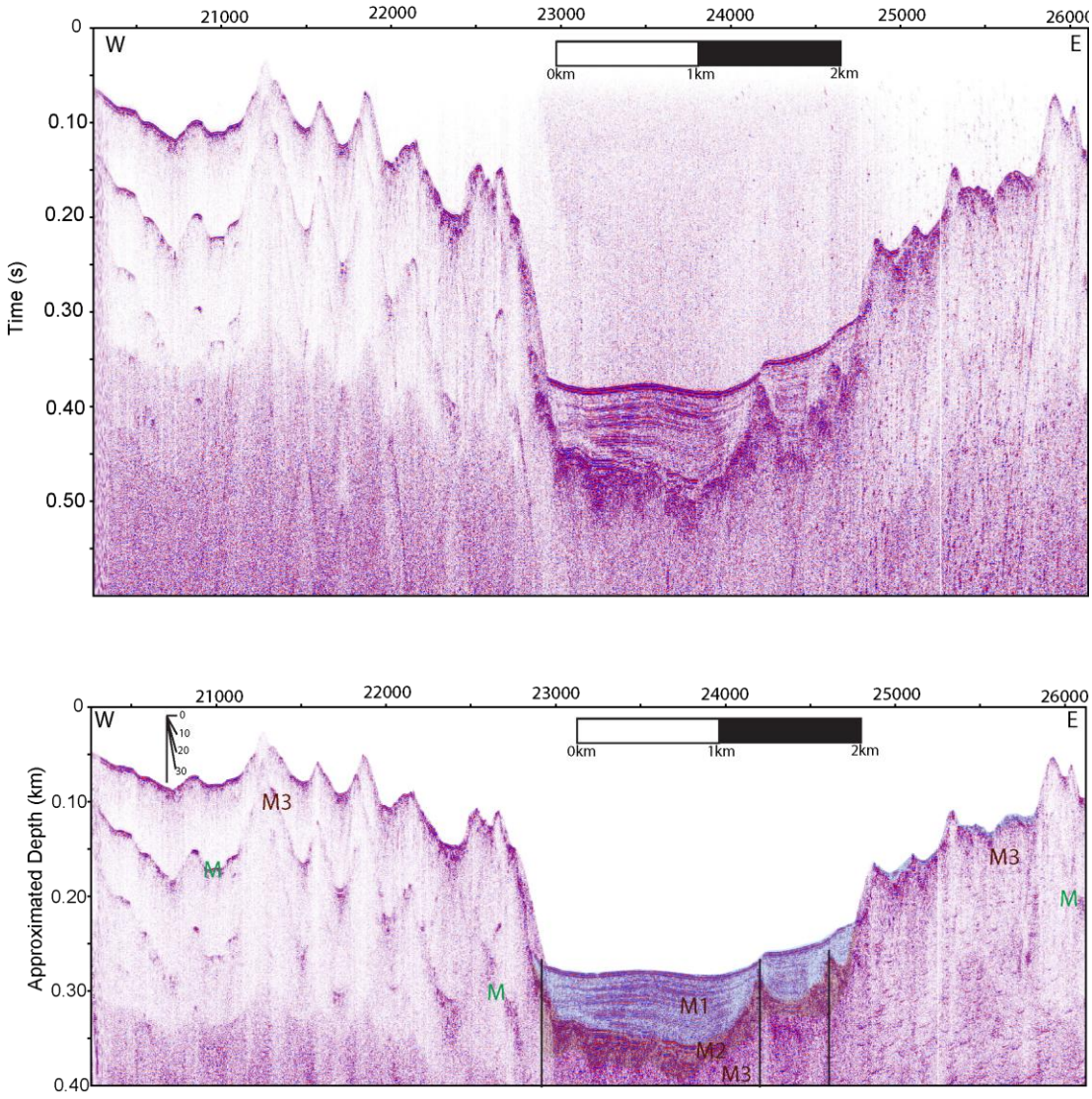

Figure 47: (top) Unmigrated traveltime stack for MS 1. (bottom) Migrated depth converted stack of MS 1. Dip meter in top right shows angle of reflectors or faults on profile.

Seismic Profile Montague Strait 2 (MS2)

The 10.1 km west-east MS 2 profile crosses the bathymetric high that extends from central Montague Strait, Green Island, in water depth that ranges from 50 m to 210 m (Figure 48). The basin extends between CMP 30,500 to 32,500. The profile was

acquired between 2:41PM and 3:55PM local time with an average boat speed of 2.3 m/s, average shot spacing of 3.1 m ,and binned CMP spacing of 1.5 m.

The unmigrated seismic section for profile MS 2 reveals reflections to more than 0.1 s two-way travel time below the water bottom reflector between CMP 30,500 and 32,500 (Figure 48). On the migrated and depth converted image, I identify Unit M1 to represent Holocene strata with a maximum of 50 m sediment thickness, consistent with 8,333 years of sediment at modern sedimentation rates of 6 mm/yr (Klein, 1983). Unit M2 is most clearly imaged between CMP 31,000 and 32,000 with a maximum thickness of 20 m. The basal seismic unit M3 represents strata below the water bottom reflector along the profile margins.

I identify three water bottom offsets that represent faults (Figure 48). A water bottom lineament is located at CMP 29,500 and the water bottom is offset by 15 m. At this location, there is a change of reflector dip within the unit across the fault. At CMP 30,600, a fault defines the southern boundary of the basin and has a water bottom offset of 50 m. At CMP 31,000, there is a 30 m water bottom offset. The fault offsets M2 strata by 50 m demonstrated by the unconformity between M1-M3, suggesting a fault with continued Holocene activity. A bathymetric high at CMP 31,400 indicates an eroded fault scarp that offsets M1 by 10 m. At this location, there is a unit M3 high with a vertical offset of unit M2. A fault at CMP 32,000 offsets the water bottom by 10 m. An unconformity between unit Holocene and Tertiary strata (M1 and M3) indicates an offset of unit M2 by 20 m. The northern basin boundary is at CMP 32,500 with a 100 m sea floor depth change. Near-surface strata of M1 are offset by at least 5 m. A 20 m water bottom offset at CMP 33,000 occurs in unit M3 strata.

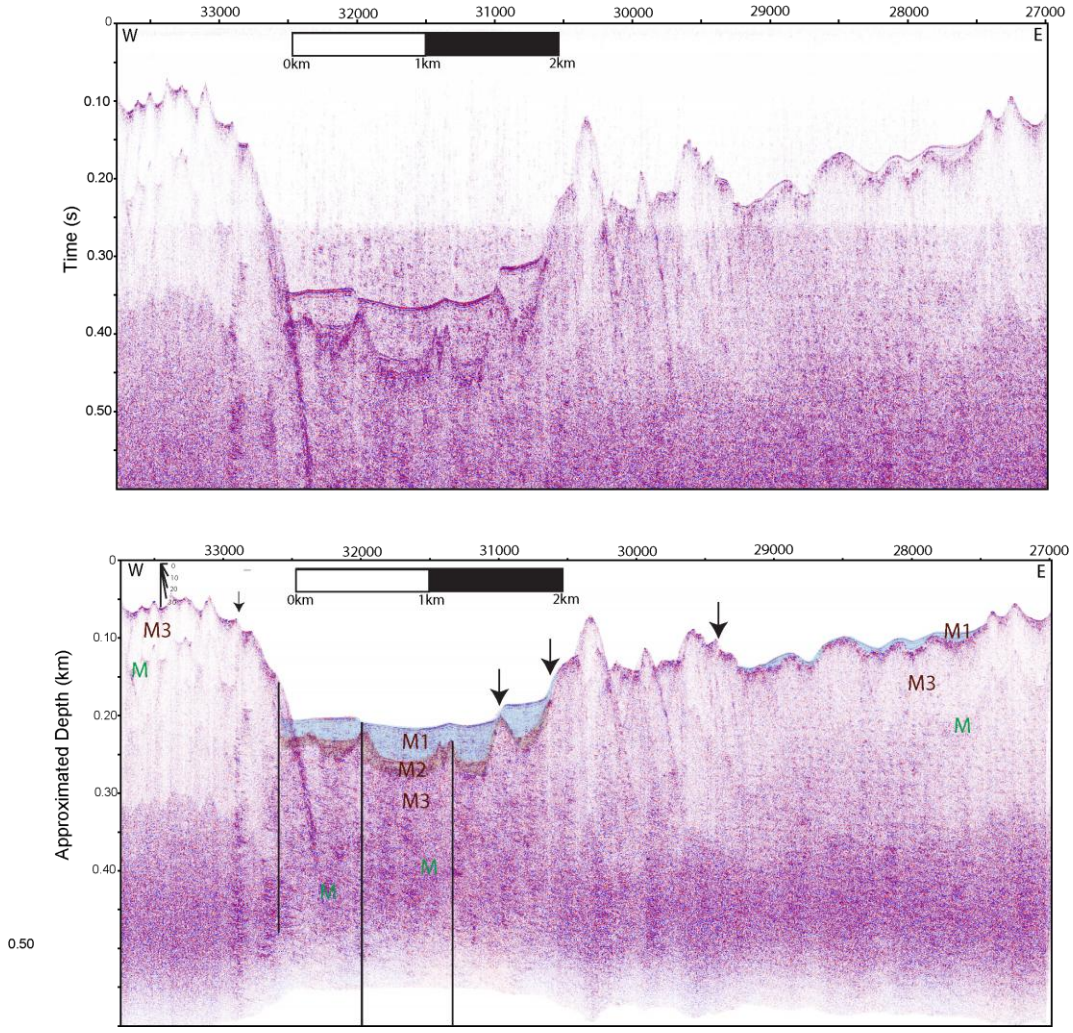

Figure 48: (top) Unmigrated traveltime stack for MS 2. (bottom) Migrated depth converted stack of MS 2. Dip meter in top right shows angle of reflectors or faults on profile.

Seismic Profile Montague Strait 3 (MS3)

The 12.5 km west-east MS3 profile was acquired from Knight Island east across the bathymetric high in the central Montague Strait in water depth that ranges from 25 m to 280 m (Figure 46; Figure 49). A bathymetric low extends between CMP 30,500 to 32,500. We collected data between 7:08PM and 8:52PM local time with an average boat speed of 2.0 m/s, an average shot spacing of 3.1 m, and binned CMP spacing of 1.5 m.

The unmigrated seismic section for profile MS3 reveals reflections to more than 0.1 s two-way travel time below the water bottom reflector between CMP 36,000 and 37,500 (Figure 49). Unit M1 is a maximum of 100 m thick. Unit M2 is most clearly imaged between CMP 36,000 and 37,500. Basal seismic unit M3 is interpreted at the water bottom surface outside CMP 36,000 to 37,500.

I identify six water bottom offsets that may represent faults within a sedimentary basin between 35,000 and 37,500. I interpret two additional faults based on reflector offsets that do not offset the water bottom surface (Figure 49). A fault at CMP 35,100 offsets M3 and the water bottom by at least 20 m. I interpret a basin bounding fault at CMP 36,000 with an 80 m total bathymetric offset and an offset of at least 10 m across M1 strata. A fault at depth at CMP 36,500 offsets M1 strata by 10 m and the boundary between unit M1 and M2 by 15 m. A fault that does not offset the sea floor does offset the contact between M1 and M2 by 50 m. Another parallel fault at CMP 37,100 offsets M1 strata with a maximum of 15 m and M2 by 30 m. A fault at CMP 37,400 offsets the contact between M1 and M2 by 30 m. At CMP 39,400, a fault offsets M3 by at least 20 m and may account for the 10 m M1 bedrock high.

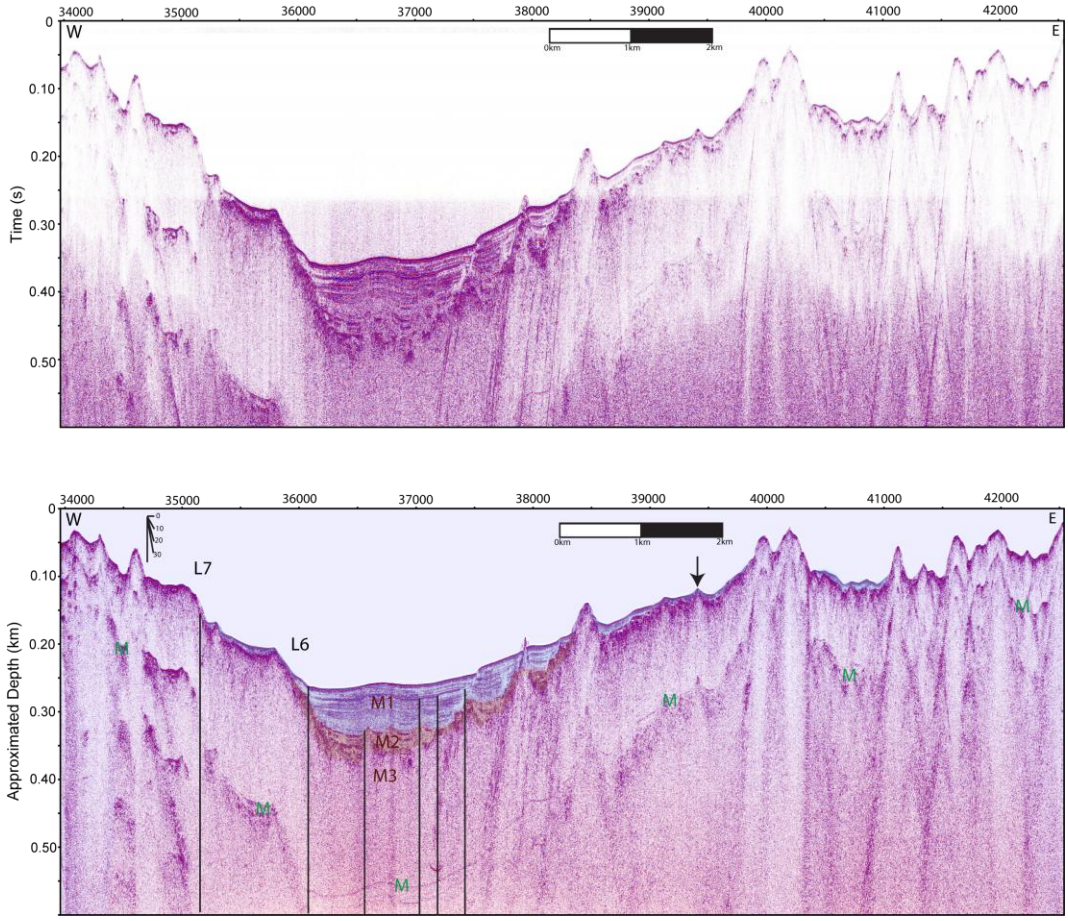

Figure 49: (top) Unmigrated traveltime stack for MS 3. (bottom) Migrated depth converted stack of MS 3. Dip meter in top right shows angle of reflectors or faults on profile.

Seismic Profile Montague Strait 4 (MS4)

Seismic profile MS4 was acquired from central Montague Strait north of Montague Island toward Knight Island (Figure 46). This 9.65 km west-east profile crosses the bathymetric high that extends from central Montague Strait in water depth that range from 220 m to 320 m (Figure 50). The basin as defined by a bathymetric low extends between CMP 52,500 to 53,300. The profile was acquired between 5:39PM and 7:32PM local time with an average boat speed of 1.42 m/s, an average shot spacing of 1.91 m, and binned CMP spacing of 1.5 m.

The unmigrated seismic section for profile MS4 reveals reflections to more than 0.1 s two-way travel time below the water bottom reflector at CMP 52,500 and 55,500 (Figure 50). Unit M1 is a maximum of 50 m thick. Unit M2 is most clearly imaged between CMP 51,500 and 53,400. Unit M1 and M2 are deposited in sedimentary basins between CMP 52,500-53,500 and 55,000-55,600. Basal seismic unit M3 is continuously exposed at the water bottom surface except within the basins.

I identify three faults as defined by offset strata with one fault having a water bottom offset (Figure 50). In addition, I identify one water bottom lineament at CMP 52,600. I interpret reflector offsets within Unit M1 across faults at CMP 53,400; 53,700; and 54,200. The boundary between M1 and M2 is offset by 30 m at CMP 52,500. I interpret a fault at 53,500 with a water bottom offset of 60 m. The fault at CMP 53,700 offsets the boundary between M2 and M3 is offset by 15 m. Faulting at CMP 54,200 offsets the boundary between M1 and M3 by 20 m.

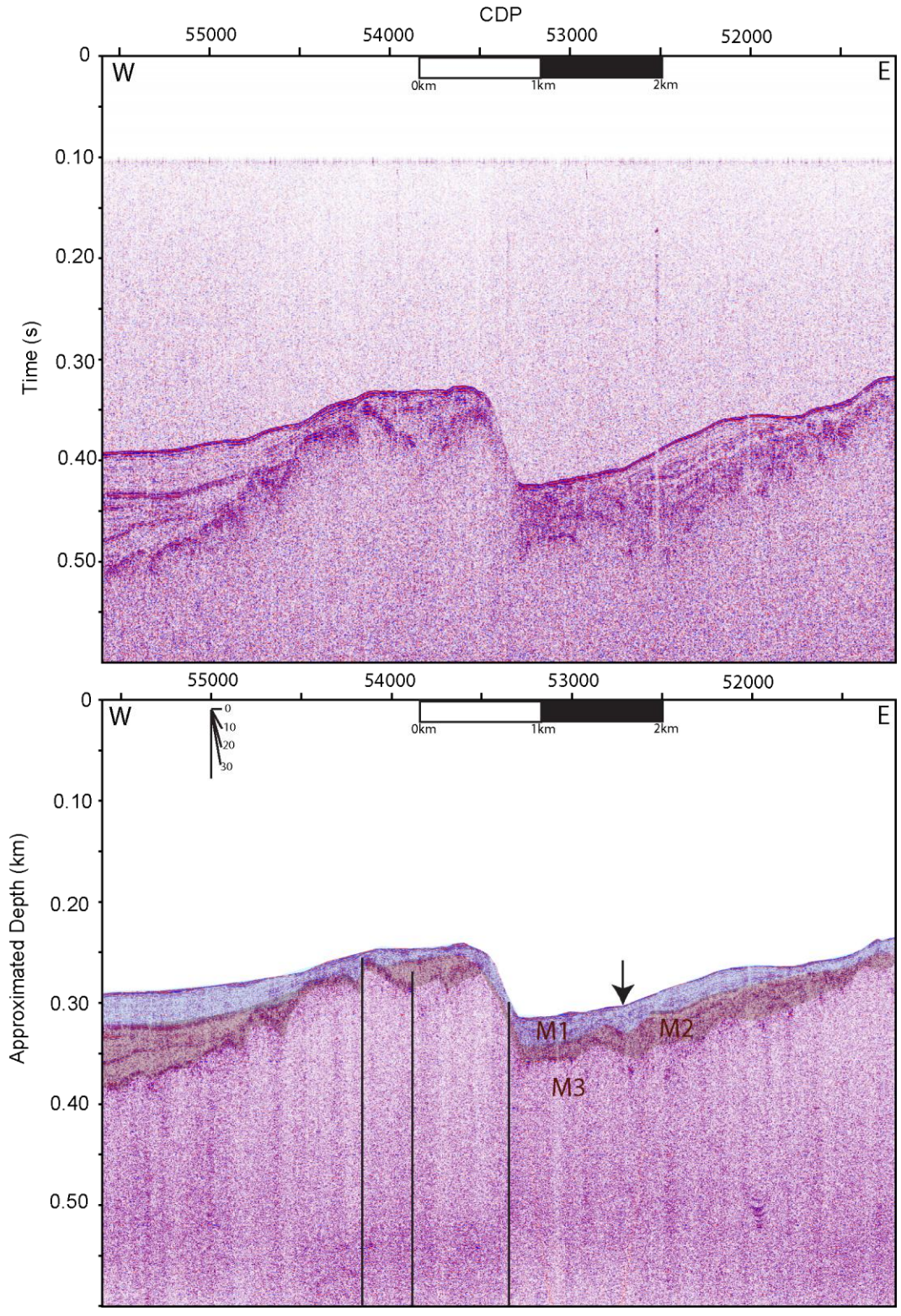

Figure 50: (top) Unmigrated traveltime stack for MS4. (bottom) Migrated depth converted stack of MS 4. Dip meter in top right shows angle of reflectors or faults on profile.

Seismic Profile Montague Strait 5 (MS5)

Seismic profile MS5 was acquired across central Montague Strait (Figure 46). This 2.0 km west-east profile crosses the bathymetric high that extends from central Montague Strait in water depth that ranges from 50 m to 210 m (Figure 51). A bathymetric low extends between CMP 63,750 to 64,250. The profile was acquired between 7:53AM and 8:10AM local time with an average boat speed of 2.0 m/s, an average shot spacing of 2.38 m, and binned CMP spacing of 1.5 m.

The unmigrated seismic section for profile MS5 reveals reflections to more than 0.05 s two-way travel time between CMP 63,750 and 64,250 (Figure 51). Unit M1 is a maximum of 15 m thick. Basal seismic unit M3 is continuously exposed at the water bottom surface except between CMP 63,750 and 64,250.

I identify three faults defined by offset stratigraphy along the profile. One fault at 63,750 shows a minimum offset of 30 m across the base of M1 (Figure 51). The second fault bounds the eastern extent of M1 at CMP 64,250 and coincides with a 20 m water bottom offset. The offset across M3 strata on the fault at 63,750 is at least 30 m. A fault at 64,450 occurs at a slope change of unit M3 and surface reflectors show at least a meter offset.

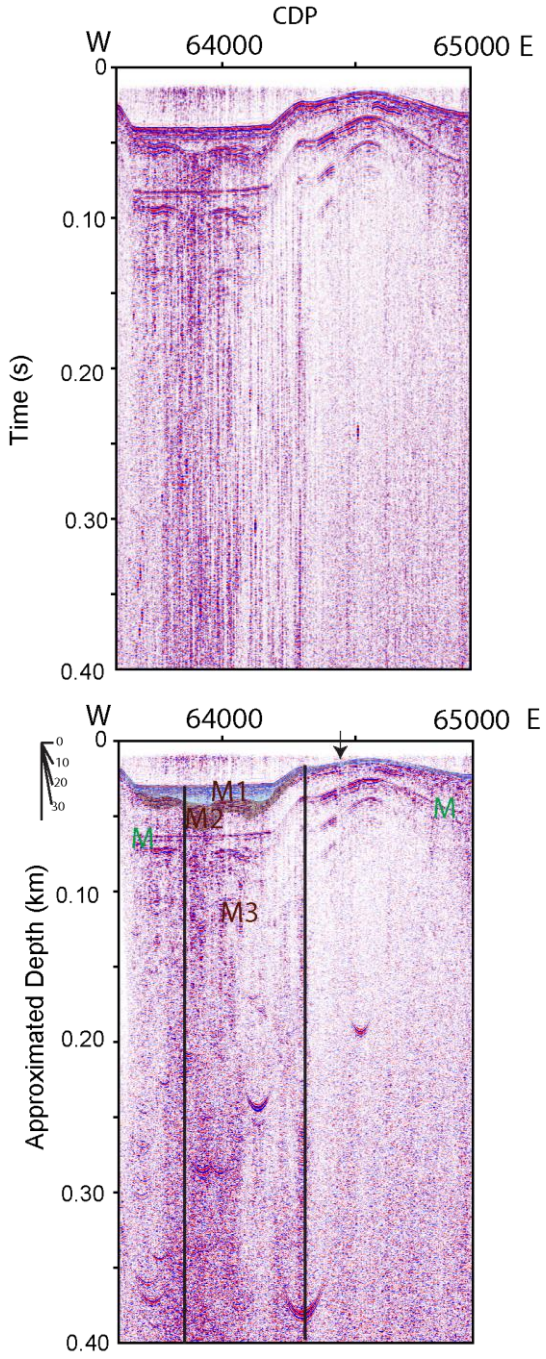

Figure 51: (top) Unmigrated traveltime stack for MS5. (bottom) Migrated depth converted stack of MS5. Dip meter in top right shows angle of reflectors or faults on profile.

Seismic Profile Montague Strait 6 (MS6)

Seismic profile MS6 was acquired from central Montague Strait, north of Montague Island (Figure 46). This 10.55 km west-east profile crosses the bathymetric high that extends from central Montague Strait in water depth that ranges from 50 m to 210 m (Figure 52). The basin interpreted by a bathymetric low extends between CMP 68,600 to 73,000. The profile was acquired between 8:18AM and 9:39AM local time with an average boat speed of 2.2 m/s, an average shot spacing of 2.7 m, and binned CMP spacing of 1.5 m.

The unmigrated seismic section for profile MS6 reveals reflections to more than 0.05 s two-way travel time below the water bottom reflector between CMP 68,000 and 72,000 (Figure 52). Unit M1 is a maximum of 25 m thick. Unit M2 is most clearly imaged between CMP 68,500 and 71,500. Basal seismic unit M3 is at the water bottom surface between 67,300 and 68,500. The upper contact of Unit M3 is not clearly imaged between 68,500 and 72,000. A bathymetric high between 71,800 and 72,800 that I interpret as lacking stratigraphic layering is a landslide deposit.

I identify four faults as defined by offset reflectors with two faults having water bottom offsets (Figure 52). I interpret a 15 m offset within unit M1 on a fault on 66,400 (Figure 52). I interpret a fault at CMP 67,300 that offsets the water bottom by 20 m and unit M2 by 30 m.

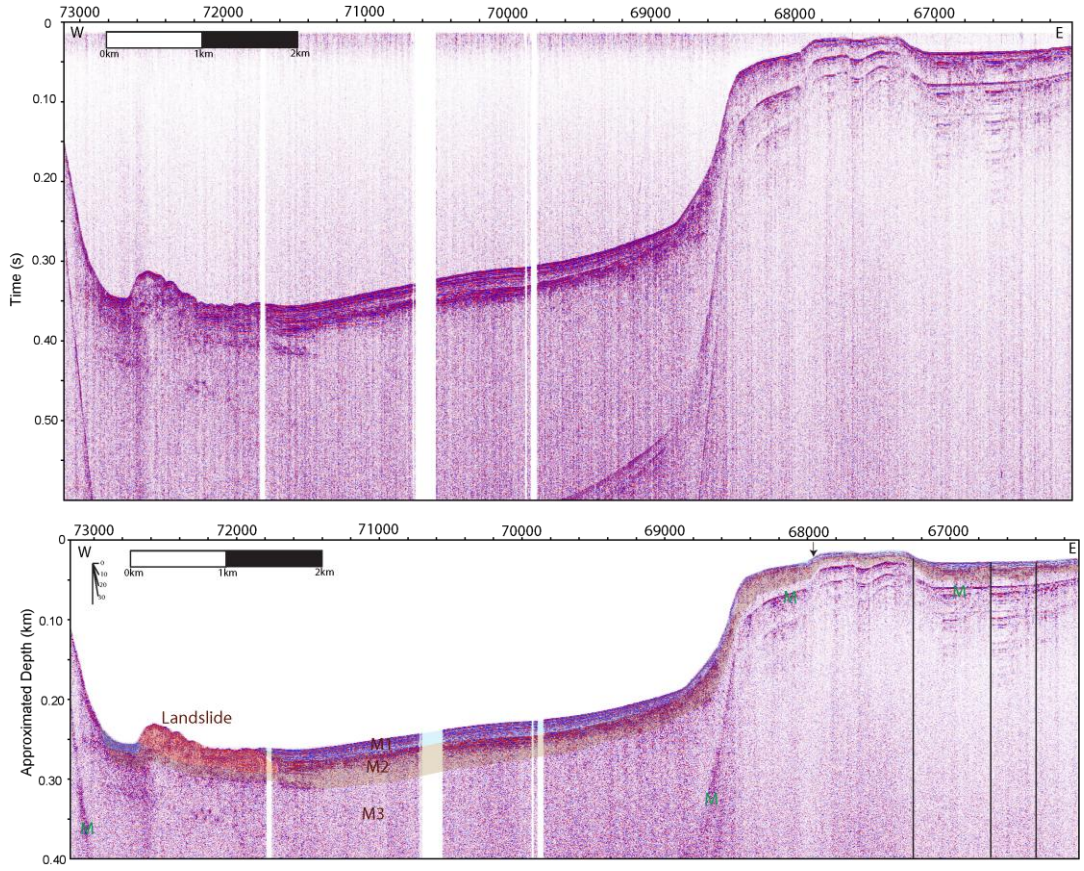

Figure 52: (top) Unmigrated traveltime stack for MS6. (bottom) Migrated depth converted stack of MS6. Dip meter in top right shows angle of reflectors or faults on profile.

Seismic Profile Montague Strait 7 (MS7)

Seismic profile MS7 was acquired from central Montague Strait toward MacLeod Harbor on Montague Island (Figure 46). This 9.6 km west-east profile crosses the bathymetric high that extends from central Montague Strait in water depth that ranges from 50 m to 170 m (Figure 53). The basin as defined by a bathymetric low extends between CMP 77,000 to the end of the profile. The profile was acquired between 10:23AM and 11:36AM local time with an average boat speed of 2.2 m/s, an average shot spacing of 3.2 m, and binned CMP spacing of 1.5 m.

The unmigrated seismic section for profile MS7 reveals reflections to more than 0.1 s two-way travel time below the water bottom reflector between CMP 77,000 and 78,500 (Figure 53). Unit M1 measures a maximum of 50 m sediment thick. Unit M2 is most clearly imaged between CMP 77,000 and 78,000. Basal seismic unit M3 represents the water bottom reflector along the length of the profile except within the basin.

I identify five faults with a subset of three faults having water bottom offsets. I interpret offsets within Unit M1 on faults at CMP 77,300; CMP 77,600; 78,400; 78,600; and 79,900 (Figure 53). Fault at CMP 77,300 has a water bottom offset of 10 m and a unit M2 offset of 50 m. Fault at CMP 77,600 offsets boundary between M1-M2 by 40 m and boundary between M2-M3 by 55 m. The water bottom offset is a 50 m offset however I interpret the Holocene offset to be less since the slope margin would change the apparent offset. The fault at CMP 78,400 has an offset of 20 m with an equivalent offset in the boundary between unit M1-M2 suggesting recent initial faulting. The fault at CMP 78,600 offsets the boundary between M1-M2 by 10 m with a zero water bottom offset. Faulting at CMP 79,900 offsets the boundary between units M1-M2 by 10 m.

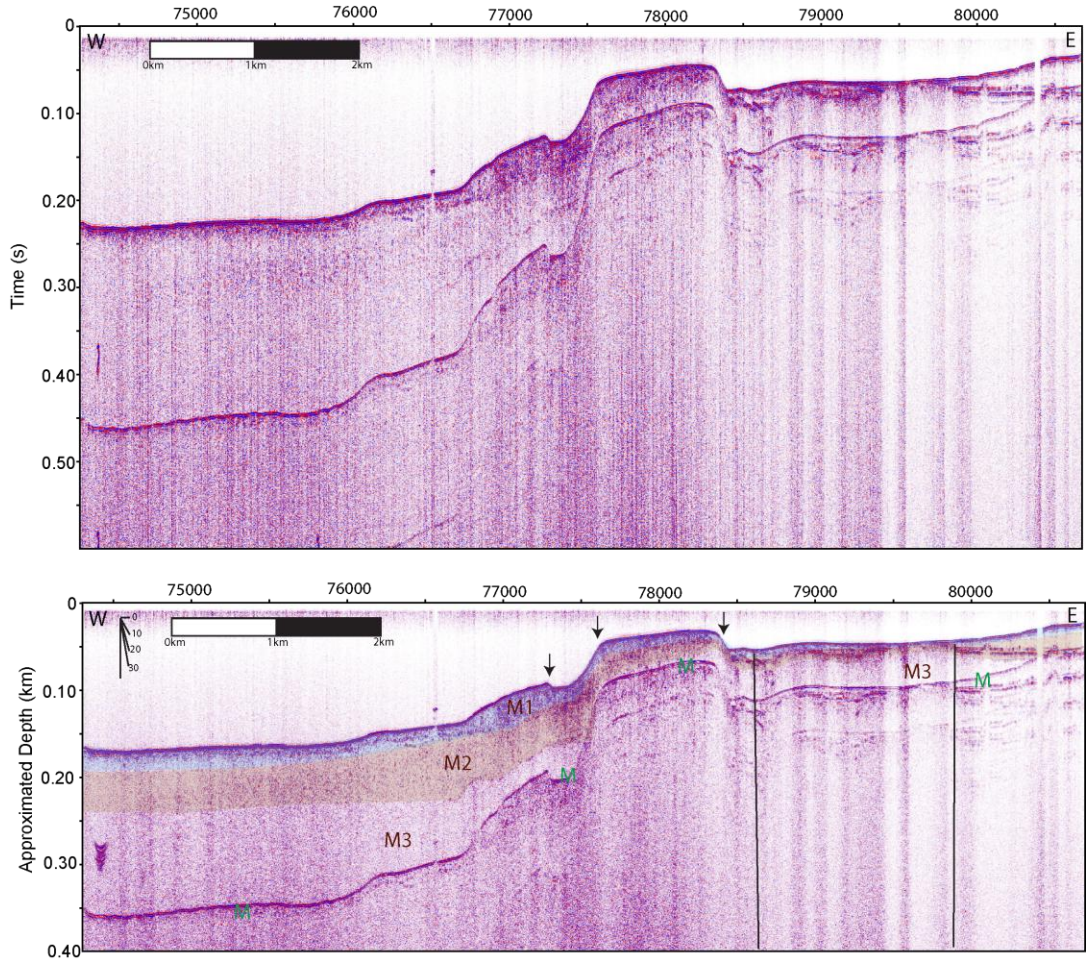

Figure 53: (top) Unmigrated traveltime stack for MS7. (bottom) Migrated depth converted stack of MS 7. Dip meter in top right shows angle of reflectors or faults on profile.

Seismic Profile Montague Strait 8 (MS8)

Seismic profile MS8 was acquired from MacLeod Harbor toward central Montague Strait north of Montague Island (Figure 46). This 5.28 km west-east profile crosses the bathymetric high that extends along Montague Island near McLeod harbor (Figure 13). Water depth ranges from 25 m to 100 m (Figure 54). One bathymetric low, a channel, is at CMP 84,100 and the second bathymetric low is at the end of the profile towards the central Montague Strait. The profile was acquired between 11:45 AM and

12:27 PM local time with an average boat speed of 2.1 m/s, an average shot spacing of 2.8 m, and binning CMP spacing of 1.5 m.

The unmigrated seismic section for profile MS8 reveals reflections to more than 0.05 s two-way travel time below the water bottom reflector between CMP 83,000 and 83,900 (Figure 54). Unit M1 represents the Holocene strata with a maximum of 40 m sediment thickness. Unit M2 clearly imaged between CMP 83,000 and 83,900. The basal seismic unit is Unit M3.

I identify three faults with two faults having water bottom offsets. Faults at CMP 83,900 and 84,200 have water bottom offsets of 50 and 40 m, respectively (Figure 54). Faults at CMP 83,900 and 84,200 offset the boundary between M1-M2 by 50 and 70 m. These two faults bound a narrow sea floor channel located between 83,900 and 84,200. I interpret an offset of boundary between M1 and M2 of 30 m from the fault located at 82,950.

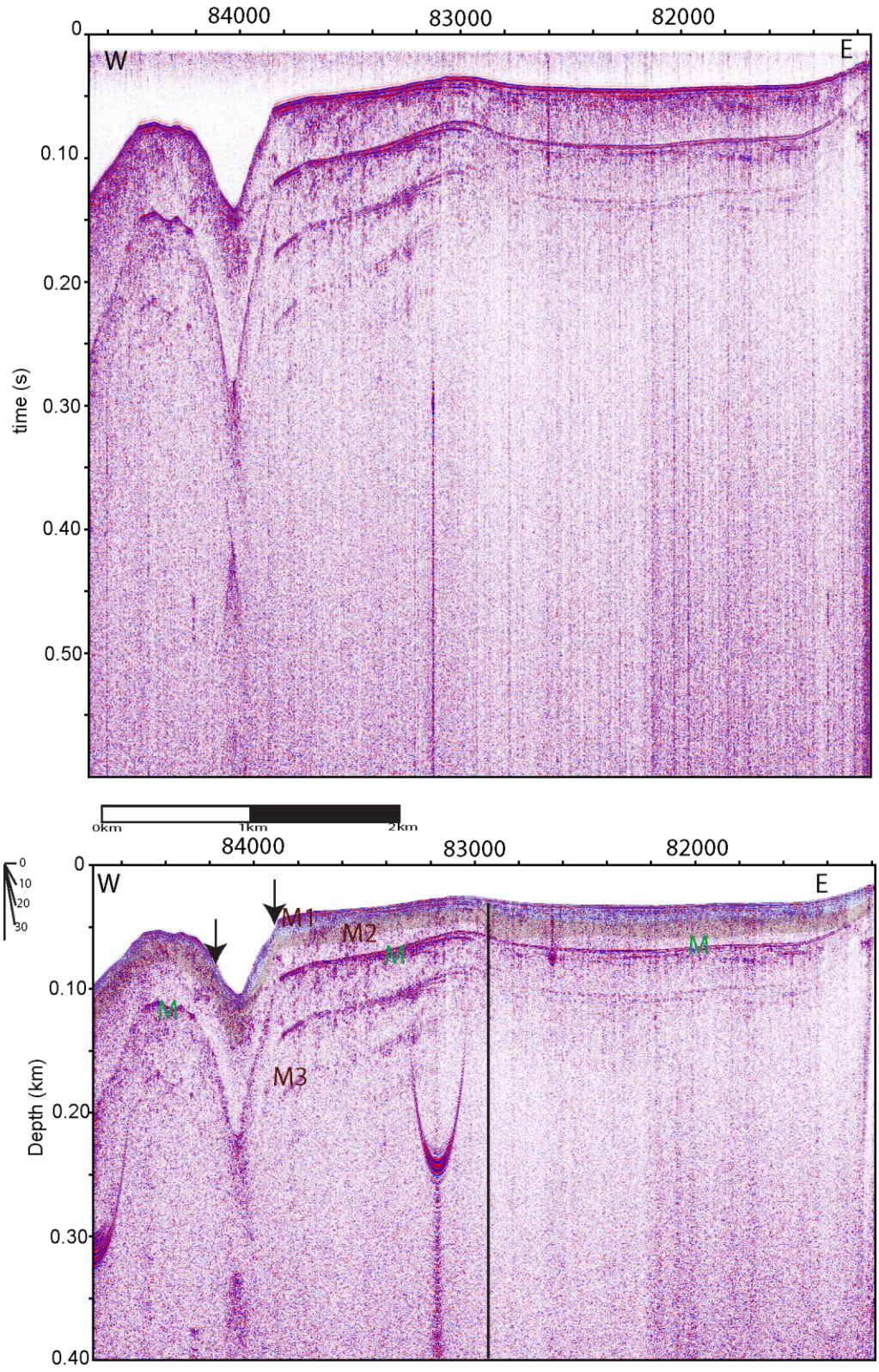

Figure 54: (top) Unmigrated traveltime stack for MS8. (bottom) Migrated depth converted stack of MS 8. Dip meter in top right shows angle of reflectors or faults on profile.

Summary

Montague Strait represents the hanging wall region of the Patton Bay and Hanning Bay thrust faults mapped on Montague Island (Figure 17; Figure 46). High signal attenuation along each profile as compared to the Orca Bay or Hinchinbrook Entrance profiles is likely due to coarse grain modern sediments coming out of suspension within Montague Strait from local sources. Unit M1 contains a maximum thickness of 70 m within Montague Strait with the greatest sediment thickness along profile MS1-MS3. Given a modern and constant sedimentation rate of 6.0 mm/year, Unit M1 represents approximately 11,666 years of sediment (Klein, 1983). Klein [1983] identified a decrease in modern sedimentation rates from east to west within Montague Strait, consistent with long-term depositional rates as measured on seismic profiles west of Knight Island Passage as compared to profiles to the east (Figure 6). Along the shoreline of Montague Strait, Orca Group Tertiary metasediments are exposed. This shoreline exposure is consistent with the Unit M3 sea floor surface along the Montague Strait basin margins. These shallow water deposits may either represent active exhumation or high velocity water currents that limit sediment deposition. Coarse grain sediments in Montague Strait suggest a local sediment source. Deep-water currents significantly affect the location of sediment deposition and erosion throughout the Montague Strait basin.

I match water bottom lineations to subbottom reflector offsets, suggesting these lineations are faults that control the northwest basin margin of Montague Strait (Figure 46). Faults trend N20˚E along the western portion of Montague Strait. Lineations trend N45˚E along the eastern portion of Montague Strait where bedrock is exposed at the sea

floor. This linear trend upon bedrock may represent the direction of glacial retreat in a region dominated by active exhumation. Fault L6 recorded on MS1 appears on profile MS2 with a step-over to Fault L7 between Profiles MS3 and MS4. I interpret Fault L7 to extend southward along the south shore of Latouche Island. I suggest MS6 does not cross the fault because the lineation and shoreline are coincident. I interpret lineations along flanks of Montague Strait as faults offsetting Holocene sediments. I interpret the Hanning Bay fault to project across Hanning Bay with approximately 1-2 m of slip during the 1964 event; Hanning Bay fault had a maximum of 5 m of slip 10 km to the southwest of Hanning Bay (Plafker, 1969). Consistent with localized uplift associated with the Hanning Bay fault (Plafker, 1969), the presence of active faulting along the northern margin of Montague Strait suggests megathrust splay faults likely surface farther north than previously identified. Furthermore, Latouche and Knight Island represent uplift from another splay fault (Plafker, 1969).

CHAPTER FIVE: DISCUSSION

Orca Bay

Orca Bay encompasses a basin for sediment source deposited from eastern PWS and from the Copper River delta through the Hinchinbrook Entrance (Klein, 1983). High angle active normal faults bound the sedimentary basin beneath Orca Bay and strike between N70E to N80E (Figure 17; Figure 18; Figure 55). Tertiary bedrock lies both beneath and adjacent to late Quaternary and younger strata that fill Orca Basin. Bathymetric highs project to exposed Tertiary bedrock, and these bedrock highs form the footwall of active normal faults (Condon and Cass, 1958; Carlson and Molnia, 1978; Wilson and Hults, 2008). Although these normal faults suggest extension, the faults may root into the hanging wall of thrust faults related to the megathrust subduction system (Collot et al., 2008; Melnick et al., 2009).

As evidenced by increasing reflector offsets with depth, many faults within Orca Bay have remained active throughout the Holocene (Figure 55). These growth faults provide an ideal opportunity to assign slip rates to address seismic hazards in Orca Bay. I calculate slip rates for Faults L1 and L2 that control the northern basin margin (Figure 55; Figure 56). Reflectors were matched across the faults. Assuming a constant rate of Holocene sedimentation (Jaeger et al., 1998), I calculate slip rates for each fault. I calculated a deposition rate of 3.0 mm/yr within the basin was calculated by assuming the underlying unconformity represents a 12 kya surface. This sedimentation rate and age of

glacial maxima (hiatus in sedimentation) is consistent with values from Klein [1983] and Jaeger et al. [1998]. Average slip rates are calculated based on least-squares fit to the reflector offsets with increasing age. From seismic profile Orca 8, I calculate an average slip rate of 1.4 m/kyr for Fault L2 and an average slip rate of 0.6 m/kyr for Fault L1 (Figure 56). From seismic profile Orca 10 where Faults L1 and L2 combine to form a single fault, I calculate an average slip rate of 1.8 m/kyr. Deviation from the average slip rates may result from changing rates of sedimentation with time, variable earthquake rupture recurrence intervals, or improper travel time to depth conversion due to sediment compaction or changes in lithology.

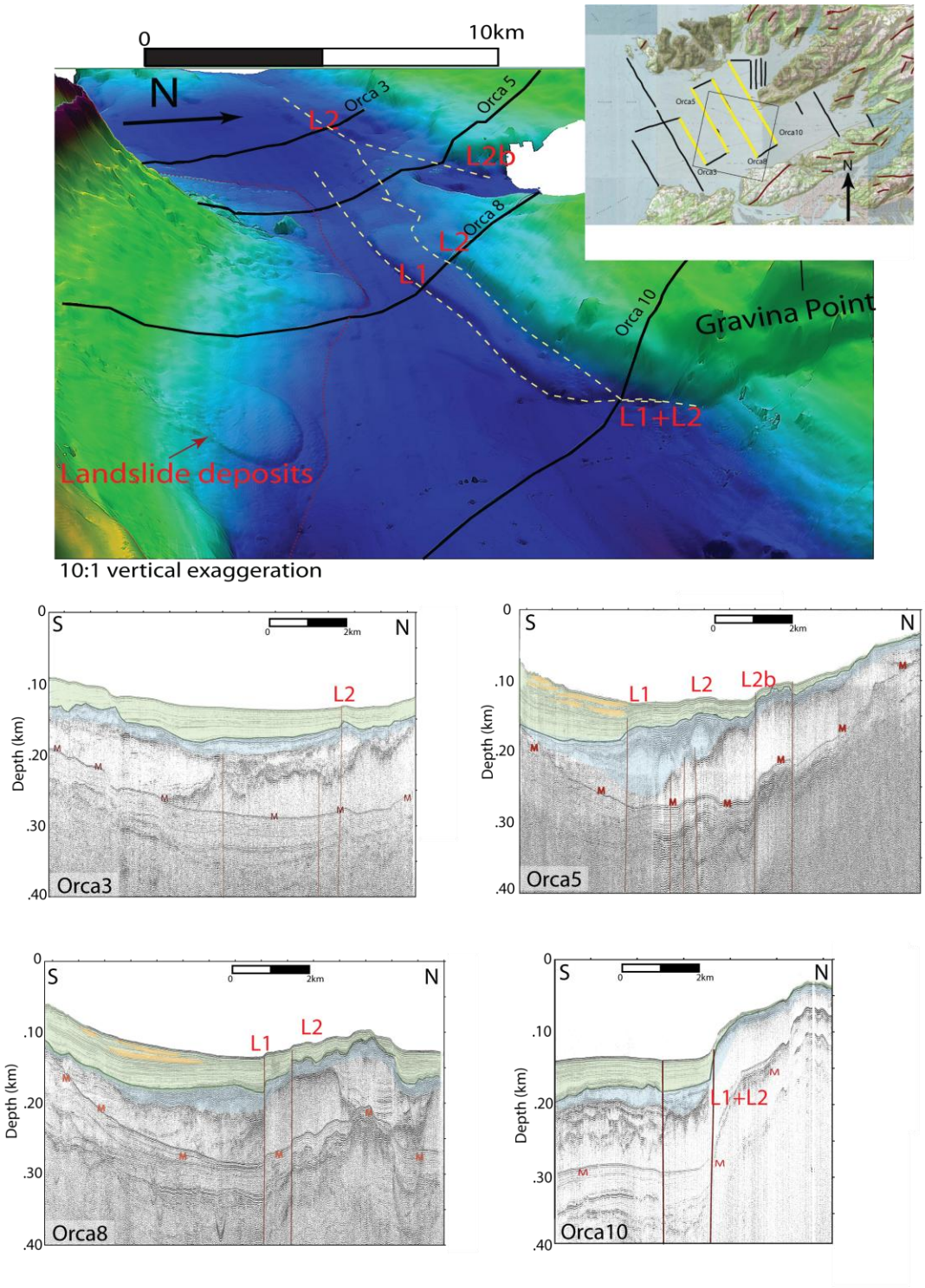

Figure 55: Orca Bay, eastern PWS bathymetry and seismic profiles (top) Perspective bathymetry of Orca Bay (NOAA database) with blue as greater water depth, seismic lines in black, dashed red line is interpreted toe of modern landslide deposits, and dashed yellow is an interpreted fault trace. (bottom) seismic profiles Orca 3,5,8,10 with interpreted faults and landslide deposits.

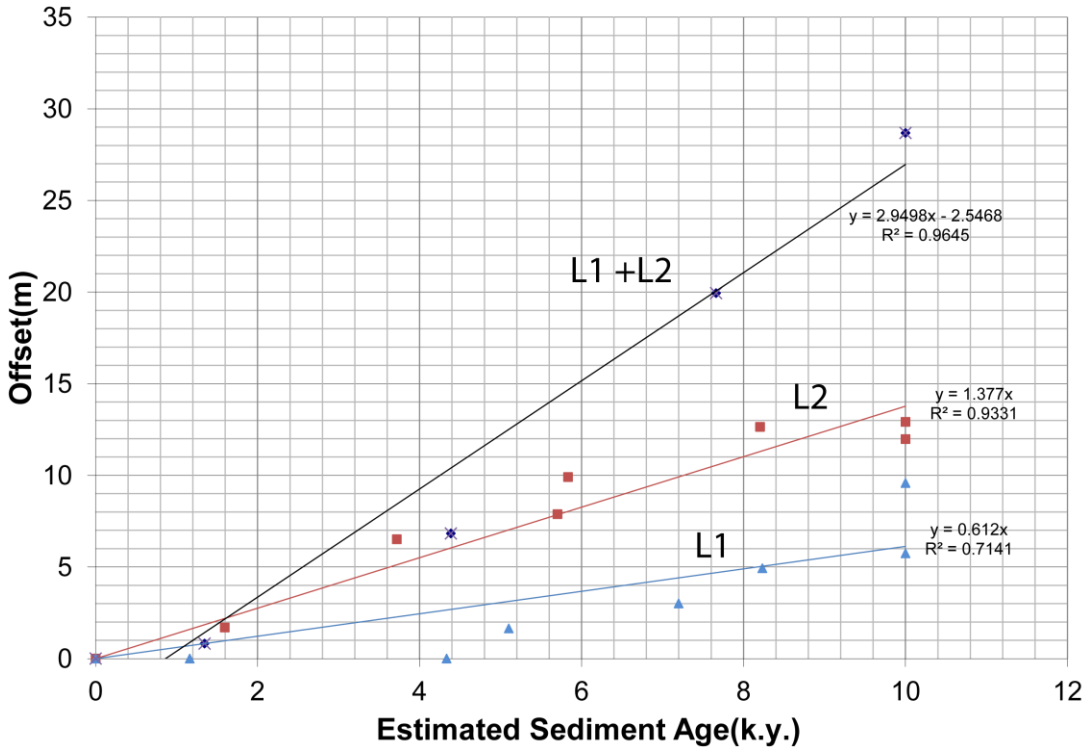

Figure 56: Fault offset vs. estimated sediment age and depth for Faults L1 and L2 within Orca Bay Fault L1 (blue), fault L2 (red), and L1+L2 (purple) from Orca 8 and Orca 10 profiles (Figure 55). Slopes provide slip rate values in m/kyr. R values represent the fit of the lines to the points.

Carver and Plafker [2008] suggest a recurrence interval of ~860 years with 2.3 m of uplift per event for the nearby Copper River delta region. I measure a long-term slip rate average of 1.8 m/ky for the combined faults A and B that control the northern margin of Orca Bay. Assuming a recurrence interval of 860 years, I estimate slip of 1.5 m per event. Alternatively, assuming 2.0 m slip per event, I calculate a recurrence interval of 1,111 years. Regardless, both estimates are consistent with the Carver and Plafker [2008] regional estimate.

Assuming a recurrence interval of 860 years, slip along the Orca Bay fault would average 1.55 m per earthquake. Using empirical relationships established by Wells and Coppersmith [1994], this average displacement per earthquake suggests the Orca Bay

fault could independently support a M 7.1 earthquake. Additional empirical relationships from Wells and Coppersmith [1994] suggest a M7.1 earthquake with an average of 1.55 m represents a fault of length 69 km. Although I measure a fault length of 40 km for the Orca Bay fault, this fault system may connect to lineations observed on land and/or to faults mapped to the west in central PWS (Condon and Cass, 1958; Wilson and Hults, 2008; Finn et al., 2011). No ruptures or differential uplift occurred on the mainland from 1964, however faults within Orca Bay and farther west may have coseismically ruptured during this event (Carver and Plafker, 2008; Finn et al., 2011). Plafker [1969] estimated between .5 and 2 m of regional vertical uplift within Orca Bay, however this study had no direct evidence to suggest faults were active beneath Orca Bay. Given the compelling evidence presented here for active faulting within Orca Bay and bathymetric evidence for a modern scarp and submarine landslides, these faults are likely an active component to the megathrust fault system. Thus, local seismic hazard for Orca Bay is higher than previously documented. Furthermore, the splay fault system related to megathrust earthquakes extends further than previously documented.

I identify four independent submarine landslides within the Holocene sediments within Orca Bay. Based on stratigraphic positioning and a constant rate of sedimentation, I estimate submarine landslide deposits formed between 1.3 kya and 4.16 kya. Additionally, modern submarine landslides appear on the Orca Bay bathymetric map (Figure 32), suggesting repeated landslides throughout late Holocene time. Although there is no direct evidence to suggest that these landslides are earthquake induced, landslides initiating local tsunamis near Valdez and Whittier caused significant damage during the Great Alaska Earthquake of 1964 (Plafker, 1969). Multiple landslide deposits

observed along the southern margins of Orca Bay (Figure 18, 21, 24, 27 and 55) indicate slope instability. The average slope offshore northern Hinchinbrook Island is measured at approximately 30˚. However, landslide deposits appear below slopes that measure as little as 10˚. I suggest that sediments may become unstable at very low angles (<10˚) and could become unstable even during minor seismic shaking (McAdoo et al., 2000).

Gravina Bay

Gravina Bay northeast of Orca Bay was investigated because of the potential for active faulting as identified from a water bottom lineation, L3 (Figure 33) (Andring et al., 2006). Water bottom lineation L3 was identified on profiles Gravina 3 through 5 (Figure 36-Figure 38). A lack of Holocene sediment near L3 on Gravina 3 through 5 limits the interpretation as being only a water bottom lineation. I identify other faults along the Gravina Bay profiles, however these faults show no recent activity as defined by the lack of offset of Holocene strata.

Hinchinbrook Entrance

The sedimentary basin below Hinchinbrook Entrance contains upwards of 200 m of late Quaternary and younger sediment above Tertiary bedrock (Figure 45; Figure 57). I interpret north to northwest dipping high angle faults to offset the water bottom and deeper reflectors. Hinchinbrook seismic profiles 1, 2, 4, 5 and 6 show predominantly northeast striking faults that correlate with bathymetric lineations and on-shore faults (Figure 40-Figure 45).

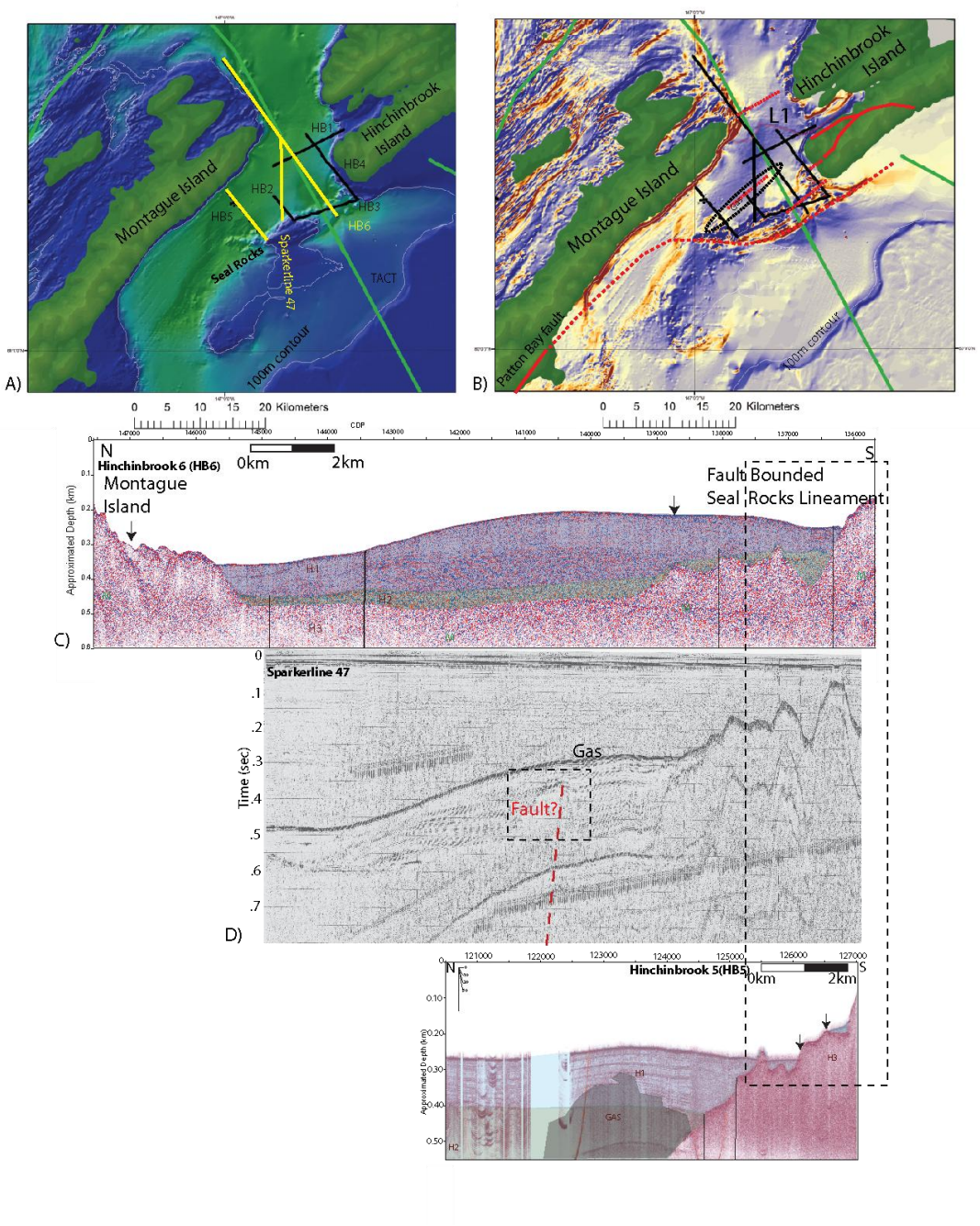

Figure 57: (A) Hinchinbrook Entrance maps and seismic profiles. (B) Bathymetric maps showing fault interpretations (red lines), Seismic images of HB 6 (C), unpublished 1974 USGS sparker line 47 (D), and HB(E). I interpret a bathymetric lineation along the southern edge of Montague Island to represent the northeastern extension of the active Patton Bay fault. A similar bathymetric lineation bounds the southern edge of Seal Rock that I interpret as a step-over and continuation of the Patton Bay fault system. Tact profile in green (Figure 58).

Although a Tertiary bedrock exposure along the seafloor alone does not indicate active faulting, it does indicate either rapid exhumation or a lack of sedimentation. Since a thick sequencing of Holocene strata surround Seal Rocks, I presume Seal Rocks represents an area of rapid exhumation. My Hinchinbrook seismic profile interpretations support the Plafker [1969] model of the Patton Bay fault extending across Hinchinbrook Entrance along an en echelon pattern of faulting (Figure 57B). Geologic mapping and aerial photographs show the Patton Bay fault continuing offshore along the southwest margin of Montague Island (Figure 17) (Plafker, 1969; Condon and Cass, 1958). Plafker [1969] mapped northwest-dipping splay faults on Montague Island and hypothesized that the steep southern shoreline was the continuation of the Patton Bay fault. I interpret the Seal Rocks bedrock high between Montague and Hinchinbrook Islands to represent the northeast extension of the Patton Bay fault. This bedrock high is fault controlled, consistent with the Patton Bay fault geometry. The bedrock high that forms Seal Rock and bathymetric high to the northeast then represents a southward step of the Patton Bay fault system. Bathymetric lineations and seismic data suggest faulting has uplifted Seal Rock where a splay fault surfaces along the southern bedrock high. I suggest Seal Rock is part of a larger fault system that may extend the Patton Bay fault system from Montague Island to Hinchinbrook Island to create a fault system that extends for nearly 200 km in length (Figure 57). Furthermore, a splay fault must appear offshore Hinchinbrook Island to account for the 2.5 m of uplift during the 1964 earthquake (Figure 5).

An unpublished crustal-scale seismic reflection data set shown between the Alaskan Trench and central PWS shows megathrust decollement and splays. Initial processing of the TACT reflection profile shows reflections from a 20 km depth that

splay to the surface at the location of Seal Rock (Figure 58). Although the splay faults are difficult to image at shallow depths, in shallow water, and within Tertiary bedrock, the bedrock high associated with Seal Rock or the northeastern extension of the Patton Bay fault are the obvious surface expression for the hanging wall of this splay fault. Other features representing uplift such as tilted strata are observed in the Holocene stratigraphy on seismic profiles H 2, 4, and 6 (Figure 41, 43, 45). These deformed strata represent folding in the hanging wall of the Patton Bay splay fault and are consistent with the greater uplift on the south shore of Hinchinbrook Island compared to uplift on the north shore.

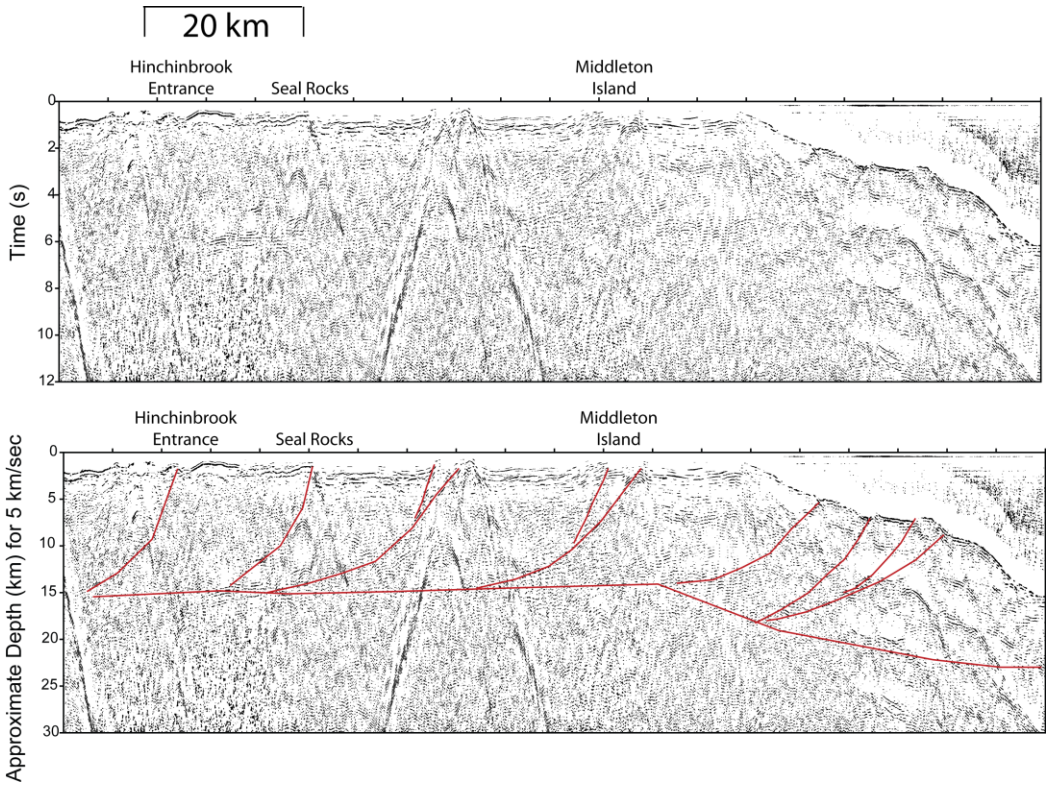

Figure 58: TACT reflection profile in time processed by stack, filtering, and AGC. Top image uninterpreted, lower image interpreted showing splay faults emerging from regional decollement (from Finn et al., 2011). TACT profile location is shown on Figure 57.

Sedimentation rates are significantly greater within Hinchinbrook Entrance than in central PWS or immediately offshore (Figure 6) (Klein, 1983; Jaeger et al. 1998). Using a maximum sediment thickness of Unit H1 of 250 m and an assumption that post glacial sedimentation initiated 10 kA, I calculate an average Holocene sedimentation rate of 25 mm/yr, consistent with rates estimated by Jaeger et al. [1998]. The sediment entering PWS from the Copper River delta and Gulf of Alaska is routed northward through the Hinchinbrook Entrance and trapped in the fault controlled basin of Hinchinbrook Entrance. I suggest the Seal Rock bathymetric high slows the current velocity and sediment drops out of suspension immediately north of Seal Rock in the Hinchinbrook Entrance. The large sediment volume creates a thick sedimentary basin and sediment high within the center of the Hinchinbrook Entrance.

Montague Strait

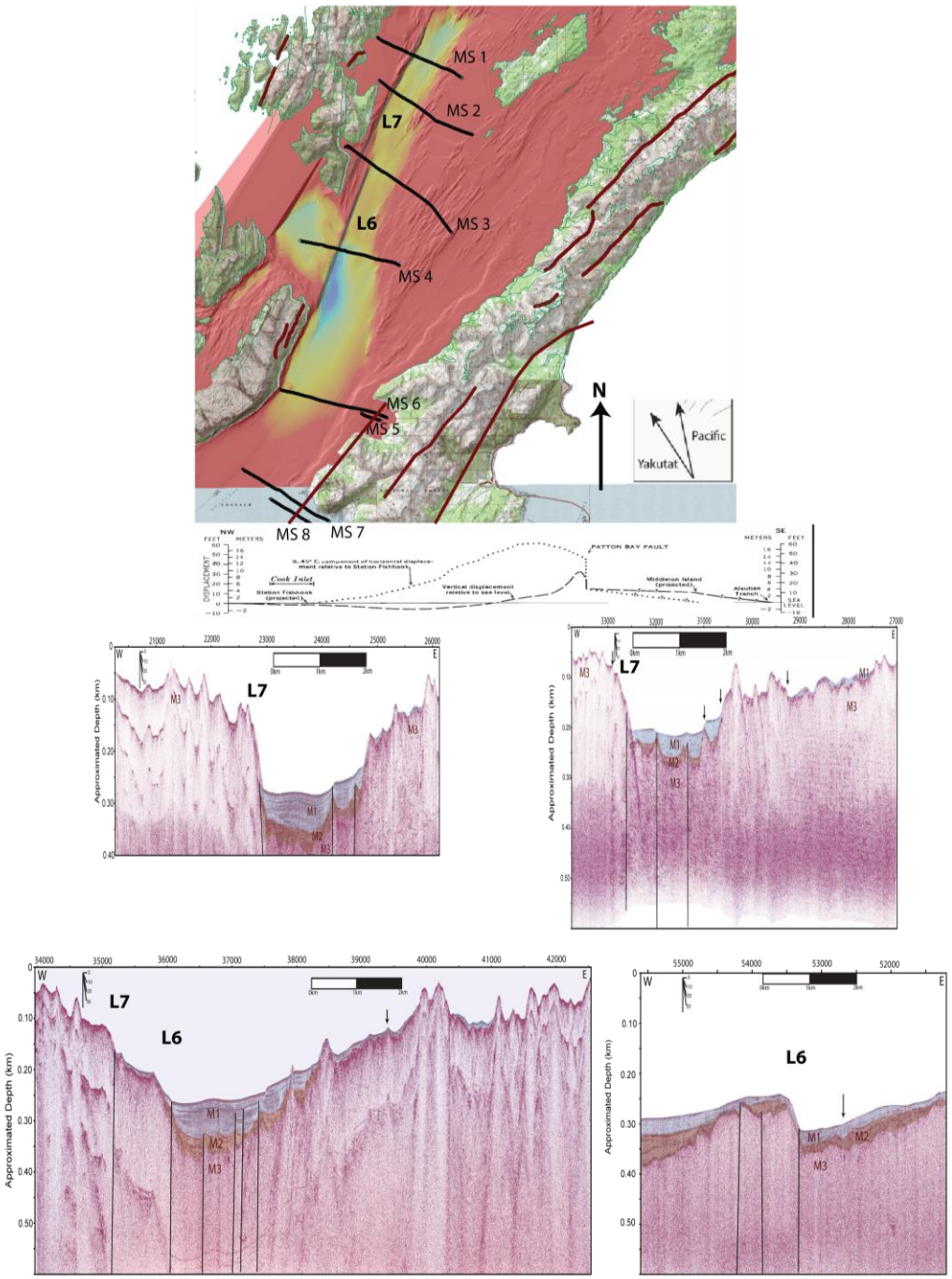

Figure 59: (top) Bathymetry of Montague Strait with blue color as deepest bathymetry (NOAA database), with seismic profiles (black lines), plate motion vectors of Pacific and Yakutat are shown, uplift profile of Montague Island (Plafker, 1969), and faults shown in red (Wilson and Hults, 2008). L6 and L7 represent water bottom scarps related to active faulting (see MS 1, 2, 3, and 4).

Beneath Montague Strait, seismic profiles reveal up to 100 m of late Quaternary and younger sediments below the sea floor. Using modern sedimentation rates from Klein [1983], a key unconformity appears at the base of Holocene strata, approximately 10 kya. Lineations in Montague Strait strike between N10˚E and N40˚E. These lineations have been imaged by both seismic profiles and a bathymetry survey. I suggest normal faults trend northeast-southwest throughout Montague Strait (Figure 56) and a late Quaternary and younger sedimentary basin forms the bathymetric low beneath Montague Strait. These lineations define a 60 km fault system that could support a M7 earthquake independent of megathrust earthquakes (Wells and Coppersmith, 1994).

To the northeast and along strike of the Montague Strait fault, a parallel lineation appears near where the Montague Strait fault terminates (Figure 59). From seismic profiles MS2 and MS3, I interpret this lineation as a continuation of the Montague Strait fault via an en echelon step over related to oblique shortening relative to modern Pacific Plate motion (Figure 47, 48, 49, 50). The extensional Montague Strait basin likely represents the footwall of the Montague Strait blind thrust fault. The Knight Island Passage bathymetric high and Knight and Latouche Islands represent the hanging wall portion of the Montague Strait fault that bounds the western margin of the Montague Strait. Sediments are deposited via syntectonic deposition (e.g., Melnick et al., 2009). Evidence for long term regional uplift is observed in northwest dipping older Quaternary strata on the hanging wall of this fault. As best illustrated on profile MS4 (Figure 50), sediment is draped over the fault and Holocene strata, and bedrock is offset by more than 100 m (Figure 50).

I would suggest structures of Montague Strait experience a different stress direction, between N80˚W and N50˚W, respectively, compared to N10˚W of Orca Bay and Hinchinbrook Entrance. I suggest Montague Strait and Orca Bay represent extensional deformation of the forearc basin bounded by and accommodating parallel splay fault system that uplift the region. As the Montague Strait lineations continue to the north, they are offset in an en echelon pattern as Plafker [1969] observed along strike of the Patton Bay fault on Montague Island. I suggest the Patton Bay fault steps southward while the Montague Strait fault steps northward because of the normal faulting that occurs within central PWS. Furthermore, I interpret this en echelon offset as the result of different stress direction acting on lineation throughout PWS.

Plafker [1969] measured the largest amount of uplift related to the 1964 earthquake near Montague Strait, in particular at the southern portion of Montague Island. The Montague Island shorelines are steep sloped and terraced with deformed Tertiary aged rock exposed; suggesting that the region has experienced high exhumation rates from independent uplift events through their history (Plafker, 1969; Carver and Plafker, 2008; Arkle, 2012). Montague Island in particular has been uplifted by at least three faults: Patton Bay, Hanning Bay, and a fault to the south of Montague Island with no on-land surface expression (Plafker, 1969). Montague Strait represents the hanging wall of all three Montague Island thrust faults. The uplift on Montague Island may result in an unstable stress condition due to an uplifted uncompensated mass that requires subsidence by extension in the Montague Strait hanging wall. Some closely spaced normal faulting may be related to sediment compaction in unconsolidated sediments (Cartwright and Dewhurst, 1998). Normal faulting is observed on other subduction

forearc such as Colombia, Japan, or Chile (Park et al. 2002; Collot et al., 2008; Melnick et al., 2009)

Splay faults surface along an outer ridge high (Montague and Hinchinbrook Islands) within the PWS megathrust fault system. The outer ridge high ruptured during the 1964 Great Alaskan Earthquake and previous megathrust earthquakes (Figure 3; Figure 60). The arcuate shape of PWS barrier island is the result of the rotation of the terrane and subduction zone geometry with respect to the North American plate (Freymueller et al., 2008), resulting in margin parallel faulting throughout the region (Plafker, 1969). Furthermore, the stress orientation is also reflected in the velocity tomograms beneath PWS (Eberhart-Phillips et al., 2006).

Megathrust splay faults are being characterized along subduction zones across the world (Japan, Indonesia, Chile, etc.) (e.g., Lay et al., 2005; Rajendran et al, 2007, Moore et al., 2007). Splay faults emerge from a regional decollement surface along a series of thrust or backthrust faults including along the outer ridge or accretionary wedge (e.g., Park et al., 2002, Mosher et al., 2008). Splay faults uplift and deform the accretionary wedge (e.g., McAdoo et al., 2000; Fujiwara et al., 2011) while generating local tsunamis during large megathrust earthquakes (e.g., Park et al., 2002, Moore et al., 2007). Landward of the accretionary prism, normal faulting and formation of a thickened sediment cover sequence occurs within the forearc (Park et al., 2002; Collot et al.,2008). Multibeam bathymetry and seismic data have been integral in examining these faults and investigating hazard.

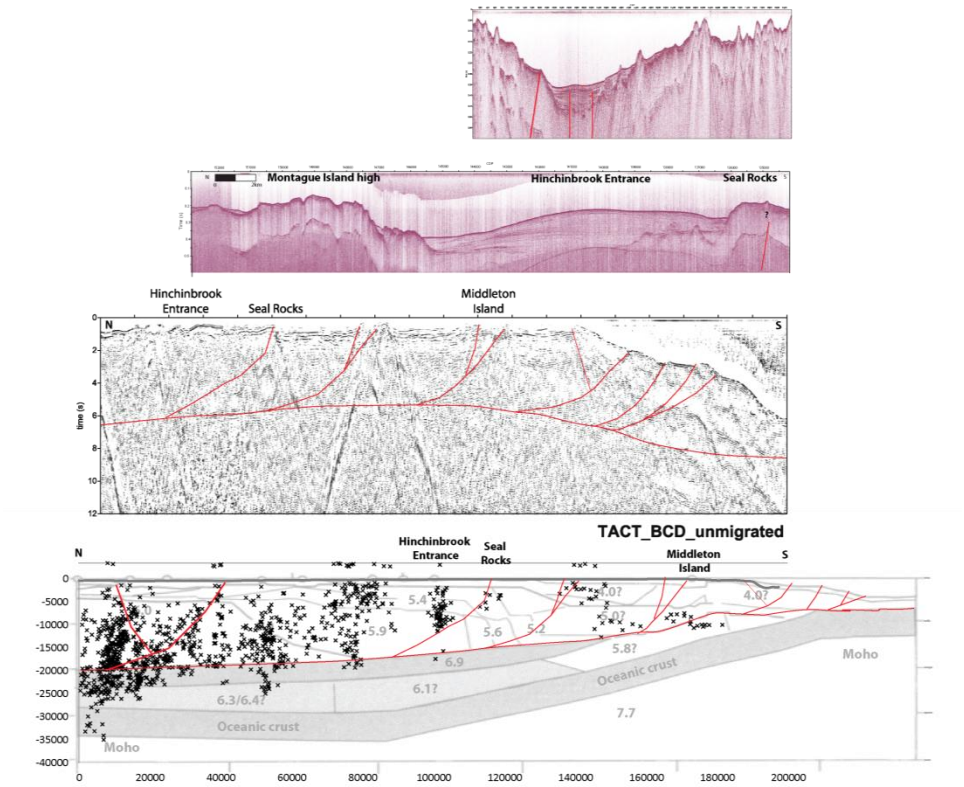

Figure 60: Three seismic profiles from MS3, HB6, and TACT. Cross-section showing earthquakes in PWS in black dots (Doser et al., 2008), faults from seismic profiles in red, and refraction velocity model as transparent layer (Brocher et al. 1994). Relocated seismicity suggests more faults may be present than those observed on reflection profiles.

I interpret active extension in the forearc region of the PWS subduction system, Orca Bay and Montague Strait (Figure 60) to be consistent with observations from other subduction zones (e.g., Park et al., 2002). A narrow zone of subsidence occurs in basins controlled by normal faulting, whereas uplift during earthquake cycles creates the islands of PWS. The normal faults change strike throughout PWS with en echelon pattern of faulting to accommodate oblique subduction of the Pacific and Yakutat terranes with respect to North America. Faulted mapped on Montague Island and Hinchinbrook Islands may be interconnected via a transfer zone beneath Hinchinbrook Island. Bathymetry maps, in addition to seismic profiles, show the Montague Strait fault extends for

approximately 100 km. Faults mapped within Orca Bay extend westward to central PWS and may link to lineations observed on Naked Island (Condon, 1966) in Montague Strait (Condon and Cass, 1958; Plafker, 1969; Wilson and Hults, 2008). If central PWS and Orca Bay are linked and experience simultaneous rupture, these faults could independently support an Mw8 earthquake (Wells and Coppersmith, 1994). If the Montague Strait or Orca Bay faults experienced independent motion, isolated from a large megathrust earthquake, a M7 is possible (Wells and Coppersmith, 1994). If these linked faults connect to offshore faults, it suggests that rupture along the entire fault length is possible during a megathrust earthquake.

CHAPTER SIX: CONCLUSION

PWS is a structurally complex terrane that experiences regional tectonic uplift and localized subsidence both spatially and temporally. General uplift and subsidence trends are accelerated during earthquakes. Similar patterns of uplift and subsidence are present at other subduction zones worldwide, the structural complexity of PWS causes dramatic changes in fault character along strike and significant uplift in the outer arc high (Plafker, 1969; Park et al., 2002; Collot et al., 2008; Finn et al., 2011). Fault dip and orientation changes throughout PWS. Regionally extensive splay faults present hazards in the form of large magnitude earthquakes (>M8). Furthermore, these hazards may present themselves in the form of an shorter recurrence earthquakes of M7 within the central PWS area. Orca Bay and Montague Strait show evidence for submarine landslides that may have activated during earthquakes. During the M9.2 1964 earthquake, submarine landslide generated local tsunamis. These submarine landslides will continue to be the largest hazard for local communities.

Seismic profiles collected throughout PWS show structures that are analogous to subduction zones around the world. Splay faults in PWS emerge from the Pacific/Yakutat decollement surface along a series of thrust or backthrust faults that uplift and deform the accretionary wedge (Japan, Indonesia, Chile, etc.) (e.g., Park et al., 2002; McAdoo et al., 2000; Lay et al., 2005; Moore et al., 2007; Rajendran et al, 2007; Mosher et al., 2008;

Fujiwara et al., 2011). Hazards from the deformation include large magnitude earthquakes followed by uplift and tsunamis (e.g., Park et al., 2002; Moore et al., 2007).

REFERENCES

Alliance For Coastal Technologies. Squid 500 Sparker. Retrieved February 1, 2012 from http://www.act-us.info/sensor_list.php?cat=Seismic&type=Physical.

Andring, M., Beaver, A., Ortiz, F. (2006). Approaches to Cordova: Saint Matthews Bayto Gravina Point. Hydrographic Title Sheet. U.S. Department of CommerceNational Oceanic and Atmospheric Administration. H11610. OPR-P158-FA-06.

Applied Accoustic. Underwater Technology. Applied Accoustic Engineering Limited. Retrived February 8, 2012 from http://www.appliedacoustics.com/.

Arkle, J. *Focused exhumation in the southern Alaska syntaxis: New insights from apatiteand zircon thermochronology.* Diss. California State University, Fullerton, 2011. Dissertations & Theses: Full Text, ProQuest. Web. 30 Apr. 2012.

Arno, N., McKinney, L. (1973). Harbor and Waterfront Facilities, in: The Great AlaskaEarthquake of 1964, National Academy of Sciences, Washington, DC, USA,Engineering, Engineering Volume, p. 526-643.

Audacity, The Free, Cross-Platform Sound Editor (2009). Retrieved August, 2009, fromaudacity.sourceforge.net .

Barnes, D.F., Morin, R.L. (1990). Gravity contour map and interpretation of gravitydata for the Chugach National Forest, Alaska, U.S. Geological Survey Miscellaneous Field Studies Map MF-1645-F.

Barry, K.M., Cavers, D.A., Kneale, C.W. (1975) Recommended Standards for DigitalTaper Formats. Geophysics. Vol. 40. No. 2. P.344-352.

Berger, A.L., Gulick, S.P.S., Spotilla, J.A., Upton, P., Jaeger, J.M., Chapman, J.B.,Worthington, L.A., Pavilis, T.L., Ridgeway, K.D., Willems, B.A., and McAleer, R.J., (2008), Quaternary tectonic response to intensified glacial erosion in an orogenic wedge: Nature Geoscience, v. 1, p. 793-799, doi:10.1038/ngeo334.

Brocher, T. M., G. S. Fuis, M. A. Fisher, G. Plafker, M. J. Moses, J. J. Taber, and N. I. Christensen (1994). Mapping the megathrust beneath the northern Gulf of Alaskausing wide-angle seismic data, J. Geophys. Res., 99, p. 11,663–11,686.

Bruns, T. R. (1983). Model for the origin of the Yakutat block, an accreting terrane in the northern Gulf of Alaska, Geology, vol 11, p. 718-721.

Bufe, C. G. (2004) Stress Transfer to the Denali and Other Regional Faults from the M 9.2 Alaska Earthquake of 1964, Bulletin of the Seismological Society of America, vol 94, p. S145-S155.

Carlson, P. R., Molnia, B.F. (1978). Minisparker profiles and sedimentologic data from R/V Acona cruise (April 1976) in the Gulf of Alaska and Prince William Sound. Open File Report, U.S Department of Interior Geological Survey.

Carlson, P. R., Golan-Bac, M., Karl, H. A., Kvenvolden KA (1985). Seismic and geochemical evidence for shallow gas in sediment of Navarin continental margin, Bering Sea, AAPG Bull 69, p. 422–436.

Cartwright, J.A., Dewhurst, D. N. (1998). Layer-bound compaction faults in finegrained sediments, Geological Society of America Bulletin, 110, p. 1242-1257.

Carver, G., Plafker, G. (2008) Paloseismicity and neotectonics of the Aleutian subduction zone – an overview, in: Active tectonics and seismic potential of Alaska, edited by: Freymueller, J., Haeussler, P., Wesson, R., and Ekstrom, G., Washington DC, AGU, Geophysical Monograph Series 179 43–63.

Clark, P.U., Archer, D., Pollard, D., Blum, J.D., Rial, J.A., Brovkin, V., Mix, A.C., Pisias, N.G., and Roy, M., (2006), The middle Pleistocene transition: Characteristics, mechanisms, and implications for long-term changes in atmospheric PCO^{-2}: Quaternary Science Reviews, v. 25, no. 23-24, p.3150-3184, doi: 10.1016/j.quascirev.2006.07.008.

Cloud, W., Scott, N.(1972). Distribution of Intensity, in: The Great Alaska Earthquake of 1964, National Academy of Sciences, Washington, DC, USA, Seismology and Geodesy, Seismology and Geodesy Volume, p. 65-108.

Cohen, J.K., Stockwell, Jr. J.W., (2011), CWP/SU: Seismic Un*x Release No. 43: an open source software package for seismic research and processing, Center for Wave Phenomena, Colorado School of Mines.

Collot, J.-Y., Agudelo, W., Ribodetti, A., Marcaillou , B., (2008),Origin of a crustal splay fault and its relation to the seismogenic zone and underplating at the erosional north Ecuador-south Colombia oceanic margin, Journal of Geophysical Research, v. 113.

Condon, W.H., Cass, J.T. (1958). Map of a part of the Prince William Sound area, showing linear geologic features as shown on aerial photographs. U.S. Geological Survey.

Condon, W.H. (1966). Map of Eastern Prince William Sound Area, Alaska Showing Fracture Traces Inferred from Aerial Photographs. U.S. Geological Survey.

Cowan, E.A., Seramur, K.C., Powell, R.D., Willems, B.A., Gulick, S.P.S., Jaeger, J.M., (2010). Fjords as temporary sediment traps; history of glacial erosion and deposition in Muir Inlet, Glacier Bay National Park, Southeastern Alaska. Geological Society of America Bulletin. v 122 no.7-8. p.1067-1080.

Deodato, L. Domingo, R. Mayor, R. Sampadian, K. (2000). Southwest Prince William Sound H11005. Descriptive Report. U.S. Department of Commerce. RA-40-04 00. H11005.

Doser, D. I., Brown, W. A. A (2001). Study of Historic Earthquakes of the Prince William Sound, Alaska, Region. Bulletin of Seismological Society of America. 91.4. p. 842-857.

Doser, D. I., Ratchkovski, N. A., Haeussler, P. J. Saltus, R. (2004). Changes in Crustal Seismic Deformation Rates Associated with the 1964 Great Alaska Earthquake. Bulletin of the Seismological Society of America, vol. 94, No. 1, p. 320-325.

Doser, D. I., de la Pena, A., Veilleux, A. M. (2008). Seismicity of the Prince William Sound Region and Its Relation to Plate Structure and the 1964 Great Alaska Earthquake, Active Tectonics and Seismic Potential of Alaska, AGU Book, p. 201-214, Washington, DC.

Eberhart-Phillips, D., Christensen, D.H., Brocher, T.M., Hansen, R., Ruppert, N.A., Haeussler, P.J., and Abers, G.A. (2006). Imaging the transition from Aleutian subduction to Yakutat collision in central Alaska, with local earthquakes and active source data: Journal of Geophysical Research, v. 111, B11303, doi:10.1029/2005JB004240.

Elliott, J.L., Larson, C.F., Freymueller, J.T., Motyka, R.J. (2010). Tectonic block motion and glacial isostatic adjustment in southeast Alaska and adjacent Canada constrained by GPS measurements, J. Geophys. Research, v. 115.

Finn, S.P., Liberty, L.M., Haeussler, P.J., Northrup, C.J., Pratt, T.L., (2011), Holocene deposition and megathrust splay fault geometries within Prince William Sound, Alaska, AGU Fall Conference Abstract, T33A-23B6.

Fisher, M.A., Brocher, T.M., Bruns, T.R., Geist, E., (1989), Seismic reflections from a possible brittle/ductile transition within the accretionary wedge near the eastern Aleutian trench, Eos. Trans., AGU, 70, 1339.

Freymueller, J.F., Woodard, H., Cohen, S.C., Cross, R., Elliot, J., Larsen, C.F., Hreinsdotti, S., Zweck, C. (2008). Active Deformation Processes in Alaska, Based on 15 Years of GPS Measurements, Active Tectonics and Seismic Potential of Alaska. Geophysical Monograph 179, American Geophysical Union, p. 1-42.

Fuis, G. S., Moore, T. E., Plafker, G., Brocher, T.M., Fisher, M.A., Mooney, W.D., Nokleberg, W.J., Page, R.A., Beaudoin, B.C., Christensen, N.I., Levander, A.R., Lutter, W.J., Saltus, R.W., Ruppert, N.A. (2008). Trans-Alaska Crustal Transect and continental evolution involving subduction underplating and synchronous foreland thrusting, *Geology*, v. 36, no. 3, p. 267-270.

Fujiwara, T., Kodaira, S., No, T., Kaiho, Y., Takahashi, N., and Kaneda, Y. (2011). The 2011 Tohoku-Oki Earthquake: Displacement Reaching the Trench Axis Toshiya, Science, 334, 1240.

Griscom, A., Sauer, P., (1990). Interpretation of magnetic maps of the northern Gulf of Alaska, with emphasis on the source of the Slope anomaly, USGS, OFR 90-348.

Gulick, S.P.S., Lowe, L., Pavlis, T.L., Gardner, J.V., and Mayer, L.A. (2007). Geophysical insights into the Transition fault debate: Propagating strike slip in response to stalling Yakutat block subduction in the Gulf of Alaska: Geology, v. 35, p. 763–766.

Haas, J.E. (1973) Geography (Human Ecology), in: The Great Alaska Earthquake of 1964, National Academy of Sciences, Washington, DC, USA, Summary, Summary and Recommendations Volume, 89-97 pp.

Hamilton, T.D. (1994).Late Cenozoic glaciations of Alaska. The Geology of North America, vol G-1, The Geology of Alaska. The Geologic Society of America.

Hofmann, M.H., Hendrix, M.S., Moore, J.N., Sperazza, M., (2006), Late Pleistocene and Holocene depositional history of sediments in Flathead Lake, Montana: Evidence from high-resolution seismic reflection interpretation, Sedimentary Geology, 184, p. 111-131.

Hoogeveen, J.H.M., Hegna, S., Tenghamn, R, Stenzel, A., and Borresen, C., (2005), Practical aspects of an innovative solid streamer concept. SEG Expanded Abstracts, ACQ 3.4.

Jaeger, J.M., Nittrouer, C.A., Scott, N.D., Milliman, J.D. (1998). Sediment accumulationalong a glacially impacted coastline: north-east Gulf of Alaska, Basin Research,v.10, p.155-173.

Kanamori, H. (1977).The energy release in great earthquakes. Journal of Geophysical Research, v.82, no. 20, p. 2981-2987.

Klein, L.H. (1983). Provenances, depositional rates, and heavy metal chemistry of sediments, Prince William Sound, southcentral Alaska, M.S. Thesis, University of Alaska, Fairbanks, AK. 96 p.

Lahr, J.C., and Plafker, G. (1980). Holocene Pacific-North American Plate interaction in southern Alaska; Implications for the Yakataga seismic gap, Geology, 8,483-486.

Lay, T., H. Kanamori, C. J. Ammon, M. Nettles, S. N. Ward, R. C. Aster, S. L. Beck, S. L. Bilek, M. R. Brudzinski, R. Butler, H. R. DeShon, G. Estorm, K. Satake, and S. Sipkin (2005). The great Sumatra-Andaman Earthquake of 26 December 2004, Science 308, p. 1127–1133.

Le Douran, S., Parsons, B. (1982) A note on the correction of ocean floor depths for sediment loading, J. Geophysics Research, v. 87, p. 4715-4722.

Lee SH, Chough SK (2003) Distribution and origin of shallow gas in deep-sea sediments of the Ulleung Basin, East Sea (Sea of Japan). Geo-Mar Lett 22, p. 204–209.

McAdoo, B.G., Pratson, L.F., Orange, D.L., (2000). Submarine landslide geomorphology, US continental slope, Marine Geology, Volume 169, Issues 1 2, p. 103-136, ISSN 0025-3227, 10.1016/S0025-3227(00)00050-5.

Melnick, D., Bookhagen, B., Strecker, M. R., Echtler, H. P. (2009). Segmentation of megathrust rupture zones from fore-arc deformation patterns hundreds to millions of years, Arauco peninsula, Chile. Journal of Geophysical Research, vol. 114.

Molnia, B. F. (1977). Surface Sedimentary Units of the Gulf of Alaska Continental Shelf: Montague Island to Yakutat Bay, USGS OFR-77-30.

Molnia, B.F. (1989). Subarctic (temperate) glacial-marine sedimentation: the northeast Gulf of Alaska. Short Course in Geology: Glacial-marine sedimentation, AGU, v. 9.

Moore, G. F., Bangs, N. L., Taira, A., Kuramoto, S., Pangborn, E., Tobin, H.J. (2007). Three dimensional splay fault geometry and implications for tsunami generation, Science, v. 318, 1128.

Mosher, D.C., Austin, J.A. Jr., Fisher, D., Gulick, S.P.S. (2008). Deformation of the northern Sumatra accretionary prism from high-resolution seismic reflection profiles and ROV observations, Marine Geology, 252, p. 89-99.

Nelson, S.W., Dunmoulin, J.A., and Miller, M.L. (1985). Geologic map of the Chugach National Forest, Alaska, U.S. Geological Survey Map MF-1645-B.

NOAA (National Oceanic and Atmospheric Administration). *Bathymetric and Elevation Models*. Silver Spring , 2012. <http://www.ngdc.noaa.gov/mgg/bathymetry/relief.html>.

Nokleberg, W.J., Plafker, G., Wilson, F. H. (1994) Geology of south-central Alaska, in Plafker, G., and Berg H. C., eds., The Geology of Alaska: Boulder, Colorado, Geological Society of America, The Geology of North America, V. G-1.

Page, D, S., Boehm, P. D., Douglas, G. S. and Bence, A. E. (1995) Identification of hydrocarbon sources in the benthic sediments of Prince William Sound and the Gulf of Alaska following the Exxon Valdez oil spill. In Exxon Valdez Oil Spill: Fate and Effects in Alaskan Waters, ASTM Special Technical Publication # 1219., eds P.G. Wells, J.N. butler and J.S. Hughes p. 41-83. American Society for Testing and Materials, Philadelphia.

Park, J, Tsuru, T, Kodaira, S, Cummins, P.R., Kaneda, Y. (2002). Splay Faulting Branching Along the Nankai Subduction Zone, Science, v.297, 1157.

Plafker, G. (1969) Tectonics of the March 27, 1964 Alaska earthquake, U.S. Geol.Survey Professional Paper 543-1, 74.

Plafker, G. Gilpin, L.M. Lahr, J.C. (1993) Neotectonic Map of Alaska. Geological Society of America.

Plafker, G. Berg, H. C. (1994). Overview of the geology and tectonic evolution of Alaska. The Geology of North America (DNAG), v.G-1.

Plafker, G., Moore, J.C., Winkler, G.R., (1994). Geology of southern Alaska margin, The Geology of Alaska (DNAG), v. G-1.

Pullan, S.E. (1990). Recommended standard for seismic (/radar) data files in the personal computer environment. Geophysics, v. 55, p 1260.

Rajendran, C. P., Rajendran, K., Anu, R., Earnest,A., Machado, T., Mohan, P. M., and Freymueller, J. (2007), Crustal Deformation and Seismic History Associated with the 2004 Indian Ocean Earthquake: A Perspective from the Andaman–Nicobar Islands, Bulletin of the Seismological Society of America, Vol. 97, No. 1A, p. S174–S191, January 2007, doi: 10.1785/0120050630.

Ratchkovski, Natalia A. Hansen, Roger A. (2002). New Evidence for Segmentation of the Alaska Subduction Zone, Bulletin of the Seismological Society of America, v. 92., No. 5., p. 1754-1765.

Ruppert, N. A. Ridgway, K. D. Freymueller, J.T. Cross, R.S. Hansen, R.A.(2008). Active Tectonics of Interior Alaska: Seismicity, GPS Geodesy, and Local Geomorphology, Active Tectonics and Seismic Potential of Alaska, p. 109-133.

Ryan, H.F. Lee, H.J. Haeussler, P.J. Alexander, C.R. Kayen, R.E. (2010). Historic and Paleo Submarine Landslide Deposits Imaged Beneath Port Valdez, Alaska: Implications for Tsunami Generation in Glacial Fiord, Submarine Mass Movements and Their Consequences, Advances in Natural and Technological Hazards Research, v. 28.

Shennan, I. Barlow, N. Combellick, R.(2008) Paleoseismological Records of Multiple Great Earthquakes in Southcentral Alaska: A 4000-Year Record at Girdwood. Active Tectonics and Seismic Potential of Alaska, p. 185-199.

Sheriff, R.E. (1984). Encyclopedic Dictionary of Exploration Geophysics, SEG Publications, vol. 2, Tulsa, O.K.

Silberling, N.J. Jones, D.L. Monger, J.W.H. Coney, P.J. Berg, H.C. Plafker, G. (1994). Lithotectonic Terrane Map of Alaska and Adjacent Parts of Canada, The Geological Society of America, Boulder, Co.

Stauder, W., Bollinger, G.A. (1966) The focal mechanism of the Alaska earthquake of March 28, 1964, and of its aftershock sequence, v. 71-22, p. 5283-5296.

Trabant, P.K. (1984) Applied High-Resolution Geophysical Methods: Boston, Ma., International Human Resources Development Corporation, p.103.

USGS. Earthquake Hazards Program. *Historic World Earthquakes*, Cited on February 8, 2012, http://earthquake.usgs.gov/earthquakes/world/historical.php.

Vaughan, S. L., Mooers, C.N.K and Gay, S.M. III. (2001), Physical variability in Prince William Sound during the SEA study (1994– 98), Fisher. Oceanogr., 10, suppl. 1, 58–80.

von Huene, R.. R. J. Malloy, and G. G. Shor, Jr., and P. Saint-Amand (1967). Geologic structures in the aftershock region of the 1964 Alaskan earthquake, J. Geophys. Res., 72, 3649.

von Huene, R., Molnia, B.F., Bruns, T.R., Carlson, P.R. (1975). Seismic profiles of the offshore Gulf of Alaska Tertiary Province, R/V Thompson, Sept.-Oct. 1974, U.S. Geological Survey, 75-0664.

Wells, D.L., Coppersmith, K. J. (1994) New Empirical Relationships among Magnitude, Rupture Length, Rupture Width, Rupture Area, and Surface Displacement, *Bulletin of the Seismological Society of America*, v. 84, no. 4, p. 974–1002.

Widess, M.B. (1973). How thin is a thin bed. Geophysics.v.38-6p1176-1180.

Wilson, F.H., Hults, C.P. (2008) (in review). Geology of the Prince William Sound and Kenai Peninsula region, Alaska, U.S. Geol Survey Scientific Investigations Map.

Winkler, G.R. Plafker, G. (1981). Geologic Map and Cross Sections of the Cordova and Middleton Quadrangles, Southern Alaska, United States Department Of The Interior Geological Survey, Open File Report 81-1164.

Xiong, Q., T.C. Royer. (1984). Coastal temperature and salinity in the northern Gulf of Alaska**,** J. Geop. Res., 89:8061-8066.

Yilmaz, O. (2001) Seismic data analysis. SEG Publications, Tulsa, O.K.